Advanced fuels from ethanol-A superstructure optimization approach

Juan-Manuel Restrepo-Flórez, Christos T. Maravelias

S1. Mathematical model of the superstructure

S1.1 Notation

Indexes are presented as lower-case italicized roman characters, sets and subsets as upper-case bold roman characters, parameters as italicized Greek characters, and variables as upper-case italicized roman characters.

Sets and Subsets

$i \in \mathbf{I}$	Superstructure elements
$\mathbf{I^{MD}}$	Modules
$\mathbf{I^{TCH}}$	Technologies
$\mathbf{I^{TG}}$	Technology groups
$\mathbf{I^{SRC}}$	Sources
$\mathbf{I^{MX}}$	Mixers
$\mathbf{I^{T}_{i'}}$	Technologies $i \in \mathbf{I^{TCH}}$ belonging to technology group $i' \in \mathbf{I^{TG}}$
$\mathbf{I^{M}_{i'}}$	Modules $i \in \mathbf{I^{MD}}$ belonging to technology $i' \in \mathbf{I^{TCH}}$
$\mathbf{I^{iSPTG}_{i'}}$	Inlet splitters to technology group $i' \in \mathbf{I^{TG}}$
$\mathbf{I^{oSPTG}_{i'}}$	Outlet splitters from technology group $i' \in \mathbf{I^{TG}}$
$\mathbf{I^{iSPT}_{i'}}$	Inlet splitters to technology $i' \in \mathbf{I^{TCH}}$
$\mathbf{I^{oSPT}_{i'}}$	Outlet splitters from technology $i' \in \mathbf{I^{TCH}}$
$\mathbf{I^{SRCA}_{i'}}$	Optional sources associated with module $i' \in \mathbf{I^{MD}}$
$r \in \mathbf{R}$	Chemical reactions
$\mathbf{R^{M}_{i}}$	Chemical reactions $r \in \mathbf{R}$ that may occur in module $i \in \mathbf{I^{MD}}$
$k \in \mathbf{K}$	Chemical components
$\mathbf{K^{Of}}$	Olefins
$\mathbf{K^{Ar}}$	Aromatics
$\mathbf{K^{BP30}}$	Components with boiling point less than 30
$\mathbf{K^{BP150}}$	Components with boiling point less than 150
$\mathbf{K^{BP160}}$	Components with boiling point less than 160
$\mathbf{K^{BP225}}$	Components with boiling point less than 225
$\mathbf{K^{BP300}}$	Components with boiling point less than 300
$\mathbf{K^{BP360}}$	Components with boiling point less than 360
$\mathbf{K^{NF}}$	Components present only in trace amount in a fuel blend
$\mathbf{K^{R}_{r}}$	Reference component $k \in \mathbf{K}$ in reaction $r \in \mathbf{R}$
$\mathbf{K^{TG}_{i}}$	Components for which technology group $i \in \mathbf{I^{TG}}$ is designed
$\mathbf{K^{SRC}_{j}}$	Components present in source stream $j \in \mathbf{J^{srcM}_{i}} \wedge i \in \mathbf{I^{MD}}$
$j \in \mathbf{J}$	Process streams
$\mathbf{J^{P}}$	Fuel product streams
$\mathbf{J^{E}}$	Electricity generation streams
$\mathbf{J^{in}_{i}}$	Inlet stream to superstructure element $i \in \mathbf{I}$
$\mathbf{J^{out}_{i}}$	Outlet stream from superstructure element $i \in \mathbf{I}$
$\mathbf{J^{srcM}_{i}}$	Optional source streams feed to conversion unit of module $i \in \mathbf{I^{MD}}$

Parameters

Economic parameters

α	Scaling exponent for capital cost equation
β^{NREL}	Reference capacity of the NREL ethanol conversion plant
δ	Conversion efficiency from heat to electricity
θ^{af}	Annualization factor
θ_i^{CC}	Reference capital cost of module $i \in \mathbf{I^{MD}}$
θ_i^{OC}	Reference operating cost of module $i \in \mathbf{I^{MD}}$
θ_i^{F}	Reference mass flow rate used to calculate reference costs of module $i \in \mathbf{I^{MD}}$
θ_j^{SRC}	Cost per kilogram of source stream $j \in \mathbf{J}$
θ_j^{P}	Sale price of product streams $j \in \mathbf{J}^{\mathrm{P}}$
θ_j^{E}	Sale price of electricity $j \in \mathbf{J}^{\mathrm{E}}$

Process parameters

$\gamma_{r,k}$	Molar yield associated with species $k \in \mathbf{K}$, establishing the amount of k produced or consumed in reaction $r \in \mathbf{R}$ per mol of reference component
$\eta_{j,j',k}$	Partition coefficient determining the amount of species $k \in \mathbf{K}$ present in stream $j \in \mathbf{J_i^{in}}$ that is directed toward stream $j \in \mathbf{J_i^{out}}$, for $i \in \mathbf{I_{i'}^{oSPT}}$
ι^{LB}	Lower bound on a stream flow
ι^{UB}	Upper bound on a stream flow
ι^{LBM}	Minimum amount of material that a module can process

Physical properties of chemical components

λ_k^{MW}	Molecular weight of species $k \in \mathbf{K}$
λ_k^{LHV}	Low heating value of species $k \in \mathbf{K}$
λ_k^{CN}	Cetane Number of pure species $k \in \mathbf{K}$
λ_k^{RON}	Research Octane Number of pure species $k \in \mathbf{K}$
λ_k^{TB}	Normal boiling of pure species $k \in \mathbf{K}$
λ_k^{ρ}	Density of pure species $k \in \mathbf{K}$
λ_k^{μ}	Dynamic viscosity of pure species $k \in \mathbf{K}$

Specifications

ϕ_j^{W}	Mol percentage of water in an ethanol feed stream $j \in \mathbf{J_i^{in}}$, $i \in \mathbf{I_{tg1}^{iSPTG}}$
ϕ_j^{SRC}	Relation between molar flow of an optional source and the feed flow to the module where this source is feed $j \in \mathbf{J_i^{srcM}} \wedge i \in \mathbf{I^{MD}}$
ϕ_j^{RON}	Minimum research octane number in product outlet stream $j \in \mathbf{J_i^{out}},\ i \in \mathbf{I^{MX}}$
ϕ_j^{CN}	Minimum cetane number of product stream $j \in \mathbf{J_i^{out}},\ i \in \mathbf{I^{MX}}$
ϕ_j^{AR}	Maximum aromatic content (% mass) in product stream $j \in \mathbf{J_i^{out}},\ i \in \mathbf{I^{MX}}$
ϕ_j^{OF}	Maximum olefin content (% mass) in product stream $j \in \mathbf{J_i^{out}},\ i \in \mathbf{I^{MX}}$
ϕ_j^{ρ}	Maximum density of product stream $j \in \mathbf{J_i^{out}},\ i \in \mathbf{I^{MX}}$
$\phi_j^{\mu max}$	Maximum viscosity of product stream $j \in \mathbf{J_i^{out}},\ i \in \mathbf{I^{MX}}$
$\phi_j^{\mu min}$	Minimum viscosity of product stream $j \in \mathbf{J_i^{out}},\ i \in \mathbf{I^{MX}}$
ϕ_j^{G30}	Maximum mol % evaporated from a gasoline when temperature reaches at 30°C
ϕ_j^{G225}	Minimum mol % evaporated from a gasoline when temperature reaches at 225°C

ϕ_j^{JF160} Maximum mol % evaporated from a Jet fuel stream when temperature reaches 160°C
ϕ_j^{JF300} Minimum mol % evaporated from a gasoline stream when temperature reaches 300°C
ϕ_j^{D150} Maximum mol % evaporated from a Diesel stream when temperature reaches 150°C
ϕ_j^{D360} Maximum mol % evaporated from a Diesel stream when temperature reaches 360°C

Variables

Real variables

Z Annual profit

Non-negative continuous variables

S^{FS} Annual fuel sales
S^{ES} Annual electricity sales
C^{CC} Annualized capital costs
C^{OC} Annual operating costs excluding feedstock
C^{FST} Annual costs of feedstock
C_i^{CCE} Total capital investment for module $i \in \mathbf{I^{MD}}$
C_i^{OCE} Total operating cost for module $i \in \mathbf{I^{MD}}$
F_j Total molar flow of stream j
FM_j Total mass flow rate of stream j
$FK_{j,k}$ Molar flow rate of species k in stream j
$Fb_{r,i}$ Molar flow rate of reference reactant in reaction $\mathbf{R_i^M}$ occurring in module $i \in \mathbf{I^{MD}}$
$SF_{i,j}$ Split fraction establishing the fraction of incoming streams to splitter $i \in (\mathbf{I_{i'}^{iSPTG}} \vee \mathbf{I_{i'}^{oSPTG}})$ directed toward stream $j \in \mathbf{J_i^{out}}$
CN_j Cetane number of a product stream $j \in \mathbf{J_i^{out}}$, $i \in \mathbf{I^{MX}}$
RON_j Research Octane Number of a product stream $j \in \mathbf{J_i^{out}}$, $i \in \mathbf{I^{MX}}$
D_j Density of a product stream $j \in \mathbf{J_i^{out}}$, $i \in \mathbf{I^{MX}}$
V_j Viscosity of a product stream $j \in \mathbf{J_i^{out}}$, $i \in \mathbf{I^{MX}}$

Binary variables

YM_i Equal to one if module $i \in \mathbf{I^{MD}}$ is selected in the final solution
YT_i Equal to one if technology $i \in \mathbf{I^{TCH}}$ is selected in the final solution
YTG_i Equal to one if technology group $i \in \mathbf{I^{TG}}$ is selected in the final solution
YF_j Equal to one if product stream $\boldsymbol{j} \in \mathbf{J^P}$, is produced in the final solution

S1.2 Mathematical model

The mathematical model of the system consists of four types of equations: mass balances around the different units of the superstructure, logical relations established based on superstructure connectivity, definitions that allow to calculate the process costs, and blending rules to estimate fuel properties.

Objective function

In this work we use annual profit [Eq. S1], defined as the difference between revenues and costs, as the objective function to be maximized. We consider two sources of revenue: fuel sales [Eq. S2], and electricity sales [Eq. S3]. Fuel sales are calculated as the sum of revenues obtained from all fuel types produced. Electricity sales on the other hand are calculated by using the low heating value of components present in the electricity generation stream. To account for thermodynamic losses, we have used a heat

to electricity conversion efficiency δ. Production costs are split into three components: annualized capital investment [Eq. S4], calculated as the sum of the total capital investment of all active modules; annual operating costs [Eq. S5], also calculated based on the active modules; and annual cost of feed streams [Eq. S6], calculated as the sum of the costs of each feedstock consumed.

$$Z = S^{FS} + S^{ES} - C^{CC} - C^{OC} - C^{FST} \quad (S1)$$

$$S^{FS} = \sum_{j \in \mathbf{J^P}} \theta_j^P FM_j \quad (S2)$$

$$S^{ES} = \sum_{j \in \mathbf{J^E}} \delta \theta_j^E \sum_{k \in \mathbf{K}} \lambda_k^{LHV} FK_{j,k} \quad (S3)$$

$$C^{CC} = \theta^{af} \sum_{i \in \mathbf{I^{MD}}} C_i^{CCE} \quad (S4)$$

$$C^{OC} = \sum_{i \in \mathbf{I^{MD}}} C_i^{OCE} \quad (S5)$$

$$C^{FST} = \sum_{i \in \mathbf{I_{tg1}^{iSPTG}}} \sum_{j \in \mathbf{J_i^{in}}} \theta_j^{SRC} FM_j \quad (S6)$$

General definitions

The model requires the definition of two general variables: the total molar flow of a stream [Eq. S7], and its total mass flow rate [Eq. S8].

$$F_j = \sum_{k \in \mathbf{K}} FK_{j,k}, \forall\, j \in \mathbf{J} \quad (S7)$$

$$FM_j = \sum_{k \in \mathbf{K}} \lambda_k^{MW} FK_{j,k}, \forall\, j \in \mathbf{J} \quad (S8)$$

Inlet/outlet splitters associated with a technology group

Inlet(outlet) splitters to(from) a technology group are modeled using two redundant mass balances: a linear component balance around the splitter [Eq. S9]; and a non-linear one in terms of split fraction $SF_{i,j}$ [Eqs. S10-S11], the non-linear balance ensures that every output stream has the same composition. Although only Eqs. S10-S11 are physically required to describe the system, we have found that adding Eq. S9 increases the speed of convergence. In principle the superstructure can formulated as a fully connected system, in which every output splitter for a technology group is connected to every input splitter from other technology groups, and to every product. This fully connected superstructure can be simplified by identifying non-productive connections in which the outlet port does not contain the substrate that is processed by the technology group to which the inlet port is attached. These connections can be eliminated without cutting off good solutions while simultaneously improving computational performance. A connectivity matrix showing the productive connections is shown in Supplementary section S3.

$$\sum_{j \in \mathbf{J_i^{in}}} FK_{j,k} = \sum_{j \in \mathbf{J_i^{out}}} FK_{j,k}, \forall \big(k \in \mathbf{K} \wedge i \in (\mathbf{I_{i'}^{iSPTG}} \vee \mathbf{I_{i'}^{oSPTG}}) \big) \quad (S9)$$

$$FK_{j,k} = \sum_{j' \in \mathbf{J_i^{in}}} SF_{i,j} FK_{j',k}, \quad \forall \big(k \in \mathbf{K} \wedge j \in \mathbf{J_i^{out}} \wedge i \in (\mathbf{I_{i'}^{iSPTG}} \vee \mathbf{I_{i'}^{oSPTG}}) \big) \quad (S10)$$

$$\sum_{j \in \mathbf{J_i^{in}}} SF_{i,j} = 1, \forall \big(i \in \mathbf{I_{i'}^{iSPTG}} \vee \mathbf{I_{i'}^{oSPTG}} \big) \quad (S11)$$

Inlet splitter to a technology

Inlet splitters to a technology result from merging the inlet splitters of individual modules part of the technology. Since at most one module can be selected for each active technology, these units can be modelled as *selection splitters*[1]. A selection splitter can be fully characterized without using bilinear terms. To achieve this simplification, it is necessary to use the binary variable (YM_i) indicating if a module is selected or not. Using the binary variable YM_i, it is possible to model this unit using three equations: a linear component mass balance [Eq. S12]; a logical constraint enforcing the selection of at most one module [Eq. S13]; and an inactivation constraint that forces the flow of streams associated with the conversion unit of an inactive module to be zero [Eq. S14]. Note that in Eq. S13, the right-hand side is the binary variable YT_i, which indicates if a technology is active, including this binary in the constraint forces all modules in a technology to be inactive if that technology is not selected, likewise, if none of the modules in a technology is selected this constraint forces the technology to be inactive.

$$\sum_{j\in\mathbf{J}_i^{\mathbf{in}}} FK_{j,k} = \sum_{j\in\mathbf{J}_i^{\mathbf{out}}} FK_{j,k}\,, \forall\big(\, k \in \mathbf{K} \,\wedge i \in \mathbf{I}_{i'}^{\mathbf{T}}\big) \tag{S12}$$

$$\sum_{i\in\mathbf{I}_{i'}^{\mathbf{M}}} YM_i = YT_{i'}, \forall\, i' \in \mathbf{I}^{\mathbf{TCH}} \tag{S13}$$

$$FK_{j,k} \le \iota^{UB} YM_i, \forall (j \in (\mathbf{J}_i^{\mathbf{iM}} \vee \mathbf{J}_{\mathbf{i}}^{\mathbf{oM}}) \wedge i \in \mathbf{I}^{\mathbf{MD}}) \tag{S14}$$

Conversion unit of a module

Within each conversion unit of a module there are r reactions that can take place. In each of these reactions we use a reference reactant ($k \in \mathbf{K}_r^{\mathbf{R}}$) to define a yield coefficient $\gamma_{r,k}$ for each species k within the system. The yield coefficient is defined as the amount of k produced or consumed in the module per mol of reference reactant. If $\gamma_{r,k}$ is greater than zero k is produced, if smaller than zero k is consumed, and if equal to zero k is an inert. The yield coefficient is a constant characteristic of the module and can be calculated *a-priori* using data from detailed simulations, or from the Techno-Economic Analysis (TEA) literature. The yield coefficient value is rich in information, lumping together the effects of both the specific catalyst selected, and the recycle policy characteristic of a design. Eqs. S15 and S16 model the conversion unit of a module, such that in Eq. S15 we define the reference reactant in a module as the sum of its molar flow in the incoming flows; and in Eq. S16 we perform a mass balance around the conversion unit using $\gamma_{r,k}$ to describe the conversion process. Additionally, we introduce a constraint to establish the minimum amount that can be processed by a module [Eq. S17], this constraint is important from a practical point of view, because it eliminates impractical solutions with excessively small modules.

$$Fb_{r,i} = \sum_{k\in\mathbf{K}_r^{\mathbf{R}}} \sum_{j\in\mathbf{J}_i^{\mathbf{in}}} FK_{j,k}, \forall\big(\, r \in \mathbf{R}_i^{\mathbf{M}}, i \in \mathbf{I}^{\mathbf{MD}}\big) \tag{S15}$$

$$\sum_{j\in\mathbf{J}_i^{\mathbf{in}}} FK_{j,k} + \sum_{r\in\mathbf{R}_i^{\mathbf{M}}} \gamma_{r,k}\, Fb_{r,i} = \sum_{j\in\mathbf{J}_i^{\mathbf{out}}} FK_{j,k}\,, \forall\big(\, k \in \mathbf{K}, i \in \mathbf{I}^{\mathbf{MD}}\big) \tag{S16}$$

$$FM_j \ge \iota^{LBM} YM_i, \forall\, (j \in \mathbf{J}_i^{\mathbf{iM}}, i \in \mathbf{I}^{\mathbf{MD}}) \tag{S17}$$

In the conversion unit of every module we have considered the possibility of adding an optional source. This element is typically used to model the addition of: inert carriers and other diluents, make-up streams containing separation agents required in extraction columns, and reactants that are not part of the components flowing through the superstructure, *e.g.* homogenous catalyst. The size of a source stream entering a module depends on two factors [Eq. S18]: the stochiometric consumption in a reaction within the module, if any; and a user determined consumption rate per mol of incoming flow, defined based on process considerations and recycle efficiency. The user determined consumption rate is

considered by introducing in Eq. S18 a constant rate of consumption (ϕ_j^{SRC}) per mol of incoming flow (see SI-8). Finally, we note that the composition of the source must be specified, in principle a source can have as many components as required, for simplicity we have assumed that each source is made of a pure component [Eq. S19], and we have defined as many sources as necessary to include all necessary external inputs.

$$FK_{j,k} = \phi_j^{SRC} \sum_{j' \in [\mathbf{J}_i^{\mathbf{in}} - \mathbf{J}_i^{\mathbf{srcM}}]} F_{j'} - \sum_{r \in \mathbf{R}_i^{\mathbf{M}}} \gamma_{r,k} Fb_{r,i}, \forall \left(k \in \mathbf{K}_j^{\mathbf{SRC}} \wedge\ j \in \mathbf{J}_i^{\mathbf{srcM}} \wedge i \in \mathbf{I}^{\mathbf{MD}}\right) \quad (S18)$$

$$FK_{j,k} = 0, \forall \left(k \in \left(\mathbf{K} - \mathbf{K}_j^{\mathbf{SRC}}\right) \wedge\ j \in \mathbf{J}_i^{\mathbf{srcM}} \wedge i \in \mathbf{I}^{\mathbf{MD}}\right) \quad (S19)$$

The total capital investment and the operating costs associated with each active module are scaled based on the size of the incoming flow using Eqs. S20-S21. For the capital cost we use a power-law expression [Eq. S20][2]. For the operating cost we use a linear equation [Eq. S21] that contains three elements: a scale dependent term that accounts for the costs of catalyst, waste treatment, utilities, and overhead; a term that allows to calculate the cost of any independent source feed to the module; and a scale independent term that account for fixed costs, in particular the cost of labor. We note that although in reality the cost of labor changes with plant size, this change does not follow a continuous trend, our assumption is reasonable and convenient since it enforces the existence of economies of scale.

$$C_i^{CCE} = \theta_i^{CC} \left[\frac{\sum_{j' \in [\mathbf{J}_i^{\mathbf{in}} - \mathbf{J}_i^{\mathbf{srcM}}]} FM_j}{\theta_i^F}\right]^{\alpha}, \quad \forall \left(i \in \mathbf{I}^{\mathbf{MD}}\right) \quad (S20)$$

$$C_i^{OCE} = \theta_i^{OC} \left[\frac{\sum_{j' \in [\mathbf{J}_i^{\mathbf{in}} - \mathbf{J}_i^{\mathbf{srcM}}]} FM_j}{\theta_i^F}\right] + \sum_{j \in \mathbf{J}_i^{\mathbf{srcM}}} \theta_j^{SRC} FM_j + \theta^{FX} YM_i, \qquad \forall \left(i \in \mathbf{I}^{\mathbf{MD}}\right) \quad (S21)$$

Outlet splitter from a technology

The outlet splitter from a technology is modelled by means of a linear relation written in terms of a partition coefficient $\eta_{j,j',k}$ [Eq. S22]. This partition coefficient is defined as the fraction of compound $k \in \mathbf{K}$ that is directed from stream $j \in \mathbf{J}_i^{\mathbf{in}}$ to stream $j' \in \mathbf{J}_i^{\mathbf{out}}$. The set $\mathbf{J}_i^{\mathbf{out}}$ contains all the possible product streams for technology $i \in \mathbf{I}^{\mathbf{TCH}}$. Hence, the coefficient $\eta_{j,j',k}$ carries all the information related to the separation processes in a module. Similar to the yield, the partition coefficient can be calculated *a-priori* from detailed process simulations. It must be highlighted though, that the set of components present in the superstructure may be larger than the set of components used in the simulations used to calculate the partition coefficient. This implies that in the superstructure optimization process we force the module to operate under slightly different conditions than those used for its design. That is, it is possible that the incoming flow to a module contains species that were not present in the original design. To deal with species not originally present in the simulation we have used two strategies: First, we have pre-assigned a partition coefficient to these species such that they are sent completely toward a product stream in accordance with their boiling point. Second, we have limited the amount of these species in a module to be less than 15% by introducing a constraint at the technology group level [Eq. S23]. This constraint ensures that the majority of chemical compounds in a module were considered in its original design.

$$FK_{j,k} = \sum_{j' \in \mathbf{J}_i^{\mathbf{out}}} \eta_{j,j',k} FK_{j,k}, \left(k \in \mathbf{K} \wedge\ j \in \mathbf{J}_i^{\mathbf{in}}\ \wedge i \in \mathbf{I}^{\mathbf{TCH}}\right) \quad (S22)$$

$$\sum_{j \in \mathbf{J}_i^{\mathbf{in}}} \sum_{k \in \mathbf{K}_i^{\mathbf{TG}}} FK_{j,k} \geq 0.85 \sum_{j \in \mathbf{J}_i^{\mathbf{in}}} F_j\,, i \in \mathbf{I}^{\mathbf{TG}} \quad (S23)$$

Technology block

A technology has three types of elements associated: an inlet splitter, an outlet splitter, and a set of module conversion units. These elements have been described previously. Thus, in this subsection we only introduce one constraint associated with the binary YT_i, this constraint [Eq. S24] sets to zero all the flows associated with the inlet and outlet splitters of the technology if $YT_i = 0$.

$$FK_{j,k} \leq \iota^{UB} YT_i, \forall \left(j \in \left(\mathbf{J_i^{in}} \vee \mathbf{J_i^{out}}\right), i \in (\mathbf{I_{i'}^{iSPT}} \vee \mathbf{I_{i'}^{oSPT}})\right) \quad (S24)$$

Technology group block

As in the case of a technology block, the elements of a technology group have already been described. However, we introduce binary variable YTG_i to indicate the existence of a technology group in the final solution. This binary is defined in Eqs. S26-S27, and it is used to inactivate all streams associated with inlet and outlet splitters in a technology group when the technology group is inactive [Eq. S28].

$$YTG_i \geq YT_{i'}, \forall\ (i' \in \mathbf{I_i^T} \wedge i \in \mathbf{I^{TG}}) \quad (S26)$$

$$YTG_i \leq \sum_{i' \in \mathbf{I_i^T}} YT_{i'}, \forall\ (i \in \mathbf{I^{TG}}) \quad (S27)$$

$$FK_{j,k} \leq \iota^{UB} YTG_i, \forall\ (k \in \mathbf{K} \wedge j \in (\mathbf{J_i^{in}} \vee \mathbf{J_i^{out}}) \wedge i \in (\mathbf{I_{i'}^{iSPTG}} \vee \mathbf{I_{i'}^{oSPTG}}) \quad \text{(S28)}$$

Output mixers

The outputs of the system are modelled using a set of mixers, whose inlet streams come from the active modules, and whose outlet streams constitute the different products, by-products and waste streams obtained from the process. These elements of the superstructure are modelled by using a component mass balance [Eq. S29]. Furthermore, we introduce a binary variable YF_j, equal to one if fuel product associated with stream j is produced. Using YF_j we define two inactivation constraints [Eqs. S30-S31]: the first one [Eq. S30] forces the flow of a fuel product to be zero if the binary associated with that product is zero; the second one [Eq. S31] establishes a lower bound on the amount of a specific fuel that is obtained; this lower bound rules out impractical solutions where a negligible amount fuel is produced.

$$\sum_{j \in \mathbf{J_i^{in}}} FK_{j,k} = \sum_{j \in \mathbf{J_i^{out}}} FK_{j,k}, \forall\ (k \in \mathbf{K} \wedge i \in \mathbf{I^{MX}}) \quad (S29)$$

$$FK_{j,k} \leq \iota^{UB} YF_j, j \in \mathbf{J^P} \quad (S30)$$

$$FM_j \geq \iota^{LB} YF_j, j \in \mathbf{J^P} \quad (S31)$$

Feedstock input

Ethanol can be feed to the superstructure with different degrees of purity. In fact, different ethanol sources with different grades can be used simultaneously as long as the total amount of ethanol processed remains equal to a constant [Eq. S32]. In principle this constant can adopt any value, to make our results comparable with most of the relevant literature we have assumed that this constant is equal to the amount of ethanol produced by the NREL lignocellulosic ethanol production plant (β^{NREL})[3]. Constraining the amount of ethanol processed ensures that even if the profit is negative a non-trivial solution is found. Every ethanol feed stream with a different grade constitutes a different source. As a general assumption we consider that ethanol streams available are constituted exclusively by ethanol and water. This assumption is enforced in Eqs. S33-S34. Eq. S33 forces every component different from ethanol and water to be zero in the ethanol feed streams. On the other hand, Eq. S34 establishes the amount of water on the feed stream based on its characteristics.

$$\beta^{NREL} = \sum_{i \in \mathbf{I}_{i'}^{\mathbf{iSPTG}}} \sum_{j \in \mathbf{J}_i^{\mathbf{in}}} FK_{j,k}, \ , i' = TG1, k = EtOH \quad (S32)$$

$$FK_{j,k} = 0, j \in \mathbf{J}_i^{\mathbf{in}} \wedge i \in \mathbf{I}_{i'}^{\mathbf{iSPTG}}, i' = TG1, k \neq (EtOH \wedge Water) \quad (S33)$$

$$FK_{j,k} = \phi_j^W F_j, j \in \mathbf{J}_i^{\mathbf{in}} \wedge i \in \mathbf{I}_{i'}^{\mathbf{iSPTG}}, i' = TG1, k = Water \quad (S34)$$

Fuel properties

The performance of a fuel is the result of the complex interaction among several physicochemical properties. The magnitude of these properties determines the fuel efficiency, safety, and emission profile[4]. Since different fuels are used in different engines then the more relevant properties as well as the optimal property ranges vary among fuel types. In this work we consider three fuels: gasoline, jet fuel and diesel. In all cases we impose constraints on viscosity [Eqs. S39-S40], density [Eqs. S41-S42], aromatic content [Eq. S43], olefin content [Eq. S44], trace components [Eq. S45], and characteristic distillation curve [Eqs. S46-S51][5–7]. Additionally, for gasoline and diesel we also impose constraints on Research Octane Number (RON) [Eqs. S37-S38], and Cetane Number (CN) [Eqs. S35-S36], respectively. The relation between fuel composition and properties is still an active area of research, and in many cases this relation is known to be non-linear *e.g.* the distillation profile of a fuel is a nonlinear function of the composition. However, the introduction of the strong non-linearities describing the relation between fuel composition and properties would render the problem intractable, especially if a global optimization approach is pursued. To mitigate this problem, we have used in this work mainly linear relations with respect to the composition, understanding that this is a necessary trade-off between tractability and accuracy. For cetane number [Eq. S35], research octane number [Eq. S37], and viscosity [Eq. S39], we have used linear mixing rules based on the mol fraction of constituents[8–10]; and for density [Eq. S41] we have used a mixing rule based on mass fraction applied to the specific volume as described by Marquard and coworkers[8,11]. Note that the equations displayed have been reformulated in terms of total and components flows since we have observed a higher speed of convergence with these forms. Among the properties required, the one that poses the biggest challenge is the distillation curve of a fuel. A distillation curve is a plot of temperature versus volume fraction of evaporated fuel. Thus, every point on the curve establishes the minimum temperature required to evaporate a specific fraction of the fuel. Constraints on the distillation curve of a fuel usually limit the minimum temperature at which a specific fraction of fuel is evaporated, or alternatively the fraction of fuel that must be evaporated when a certain temperature is reached. A compact notation to describe these constraints uses a mol fraction symbol with a sub-index to indicate the temperature involved in the constraint (*e.g.* $X_T \leq a$ can be interpreted as: at temperature *T* the fraction of fuel evaporated should be less than *a*). In this work we consider two constraints on the distillation curve of each fuel: for gasoline $X_{30} \leq 5\%$ and $X_{215} \geq 98\%$, for jet fuel $X_{160} \leq 5\%$ and $X_{300} \geq 98.5\%$, and for diesel fuel $X_{150} \leq 5\%$ and $X_{360} \geq 95\%$. The first of these constraints corresponds to the typical initial boiling point for the fuel; the second one is determined as the largest temperature regulated by the ASTM standard[5–7]. Note that by constraining these two points we give the optimizer enough flexibility in terms of possible distillation curves, while ensuring that the boiling range of is within typical standards. In general, modelling the distillation curve requires the introduction of a thermodynamic model for the estimation of activity coefficients, and the solution of a system of differential equations, this procedure is computationally expensive[8]. As an approximation we use two simplifying assumptions introduced by Koeing and coworkers[11]: first, instead of using volume fraction we use mol fraction; and second, we use the concept of true boiling point to estimate the shape of the distillation curve. In the true boiling point approximation, it is assumed that the distillation temperature is dominated by the species

with the lowest boiling point present in the mixture. In other words, the distillation curve can be approximated as a step function. Mathematically, this has been modelled by introducing a set of binaries used to find the lowest boiler among the present species. Although this approach has been successful we have decided to use an even simpler representation: in our approach we have predefined six sub-sets of components ($\mathbf{K^{BP30}}$, $\mathbf{K^{BP150}}$, $\mathbf{K^{BP160}}$, $\mathbf{K^{BP225}}$, $\mathbf{K^{BP300}}$, $\mathbf{K^{BP360}}$) each of these sets contains all the chemical species in the system with a boiling point lower than the value presented in the super-index of the set (*e.g.* $\mathbf{K^{BP30}}$ contains all the species with a boiling point lower than 30°C), these sets are conveniently designed based on the required distillation temperature constraints of the studied fuels. By introducing these sets it is possible to formulate all constraints on the distillation curve as a linear function without introducing additional binary variables [Eqs. S46-S51].

$$F_j CN_j = \sum_{k \in \mathbf{K}} \lambda_k^{CN} FK_{j,k}, j \in \mathbf{J^P} \quad (S35)$$

$$CN_j \geq \phi_j^{CN}, j \in \mathbf{J^P} \quad (S36)$$

$$F_j RON_j = \sum_{k \in \mathbf{K}} \lambda_k^{RON} FK_{j,k}, j \in \mathbf{J^P} \quad (S37)$$

$$RON_j \geq \phi_j^{RON}, j \in \mathbf{J^P} \quad (S38)$$

$$F_j V_j = \sum_{k \in \mathbf{K}} \lambda_k^{\mu} FK_{j,k}, j \in \mathbf{J^P} \quad (S39)$$

$$\phi_j^{\mu min} \leq V_j \leq \phi_j^{\mu max}, j \in \mathbf{J^P} \quad (S40)$$

$$FM_j = D_j \sum_{k \in \mathbf{K}} \frac{\lambda_k^{MW}}{\lambda_k^{\rho}} FK_{j,k}, j \in \mathbf{J^P} \quad (S41)$$

$$D_j \leq \phi_j^{\rho}, j \in \mathbf{J^P} \quad (S42)$$

$$\sum_{k \in \mathbf{K^{AR}}} \lambda_k^{MW} FK_{j,k} \leq \phi_j^{AR} FM_j, j \in \mathbf{J^P} \quad (S43)$$

$$\sum_{k \in \mathbf{K^{OF}}} \lambda_k^{MW} FK_{j,k} \leq \phi_j^{OF} FM_j, j \in \mathbf{J^P} \quad (S44)$$

$$\lambda_k^{MW} FK_{j,k} \leq 0.01 FM_j, k \in \mathbf{K^{NF}} \wedge j \in \mathbf{J^P} \quad (S45)$$

$$\sum_{k \in \mathbf{K^{BP30}}} FK_{j,k} \leq \phi_j^{G30} F_j, j = gasoline \quad (S46)$$

$$\sum_{k \in \mathbf{K^{BP225}}} FK_{j,k} \geq \phi_j^{G225} F_j, j = gasoline \quad (S47)$$

$$\sum_{k \in \mathbf{K^{BP160}}} FK_{j,k} \leq \phi_j^{JF160} F_j, j = Jet\ Fuel \quad (S48)$$

$$\sum_{k \in \mathbf{K^{BP300}}} FK_{j,k} \geq \phi_j^{JF300} F_j, j = Jet\ Fuel \quad (S49)$$

$$\sum_{k \in \mathbf{K^{BP150}}} FK_{j,k} \geq \phi_j^{D150} F_j, j = Diesel \quad (S50)$$

$$\sum_{k \in \mathbf{K^{BP360}}} FK_{j,k} \geq \phi_j^{D360} F_j, j = Diesel \quad (S51)$$

S2. Summary of technology groups technologies and modules used in the superstructure

In table S2-1 we show the different technology groups, technologies and modules considered in this work. Additionally, we show the catalyst and reactions associated with each module. We also include a list of the different products that can be obtained from a technology group. We label these products based on the composition of these streams. These labels are assigned considering two criteria: first, the dominant functional groups present in the stream, *i.e.* olefins, alcohols, ethers, etc.; and second, the carbon number distribution of the species in the stream. There are also two streams labeled as Burn and waste; the first one is used to generate electricity and contains mixtures of chemical species usually of low molecular weight; the second one contains waste streams, either waste water or gaseous streams like CO_2. We note that sometimes a catalyst can be assigned to more than one module. Differences among modules associated with the same catalyst arise due to three main reasons. First, in some instances, we have modules synthesized using the same catalyst for the transformation of different feedstocks (*e.g.* dehydration processes based on ethanol feedstocks with 50%, 83%, and 100% ethanol by mol have been included). Second, the separation processes selected may be different between two processes, either because they use a different set of separation technologies or because yield a different set of products. Finally, in some instances, we have included processes that use the same catalyst but employ a different set of operating conditions.

Table S2-1. Brief summary of the different technology groups used in this study (column 1), as well as the technologies associated with each technology group (column 2). Additionally, we present the catalysts selected for the realization of each chemistry, the modules that were designed employing each catalyst, and the reactions associated with these modules (column 3). Finally, we show the possible products from each technology group (column 4). Note that the substrate for which a technology group is designed is indicated in parenthesis in column 1.

Technology group (Substrates)	Technologies	Processes			Outputs
		Catalyst	Modules	Reactions	
TG1 (Ethanol)	Dehydration (T1)	Syndol	M1	R1	1.Ethylene 2.Burn 3. Waste 4. Olefin (C4-C12) 5. Olefin (C4-C3) 6. Olefin (C3) 7. CO2 8. Olefin (C2-C4-H2) 9. Alcohol (C4+) 10. Alcohol (C6+) 11. Alcohol (C8+) 12. Alcohol (C6OH) 13. Alcohol (C4OH)
		MCM-41	M2-M4	R2	
		LA-PHZSM	M5-M7	R3	
	DH + Condensation (T2)	Vertimas®	M8	R4	
		P-HZSM	M9	R8	
			M10	R9	
	Condensation (T3)	$ZnZrO_2$	M11	R5	
		In_2O_3-Zβ	M12	R6	
		$LaZrO_2$	M13	R7	
	Guerbet coupling (T4)	Ni-La_2O_3-γ-Al_2O_3	M14-M15	R10	
		Ni(8%)-γ-Al_2O_3	M16-M17	R11	
			M18-M20,	R12	
		Ca-HAP	M25-M27	R15	
			M28-M29	R16	
		Pa-Hydrotalcite	M21-M22	R13	
		Pd-MgO	M23-M24	R14	
TG2 (Ethylene)	Oligomerization (T5)	Ni-LASA	M30-M32	R18	1.Waste 2. Burn 3. Olefin (C3) 4. Olefin (C3+) 5. Olefin (C4) 6. Olefin (C6) 7. Olefin (C8+) 8. Olefin (C4+) 9. Olefin (C5+)
		HZSM-5	M33-M35	R19	
		Alphabutol™	M36	R20	
		Alphaselect™	M37	R21	
		NiSAIB	M38-M40	R22	
		Ni-AISBA	M41-M43	R23	
		Chevron-Philips™	M44-M46	R24	
TG3	Oligomerization (T6)	Ni-HZSM-5	M47-M48	R25	1.Olefin (C6)

(Propylene)		Pell-SAPO-11 HZSM-23 SO_3-10%-NiO-γ-Al_2O_2	M49-M50 M51-M52 M53-M54	R26 R27 R28	2. Olefin (C6+) 3. Olefin (C8+)
TG4(Isobutene)	Oligomerization (T7)	H-Zeolite-Y-P Sulfated titania	M55 M56	R29 R30	1.Olefin (C6) 2. Olefin (C8+)
TG5 (Isobutene+Propene)	Oligomerization (T8)	SPA CT275 MTW-10%P-H_3PO_4	M57-M58 M59-M60 M61-M62	R31 R32 R33	1.Olefin (C6) 2. Olefin (C6+) 3. Olefin (C8+) 4. Olefin (C12+)
TG6 (Butene)	Oligomerization (T9)	ATHZ5-Cs HZSM-57 2A-Co-C-230 ASA-13 HZSM5	M63-M64 M65-M66 M67 M68 M69	R34 R35 R36 R37 R38	1.Burn 2. Olefin (C6) 3. Olefin (C6+) 4. Olefin (C8+) 5. Olefin (C12+)
TG7 (Hexene)	Oligomerization (T10)	SO4/ZrO2	M70	R39	1.Olefin (C12+)
TG8 (Octene)	Oligomerization (T11)	ASA HZSM-5	M71 M72	R40 R41	1.Olefin (C12+)
TG9 (Olefins C3-C8)	Oligomerization (T12)	ATHZ5-Cs	M73	R42-R47	1.Olefin (C12+)
TG10 (Butanol)	Dehydration (T13)	AM-11	M74	R48	2. Ether 3. Olefin (C4) 4. Waste 5. Burn 6. Olefin (C8+) 7. Alcohol (C8+)
	Etherification (T14)	Amberlyst-70	M75	R49	
	Guerbet coupling (T15)	Ca-HAP	M76	R50	
TG11 (Hexanol)	Dehydration (T16)	Syndol	M77	R51-R52	1.Ether 2. Olefin (C6) 3. Waste 4. Burn 5. Olefin (C8+) 6. Alcohol (C8+)
	Etherification (T17)	Amberlyst-70	M78	R53	
	Guerbet coupling (T18)	Ca-HAP	M79	R54	
TG12 (Octanol)	Dehydration (T19)	Syndol	M80	R55-R56	1.Ether 2. Olefin (C8) 3. Waste 4. Burn 5. Olefin (C8+) 6. Alcohol (C8+)
	Etherification (T20)	Amberlyst-70	M81	R57	
	Guerbet coupling (T21)	Ca-HAP	M82	R58	
TG13 (Mixed alcohols)	Dehydration (T22)	Syndol	M83-M84	R59-R72	1.Ether 2. Olefin (C4) 3. Olefin (C6) 4. Olefin (C4+) 5. Olefin (C8) 6. Olefin (C8+) 7. Waste 8. Burn 9. Mixed oxygenates
	Etherification (T23)	Amberlyst-70	M85	R73-R85	
	Guerbet coupling (T24)	Ca-HAP	M86	R86-R88	
TG14 (Olefins C2-C30)	Hydrogenation (T25)	CoMo	M87	R89-R113	1.Paraffins (C1-C3) 2. Paraffins (C4-C8) 3. Paraffins (C8-C10) 4. Paraffins (C11-C12) 5. Paraffins (C13-C16) 6. Paraffins (C17-C20) 7. Paraffins (C20+)

S3. Superstructure connectivity

In table S3-1 we present the connectivity matrix. The first column contains all technology groups (1-14), and feedstock sources (S1-S3); the second column shows the technology group outputs; finally, the first row shows all the possible destinations, *i.e.* technology group inputs, and superstructure products. Productive connections between an element in column two and an element in row one are marked as "1". Productive connections between technology groups can be identified by checking if the identity of an outlet stream (Column 4 Table S2-1) overlaps with the substrate associated with inlet stream to a technology group (Column 1 Table S2-1).

Table S3-1. Connectivity matrix for superstructure elements.

		1.1	1.2	1.3	2	3	4	5	6	7	8	9	10	11	12	13	14	G	JF	D	E	W
1	1				1																1	
	2																				1	
	3																					1
	4																1	1	1	1	1	
	5						1	1				1					1	1	1	1	1	

	6					1						1									1	
	7																					1
	8				1				1			1					1				1	
	9															1		1	1	1	1	
	10															1		1	1	1	1	
	11														1	1		1	1	1	1	
	12													1		1		1	1	1	1	
	13												1			1		1	1	1	1	
2	1																					1
	2																				1	
	3					1						1					1				1	
	4											1					1	1	1	1	1	
	5								1			1					1	1			1	
	6									1		1					1	1	1	1	1	
	7										1	1					1	1	1	1	1	
	8											1					1	1	1	1	1	
	9											1					1	1	1	1	1	
3	1									1		1					1	1	1	1	1	
	2											1					1	1	1	1	1	
	3										1	1					1	1	1	1	1	
4	1									1		1					1	1	1	1	1	
	2										1	1					1	1	1	1	1	
5	1									1		1					1	1	1	1	1	
	2											1					1	1	1	1	1	
	3										1	1					1	1	1	1	1	
	4																1	1	1	1	1	
6	1																				1	
	2									1		1					1	1	1	1	1	
	3											1					1	1	1	1	1	
	4										1	1					1	1	1	1	1	
	5																1	1	1	1	1	
7	1																1	1	1	1	1	
8	1																1	1	1	1	1	
9	1																1	1	1	1	1	
10	1																	1	1	1	1	
	2								1			1					1	1			1	
	3																					1
	4																				1	
	5										1	1					1	1	1	1	1	
	6														1	1		1	1	1	1	
11	1																	1	1	1	1	
	2									1		1					1	1	1	1	1	
	3																					1
	4																				1	
	5										1	1					1	1	1	1	1	
	6														1	1		1	1	1	1	
12	1																	1	1	1	1	
	2										1	1					1	1	1	1	1	
	3																					1
	4																				1	
	5										1	1					1	1	1	1	1	
	6															1		1	1	1	1	
13	1																	1	1	1	1	
	2								1			1					1	1			1	
	3									1		1					1	1	1	1	1	
	4											1					1	1	1	1	1	
	5										1	1					1	1	1	1	1	
	6										1	1					1	1	1	1	1	
	7																					1
	8																				1	
	9																1	1	1	1	1	
14	1																				1	
	2																	1			1	
	3																	1	1		1	
	4																	1	1	1	1	
	5																		1	1	1	
	6																			1	1	
	7																				1	
S1	1	1																				
S2	2		1																			
S3	3			1																		

S4. List of chemical species considered and their properties

In table S4-1 we present all chemical species involved in the reactions considered in this work, as well their chemical properties used. In the table chemical names of carbon containing molecules have two parts: one alphabetic indicating the functional group, and one numerical indicating the number of carbons. We consider the following functional groups: alcohols (A), aldehydes (Al), ketones (K), esters (Es), olefins (O), aromatics (Ar), and ethers (E). Importantly, details on the chemical identity of aromatic species involved in the studied reactions are often not revealed, the species included in the table are meant to be representative of a complex group, and should be interpreted in this light. Other minor molecules present in the production process are included at the end of the table and are labeled using their chemical name; they include water (H_2O), hydrogen (H_2), carbon monoxide (CO_2), carbon dioxide (CO), triethylaluminum ($C_6H_{15}Al$), sodium hydroxide (NaOH), sodium aluminate ($Na_2Al_2O_4$), and nitrogen (N_2). Properties included in the table are required for the estimation of bulk fuel properties and include: molecular weight (λ_k^{MW}), low heating value (λ_k^{LHV}), cetane number (λ_k^{CN}), research octane number (λ_k^{RON}), normal boiling point (λ_k^{TB}), density (λ_k^{ρ}), and viscosity (λ_k^{μ}). Values for these properties are extracted from the Aspen plus® database (λ_k^{MW}, λ_k^{LHV}, λ_k^{TB}, λ_k^{ρ}, and λ_k^{μ}), or from the open literature (λ_k^{CN}, and λ_k^{RON})[12–18]. In some instances, especially for the estimation of RON, data for some molecules were not available. In this study we did not implement a QSPR approach, but rather we performed an informed guess based on the value of that property of a similar molecule; usually this guess is a pessimistic one. Property values for which an exact estimation was not available are indicated in red. Finally, the last column of the table is a binary parameter, equal to 1 if that molecule is not a trace element of a fuel.

Table S4.1 List of molecules considered in this study and their relevant physical properties.

Species	Code	λ_k^{MW} [Kg/mol]	λ_k^{LHV} [J/mol]	λ_k^{μ} [Pa-s]	λ_k^{CN} [-]	λ_k^{RON} [-]	λ_k^{TB} [°C]	λ_k^{ρ} [kg/m³]	Fuel [-]
A2	Ethanol	0.046	1212214.382	0.000895	12	109	78.290	777	1
A4	Butanol	0.074	2413246.391	0.001997	17	98	118.750	796	1
A6	1-Hexanol	0.102	3614020.296	0.003363	23	69	156.750	809	1
A6_2	2-Ethyl-1-Butanol	0.102	3614682.057	0.003525	17	93	147.000	822	1
A8	1-Octanol	0.130	4816589.467	0.005222	39	58	193.950	818	1
A8_2	2-Ethyl-hexanol	0.130	4816589.467	0.004305	24	83	184.450	822	1
A12_2	2-Butyl-1-Octanol	0.186	7218210.128	0.010763	64	0	263.950	819	1
A16	1-Hexadecanol	0.242	9626596.196	0.019825	68	0	324.850	825	1
AL2	Acetaldehyde	0.044	1081154.530	0.000198	0	111	21.000	761	1
AL4	Butyraldehyde	0.072	2264681.096	0.000368	41	117	74.790	787	1
AL6	1-Hexanal	0.100	3466910.161	0.000641	75	0	128.000	809	1
AL8	1-Octanal	0.128	4668511.981	0.001025	109	0	172.000	811	1
AL8_2	2-Ethyl-hexanal	0.128	4668511.981	0.000854	109	0	172.000	807	1
AL12	1-Dodecanal	0.184	7068281.615	0.002416	109	0	248.850	849	1
AL16	Hexadecyl-Aldehyde	0.240	9462089.121	0.003557	109	0	320.613	933	1
K3	Acetone	0.058	1631365.359	0.000280	0	110	56.290	775	1
K5	Methyl-Propyl-Ketone	0.100	3435798.519	0.000422	10	107	117.400	793	1
ES4	Ethyl-Acetate	0.088	2024145.120	0.000386	17.4	116	77.060	882	1
E4	Diethyl-ether	0.074	2462589.629	0.000204	150	0	34.430	696	1
E8	Butyl-ether	0.130	4867767.152	0.000601	115	0	141.000	756	1
E10	Di-pentyl-ether	0.158	6073735.620	0.000836	111	0	459.900	772	1
E12	Di-hexyl-ether	0.186	7268582.523	0.002051	117	0	225.700	782	1
E16	Di-Octyl-ether	0.242	9671022.917	0.004229	118	0	286.500	796	1
E24	Di-dodecyl-ether	0.355	14502218.581	0.007266	118	0	421.447	1009	1
O2	Ethylene	0.028	1304664.528	0.000039	13	97	-103.74	213	0
O3	Propylene	0.042	1898461.792	0.000071	11	102	-47.700	487	1
OI4	Isobutene	0.056	2487209.060	0.000166	17.0	92.9	-6.900	575	1
O4	1-Butene	0.056	2487209.060	0.000143	17.0	98.8	-6.240	574	1
O5	1-Pentene	0.070	3083385.657	0.000198	20	88	30.070	625	1
O6	1-Hexene	0.084	3683507.753	0.000244	27	76	63.480	660	1
O7	1-Heptene	0.098	4284021.390	0.000307	32	55	93.640	686	1
O8	1-Octene	0.112	4886192.882	0.000427	41	29	121.260	705	1
O9	1-Nonene	0.126	5486965.732	0.000522	51	11	146.868	718	1
O10	1-Decene	0.140	6087351.847	0.000668	49	18	170.600	731	1

O11	1-Undecene	0.154	6688685.854	0.000852	65	0	192.670	740	1
O12	1-Dodecene	0.168	7289007.074	0.001096	57	0	213.000	748	1
O13	1-Tridecene	0.182	7889965.943	0.001307	57	0	232.840	755	1
O14	1-Tetradecene	0.196	8489663.120	0.001577	83	0	251.100	762	1
O15	1-Pentadecene	0.210	9089226.194	0.001896	76	0	268.460	766	1
O16	1-Hexadecene	0.224	9689165.410	0.002291	76	0	284.870	772	1
O18	1-Octadecene	0.252	10892896.662	0.003097	90	0	314.820	776	1
O20	1-Eicosene	0.281	12094350.210	0.004179	90	0	342.390	784	1
O21	1-Heneicosene	0.295	12675796.498	0.005861	90	0	379.424	980	1
O24	1-Tetracosene	0.337	14504211.037	0.008542	90	0	390.000	796	1
DO4	1,2-Butadiene	0.054	2375976.427	0.000155	0	103	-4.410	633	1
DO6	1,2-Hexadiene	0.082	3559936.775	0.000225	18	71	76.000	703	1
DO8	2,4-Octadiene	0.110	4773249.137	0.000417	24	82	117.061	735	1
DO12	1,3-Dodecadiene	0.166	7177590.925	0.001183	57	0	210.883	770	1
DO16	2,4-Hexadecadiene	0.222	9579302.229	0.002511	76	0	283.197	791	1
P1	Methane	0.016	789129.898	0.000002	0	127	-161.49	162	0
P2	Ethane	0.030	1405907.163	0.000030	-20	111	-88.600	231	0
P3	Propane	0.044	2011124.427	0.000086	-20	111	-42.040	474	1
P4	Butane	0.058	2606891.694	0.000145	21	94	-0.500	561	1
P5	Pentane	0.072	3194792.817	0.000205	30	62	36.070	612	1
P6	Hexane	0.086	3795546.856	0.000269	45	19	68.730	647	1
P7	Heptane	0.100	4395844.412	0.000353	56	0	98.430	673	1
P8	Octane	0.114	4995955.957	0.000454	58	0	125.680	694	1
P9	Nonanane	0.128	5597008.192	0.000582	61	0	150.820	709	1
P10	Decane	0.142	6197523.847	0.000739	66	0	174.155	720	1
P11	Undecane	0.156	6797068.080	0.000932	79	0	195.928	730	1
P12	Dodecane	0.170	7398125.465	0.001147	73	0	216.323	739	1
P13	Tridecane	0.184	7998347.332	0.001402	88	0	235.466	744	1
P14	Tetradecane	0.198	8598998.178	0.001718	95	0	253.577	752	1
P15	Pentadecane	0.212	9199503.785	0.002101	98	0	270.685	757	1
P16	Hexadecane	0.226	9799615.958	0.002506	100	0	286.864	763	1
P18	Octadecane	0.255	11001930.856	0.003391	110	0	316.710	770	1
P20	Eicosane	0.283	12205373.846	0.004371	112	0	343.780	772	1
P21	Heneicosane	0.297	12805977.298	0.004619	83	0	356.500	780	1
P24	Tetracosane	0.339	14607870.092	0.007045	88	0	391.300	787	1
AR6	Phenol	0.078	3092754.343	0.000545	14	98	80.090	797	1
AR7	Toluene	0.092	3676479.426	0.000962	-1	116	110.630	813	1
AR8	Etylbenzene	0.106	4271558.793	0.001365	-4	116	138.360	837	1
AR10	Naphthalene	0.128	4932923.348	0.001619	22	86	217.993	1013	1
Ar11	1-Methylnaphthalene	0.142	5520701.878	0.005094	0	105	244.683	901	1
Ar12	Biphenyl	0.156	6120161.831	0.007213	-7	105	258.330	861	1
H2	Hydrogen	0.00201588	241722	0.000000	0	0	-252.76	31	0
CO	Carbon Monoxide	0.0280104	282794	0.000023	0	0	-191.45	295	0
CO2	Carbon Dioxide	0.0440098	0	0.000050	0	0	-78.45	511	0
W	Water	0.0180153	0	0.000740	0	0	100	991	0
TEA	TEA	0.228	0	-	0	0		882	0
NaOH	Sodium hydroxide	0.0399999	0	-	0	0		2113	0
NaAl2O2	Sodium aluminate	0.10895165	0	-	0	0		613	0
N2	Nitrogen	0.028	0	-	0	0		314	0

S5. A survey of catalyst available for the different chemistries involved in the superstructure

As it is mentioned in the main text, we group together catalysts with similar performance and optimal operating conditions on the basis of five criteria relevant for process design: *optimal operation temperature*, *optimal operation pressure*, *single pass conversion*, *product distribution*, and *catalysis phase*. The *optimal catalyst temperature* is strongly coupled with the reactor and utilities needed. Based on this criterion we consider two different kinds of catalyst: those that operate above the threshold temperature of 280°C, and those that operate below it. This threshold is selected considering than above 280°C it is common to use furnaces in endothermic reactions, and to implement heat recovery strategies based on direct steam generation in exothermic reactions. In contrast, if the required temperature is below 280°C a reactor designed as a heat exchanger usually suffices. The *optimal operation pressure* controls the need for compression units, which is especially important in gas phase systems where capital-intensive compressors are required. We consider two kinds of catalyst based on the optimal operating pressure: Catalyst that can operate at atmospheric pressure, and as such have minimal compression requirements;

and catalyst that operate above atmospheric pressures and therefore have compression needs. The *single pass conversion* obtained from a catalyst, determines the amount of catalyst needed, the size of the recycle streams, and to a certain extent the sequence of separation operations employed. At high conversion the recycle stream is small or non-existing and the separations units required to recover the feedstock are small as well. On the contrary, at low conversion both recycle streams and the operation units required to produce them are large. To capture these effects, we classify catalyst based on their single pass conversion into three levels: high conversion ($X \geq 70$), medium conversion ($40 < X \leq 70$), and low conversion ($X \leq 40$). A fourth factor used to classify the catalysts available is the *product distribution*, catalyst differ from each other based on the selectivity toward particular products, or groups of products. For each studied chemistry we have identified a set of products of interest and sorted the catalyst based on the selectivity toward these products. We note that in general the selectivity toward the products of interest has a direct impact on the overall yield of the process, and the selected separation train. Finally, we use the *catalysis phase* as a clustering criterion. In general, and in accordance with the principles of green engineering we have placed a heavy emphasis on heterogenous catalyst, since they usually lead to processes yielding less waste, and result in simpler flowsheets in which catalyst recycle is not necessary[19]. For completeness however, we have included a few homogenous processes, especially for ethylene oligomerization, where this kind of approach has been commercially studied.

In what follows we present a survey of the different catalyst available for each chemistry and we discuss in detail the clustering procedure followed in each case. The different clusters associated with each chemistry are shown using different colors in the tables. Representative catalysts of each cluster selected for process synthesis in this work are highlighted in bold blue characters. For each catalyst we show details on the following conditions: optimal temperature, optimal pressure, contact time or a related variable (WHSV, GHSV or LHSV), single pass conversion, and carbon selectivity toward major products. For compactness we will use in the same notation for chemical species described in S4.

S5.1 Alcohol dehydration

The dehydration of ethanol (Technology 1, in Technology group 1) for the production of ethylene is a widely studied chemistry[20–22]. The main product is ethylene, and a stochiometric amount of waste water is produced. Common by-products include diethyl ether, low molecular weight olefins, as well as carbon dioxide and monoxide. For this chemistry numerous catalysts have been developed; and significant advances in terms of stability, conversion, and selectivity have been obtained[21,23]. This technology has been gaining attention in recent years. The possibility of producing plastics with a reduced carbon footprint, coupled with the availability of ethanol in countries like Brazil have contributed to the momentum gained by this technology. An example of the maturity reached is the Braskem plant in Triunfo, Brazil with production capacity nearing 200.000 Ton/year[21]. In this work we have clustered catalyst available for ethanol dehydration into three groups: The first group (light blue), consists of catalyst that operate at high temperature ($T > 280°C$), operate at pressure above 1 atm, and in terms of selectivity produce a complex blend of products, dominated by ethylene but with minor amounts of other elements including CO_2 and CO, these elemental traces of carbon oxides are important because they may act as catalyst poisons, thus imposing the need to design complex separation trains, able to remove these compounds. In this group we have only one catalyst, SYNDOL®, which is commercial, low cost and has

been tested at industrial scale for several years[20,24]. The second group (light yellow) is constituted by catalysts that operate at high temperatures $T > 280°C$, in contrast with the first group, they do not require pressurization, and more importantly, their product distribution does not include CO_2 and CO, likely simplifying the separation needs associated with the process. Among the available options we have selected MCM-41[25], a catalyst that simultaneously displays total conversion and 100% selectivity toward ethylene, thus ensuring that the required separation train is the simplest possible. Finally, in the third group (light green), we find catalysts that operate at low temperature ($T \leq 280°C$), require compression, and yield product distribution similar to those described for the second group. We have selected 0.5%La-2%-P-HZSM-5 as representative of this group[26], provided that it offers desirable conversion and selectivity characteristics, both near 100%, while operating at the lowest temperature for the catalyst in the group.

Table S5.1. Catalyst for ethanol dehydration to ethylene

	T	P	Contact			X	Carbon selectivity										
			WHSV	LHSV	GHSV		P2	O2	O3	O4	O5+	DO4	Al2	E4	CO2	CO	Ref
	°C	Atm	h^{-1}	h^{-1}	h^{-1}	%											
SYNDOL	**425**	**5**	**1**	**-**	**-**	**0.27**	**98.80**	**0.06**	**0.00**	**0.00**	**0.50**	**0.20**	**0.05**	**0.07**	**0.32**	**0.27**	20
SAPO34	450	1	-	3	-	0.00	100.00	0.00	0.00	0.00	0.00	0.00	0.00	0.00	0.00	0.00	27
Al_2O_2	440	1	-	52	-	0.00	91.00	0.00	0.00	0.00	0.00	1.00	8.00	0.00	0.00	0.00	28
10%Ti/g-Al_2O_2	400	1	18	-	-	0.19	99.50	0.24	0.04	0.00	0.00	0.00	0.00	0.00	0.00	0.19	
7.4P-ZSM-5	400	1	3	-	-	0.00	99.40	0.00	0.29	0.00	0.00	0.00	0.30	0.00	0.00	0.00	29
H-ZSM-5 st.	360	1	1	-	-	0.00	99.00	0.00	1.00	0.00	0.00	0.00	0.00	0.00	0.00	0.00	30
$LaPO_4$-M1	350	1	-	-	600	0.00	100.00	0.00	0.00	0.00	0.00	0.00	0.00	0.00	0.00	0.00	31
MCM-41	**350**	**1**	**-**	**3**	**-**	**0.00**	**100.00**	**0.00**	**0.00**	**0.00**	**0.00**	**0.00**	**0.00**	**0.00**	**0.00**	**0.00**	25
NiAPSO-34	350	1	-	3	-	0.00	98.30	0.00	0.00	0.00	0.00	0.30	1.10	0.00	0.00	0.00	28
SAPO-34	325	1	1	-	-	0.00	94.30	0.00	0.00	0.00	0.00	0.30	5.30	0.00	0.00	0.00	28
H-ZSM-5 st	325	1	1	-	-	0.00	97.77	0.00	0.00	0.23	0.00	0.00	0.00	0.00	0.00	0.00	32
H-ZSM-5 abs	**300**	**1**	**139**	**-**	**-**	0.00	99.78	0.00	0.00	0.22	0.00	0.00	0.00	0.00	0.00	0.00	32
H-ZSM-5	300	1	-	3	-	0.00	100.00	0.00	0.00	0.00	0.00	0.00	0.00	0.00	0.00	0.00	33
HZSM5	300	1	3	-	-	0.00	98.50	0.00	0.00	0.00	0.00	0.50	0.50	0.00	0.00	0.00	28
TPA-MCM-41	270	1	3	-	-	0.00	100.00	0.00	0.00	0.00	0.00	0.00	0.00	0.00	0.00	0.00	34
STA-MC-41-c	260	1	2	-	-	0.00	100.00	0.00	0.00	0.00	0.00	0.00	0.00	0.00	0.00	0.00	35
2%PHZSM5	250	1	3	-	-	0.00	97.40	0.00	0.00	2.60	0.00	0.00	0.00	0.00	0.00	0.00	26
STA-MCM-41	240	1	2	-	-	0.00	99.90	0.00	0.00	0.00	0.00	0.00	0.10	0.00	0.00	0.00	35
0.5%La-2%P-HZSM-5	**240**	**1**	**2**	**-**	**-**	**0.00**	**99.90**	**0.00**	**0.00**	**0.10**	**0.00**	**0.00**	**0.00**	**0.00**	**0.00**	**0.00**	26

The chemistry of higher alcohol dehydration, is similar to that described for ethanol; that is, the main product is an olefin, water is produced as main waste, and the byproduct chemistry is similar, been the only difference the amount of carbons of the resulting products[31,36–40]. However, industrial processes have not been developed to the point of current ethanol dehydration plants. In this work we are concerned with the dehydration reaction of four higher alcohol substrates: butanol (Technology 13, part of Technology group 10), hexanol (Technology 16, part of Technology group 11), octanol (Technology 19, part of Technology group 12), and a general mixture containing alcohols with 4 to 12 carbons (Technology 22, part of Technology group 13). As it is seen in Table S5.2 we have less data for these reactions, such that only one cluster is defined for each of these substrates. In the case of butanol, the only substrate for which there are data for more than one catalyst, we have selected AM-11[36], due to its high selectivity toward the olefin main product (butene). For all the other technologies we have use data on the available catalyst[39], Syndol®. Importantly, the results for the mixed alcohol catalyst have been assumed, and do not correspond to any experimental work, but rather represent the optimistic limit of an ideal catalyst developed for this task.

Table S5.2 Catalysts for higher alcohol dehydration

Feed		Catalyst	T	P	Contact WHSV	X	Carbon selectivity												Ref.
			°C	Atm	h^{-1}	%	C4	C5	C6	C7	C8	C9	C10	C11	C12	E4	E6	E8	
Butanol		AM-11	250	1	2	100	100	0	0	0	0	0	0	0	0	0	0	0	[36]
		S/ZrO_2	200	1	32.2	59.8	94.5	0	0	0	0	0	0	0	0	5.5	0	0	[37]
		$LaPO_4$-M1	320	1	2.83	100	100	0	0	0	0	0	0	0	0	0	0	0	[31]
Hexanol		Syndol	350	1	2.65	94	0	0	95	0	0	0	0	0	0	0	2.8	0	[39]
Octanol		Syndol	350	1	3.39	97	0	0	0	0	97	0	0	0	0	0	0	2.2	[39]
Mixed Alcohols	A4	Hypothetical*	250	1	2	100	100	0	0	0	0	0	0	0	0	0	0	0	-
	A5					100	0	100	0	0	0	0	0	0	0	0	0	0	
	A6					100	0	0	100	0	0	0	0	0	0	0	0	0	
	A7					100	0	0	0	100	0	0	0	0	0	0	0	0	
	A8					100	0	0	0	0	100	0	0	0	0	0	0	0	
	A9					100	0	0	0	0	0	100	0	0	0	0	0	0	
	A10					100	0	0	0	0	0	0	100	0	0	0	0	0	
	A11					100	0	0	0	0	0	0	0	100	0	0	0	0	
	A12					100	0	0	0	0	0	0	0	0	100	0	0	0	

***The cost of this catalyst has been assumed to be similar to that of Syndol®**

S5.2 Direct dehydration and oligomerization of ethanol

Direct dehydration and oligomerization of ethanol is also a well-studied chemistry[41–43]. This kind of reaction proceeds following the well-known pool mechanism in zeolitic catalysts rich in acidic groups[23]. The product distribution usually consists of a blend of light hydrocarbons, and a slate of olefins and aromatics with C5+ carbon atoms, typically between 20-60% of the final product. Within this chemistry we have defined two catalyst clusters (Table S5.3): First (Light blue), we have catalysts characterized by producing a blend consisting mainly of aromatics ($> 50\%$). The only element in this cluster among the catalysts analyzed is the Vertimas alternative. This catalyst has been included in this study noting that detail performance results are available, and that a process near to commercialization has been recently published by the Vertimas[LLC] team[41]. Second (light yellow), we have a cluster of catalysts whose main product is a blend of C2-C4 olefins ($\sim 80\%$), suitable for a subsequent oligomerization step. Among the available catalyst we have selected the catalyst PZ-80-05[42], that produces the largest amount of the reactive species propene-isobutene.

Table S5.3 Catalyst for the direct dehydration and oligomerization of ethanol

	T	P	Contact			X	Carbon selectivity												Ref.
			WHSV	LHSV	Tau		P1	P2	P2	P3	P4	P5+	O2	O3	OI4	O4	O5+	Ar	
	°C	Atm	h^{-1}	h^{-1}	h^{-1}	%													
Vertimas™	350	1	-	-	-	-	9.9	0	0	0	6.8	22	0	0	0	0.3	12.3	47.9	[41]
PZ-80-05	550	1	1.21	-	-	100	2.4	0.0	0.0	0	0	0	27.2	32.9	17.6	0.0	0	19.9*	[42]
HZSM-5(Ga)	500	1	-	-	0.03	100	0.0	0.0	5.4	**0**	**0**	**0**	37.8	23.3	14.2	5.4	**0**	14.0*	[44]
HZSM-5 (SIO_2/AL_2O_3)	500	1	-	-	0.003	100	0.2	0.5	5.9	**0**	**0**	**0**	21.4	23.6	16.5	5.4	**0**	26.5*	[45]

* Also includes aliphatic species

S5.3 Ethanol condensation

The direct conversion of ethanol to C_3-C_4 olefins can proceed through condensation reactions typically yielding a catalyst dependent blend of C_2-C_4 olefins[23,46–53]. The main products of these blends are propene and isobutene, two light olefins more reactive than ethylene, thus making them very suitable for a subsequent oligomerization step. The main drawback of condensation reactions is the unavoidable carbon loss caused by the production of CO_x species as part of the mechanism. In this work we have clustered catalyst for condensation reactions in three groups (Table S5.4). The only relevant criteria for the definition of these groups was the product selectivity. The first group of catalysts (light blue), is characterized by producing propene as its main output. From this group we have selected the catalyst In_2O_3-β Z as representative, although the other catalyst in the group display a better performance at first sight, its carbon balance had higher inaccuracy, thus we decided to include the catalyst for which better data was available. The second group (light yellow), produces a blend of ethylene and propene as main products. La(1)/ZrO was selected as the catalyst in this group, differences among catalyst in this group were not very significant but we found that La(1)/ZrO produced a higher amount of propene. Finally, the third group (light green) contains catalyst whose main output is isobutene. In this group we have included $ZnZr_{2.5}Oz$, a catalyst that has been tested at PNNL for the production of jet fuel[52].

Table S5.4. Catalysts for ethanol condensation reactions

	T	P	Contact			X	Carbon selectivity								Ref.
			WHSV	LHSV	Tau		P1	O2	O3	OI4	AI2	K3	CO_x	BTX	
	°C	Atm	h^{-1}	h^{-1}	h^{-1}	%									
In_2O_3-β Z	460	1	0.2	-	-	100	0.8	4.6	50.0	6.1	0.0	1.5	26.9	3.1	46
Sc 3%-In2O3	550	1	-	687	-	100	2.0	1.1	55.5	13.2	2.6	0.1	23.8	0.0	51,54
0.03Y/ZrO2	450	11	-	-	0.045	92.2	0.6	31.3	44.0	0.0	0.9	3.3	11.7	0.0	47
La(1)/ZrO_2	450	11	-	-	0.045	93.6	0.0	35.8	45.2	0.0	0.0	1.9	11.2	0.0	49
Sr(1)/ZrO_2	450	11	-	-	0.045	93.7	0.0	50.6	35.7	0.5	0.0	1.8	9.2	0.0	50
$ZnZr_{2.5}Oz$	450	13.6	-	656	-	100	12.1	2.1	8.5	44	0	0.5	32.6	0	52

S5.4 Guerbet coupling of ethanol

Guerbet chemistry discovered by Marcel Guerbet as early as 1899 allows the condensation of alcohols. This condensation can occur either as a self-condensation reaction, or alternatively between two alcohols of different chain length. The resulting product is therefore a mixture of higher alcohols, whose composition is highly dependent on the feedstock composition and the selected catalyst[15,55–62]. Typical by-products include, olefins, dienes, aldehydes, and ethers. Additionally, water is always produced as a waste product, and CO_x species appear for some catalyst. Guerbet chemistry has been explored using both homogeneous or heterogenous catalysts. We will focus in this work only on heterogenous catalysts, provided that homogeneous catalysis for this process still pose significant challenges in terms of separations and catalyst cost[23]. In principle Guerbet chemistry can be used to process any feed containing alcohols. In this work we are interested in the processing of five different feedstocks: ethanol (Technology 4, part of Technology group 1), butanol (Technology 15, part of Technology group 10), hexanol (Technology 18, part of Technology group 11), octanol (Technology 21, part of Technology group 12), and a mixed feedstock consisting of alcohols of different chain length (Technology 24, part of Technology group 13). If the feedstock consists of pure ethanol the heterogenous catalysts considered can be clustered in 9 different groups (Tables S5.5-S5.6). In the construction of these groups we have found that four criteria were relevant: temperature, pressure, conversion, and selectivity toward higher alcohols (See Table S5.6 for details on each cluster). The first three of these criteria have already

been described, the selectivity criterion is chemistry dependent, in this case we have used selectivity toward alcohols, such that we group together catalyst with selectivity higher/lower than 75%. Among the available catalyst Ca-HAP was selected as representative of the first five groups[15]. Two important clarifications need to be done: First, we have not included an independent catalyst for the first and third group, provided that the performance of catalysts in these groups is similar to that of those in groups 2 and 4, respectively, except for the need of pressurization. Second, the selection of the same catalyst as representative of different clusters is explained by the fact that the carbon distribution of the products is a function of the conversion, a variable that changes among clusters. For the sixth group, we selected Pd-hydrotalcite[61], this patented catalyst presents one of the highest selectivities toward higher alcohols (86%) while still maintaining 70% conversion. Pd-MgO is selected in the seventh cluster[60] and 8(wt%)Ni-4.5(wt%)-La_2O_3/γ-Al_2O_3 in the eight[55]. Finally, we include Ni(8%)-γ-Al_2O_2 as representative of the last cluster[62].

Table S5.5. Heterogeneous catalyst for Guerbet reaction of ethanol.

	T	P	Contact			Carbon Selectivity															Ref.
			WHSV	GHSV	X	P1	P3	O2	O4	O6	DO4	DO6	A4	A5	A6	A7	A8	E4	Al2	Al4	CO_x	
	°C	Atm	h^{-1}	h^{-1}	%																	
3%Cu-K/ZrO2	360	34	-	600	88.0	0.0	0.0	0.0	0.0	0.0	0.0	0.0	38.0	0.0	28.0	0.0	0.0	1.0	0.0	0.0	0.0	57
3%Pd/ZrO2	360	34	-	600	78.0	0.0	0.0	1.0	0.0	0.0	0.0	0.0	51.0	0.0	22.0	0.0	0.0	4.0	0.0	0.0	0.0	57
Ca-HAP	**350**	**1**	**0.05**	**-**	**75.0**	**0.0**	**0.0**	**3.0**	**3.4**	**1.6**	**4.7**	**3.5**	**3.1**	**26.7**	**11.2**	**9.6**	**14.2**	**0.0**	**0.0**	**0.0**	**0.0**	15
MgO-Al2O3	345	2.41	1.00		60.0	0.0	0.0	0.0	0.0	0.0	0.0	0.0	69.2	8.0	13.5	2.8	1.0	0.0	0.0	0.0	0.0	59
3%Cu-Li/g-Al2O2	400	34	-	600	57.0	0.0	0.0	0.0	0.0	0.0	0.0	0.0	70.0	0.0	14.0	0.0	0.0	8.0	0.0	0.0	0.0	58
Ca-HAP	350	1	0.56	-	50.0	0.0	0.0	2.4	1.7	0.5	4.0	1.9	49.3	0.0	20.2	0.0	9.0	0.0	0.0	0.0	0.0	15
Ca-HAP	350	1	0.56	-	25.1	0.0	0.0	1.9	0.6	0.1	3.1	0.7	71.0	0.0	13.1	0.0	1.9	0.0	0.0	0.0	0.0	15
Pd-Hydrotalcite	**250**	**34**	**-**	**600**	70.0	**0.0**	**0.0**	**14.0**	**0.0**	**0.0**	**0.0**	**0.0**	**67.0**	**0.0**	**19.0**	**0.0**	**0.0**	**0.0**	**0.0**	**0.0**	**0.0**	61
Pd-MgO	**250**	**34**	**-**	**>600**	41.0	**0.0**	**0.0**	**0.0**	**0.0**	**0.0**	**0.0**	**0.0**	**77.0**	**0.0**	**16.0**	**0.0**	**0.0**	**0.0**	**0.0**	**0.0**	**0.0**	60
1%Ni-0.6%Pd-2.1Ge-MgO	250	34	-	>600	40.0	0.0	0.0	0.0	0.0	0.0	0.0	0.0	83.0	0.0	9.0	0.0	0.0	0.0	0.0	0.0	0.0	60
0.05Pt--0.6Pd-2.1Ge-MgO	250	34	-	>600	45.0	0.0	0.0	0.0	0.0	0.0	0.0	0.0	80.0	0.0	12.0	0.0	0.0	0.0	0.0	0.0	0.0	60
8 wt% Ni/4.5 wt% La2O3/γ-Al2O3	250	100	0.80	-	41.0	13.7	2.3	0.0	0.0	0.0	0.0	0.0	56.0	0.0	11.6	0.0	1.6	1.7	2.7	0.6	4.0	55
Ni8%/G-Al2O2	**250**	**176**	**6.40**	**-**	**35.0**	**0.0**	**0.0**	**0.0**	**0.0**	**0.0**	**0.0**	**0.0**	**62.4**	**0.0**	**24.6**	**0.0**	**0.0**	**0.0**	**0.0**	**7.1**	**0.0**	55
1 wt% Ni/9 wt% La2O3/γ-Al2O3	210	100	0.80	-	29.0	8.0	3.1	0.0	0.0	0.0	0.0	0.0	50.9	0.0	18.2	0.0	5.2	0.8	1.2	0.9	2.8	55
Ga-hydrotalcite	270	17	-	600	28.0	0.0	0.0	9.7	0.0	0.0	0.0	0.0	70.0	0.0	20.3	0.0	0.0	0.0	0.0	0.0	0.0	61
Ni-MgAlO2	250	30	3.20	-	18.8	0.0	0.0	0.0	0.0	0.0	0.0	0.0	55.0	0.0	23.4	0.0	7.9	0.0	0.0	0.0	0.0	56

Table S5.6. Criteria applied for the clustering of catalyst used for the Guerbet reaction of ethanol

	Optimal temperature	Optimal pressure	Conversion	Higher alcohol selectivity
Cluster 1	$T > 280°C$	$P > 1\ atm$	$X \geq 75\%$	$S < 75\%$
Cluster 2	$T > 280°C$	$P = 1\ atm$	$X \geq 75\%$	$S < 75\%$
Cluster 3	$T > 280°C$	$P > 1\ atm$	$35\% < X < 75\%$	$S \geq 75\%$
Cluster 4	$T > 280°C$	$P = 1\ atm$	$35\% < X < 75\%$	$S \geq 75\%$
Cluster 5	$T > 280°C$	$P = 1\ atm$	$X \leq 35\%$	$S \geq 75\%$
Cluster 6	$T \leq 280°C$	$P > 1\ atm$	$35\% < X < 75\%$	$S \geq 75\%$
Cluster 7	$T \leq 280°C$	$P > 1\ atm$	$35\% < X < 75\%$	$S \geq 75\%$
Cluster 8	$T \leq 280°C$	$P > 1\ atm$	$35\% < X < 75\%$	$S < 75\%$
Cluster 9	$T \leq 280°C$	$P > 1\ atm$	$X \leq 35\%$	$S \geq 75\%$

The study of Guerbet chemistry of higher alcohols has been less frequent in comparison with their ethanol counterpart. However, there are some studies dealing with the chemistries of interest[15,63] (Table S5.7). In the cases of butanol, hexanol, and octanol we have used results

reported for Ca-Hydroxyapatite. In the case of mixed alcohols, catalyst performance is highly dependent on the feed composition. Thus, it is difficult to find a representative mixture. As an initial approximation to the problem we have decided to assume the availability of a hypothetical catalyts (Table S5.7 fifth cluster) able to catalyze the self-condensation reaction of every alcohol in the feed. The only constraint associated with this hypothetical catalyst establishes that linear alcohols are more prone to form alcohol condensation products, while branched alcohols show higher selectivity toward the olefins, as in fact has been observed experimentally in Ca-Hydroxyapatite[15].

Table S5.7 Heterogeneous catalyst for the Guerbet reaction of higher alcohols

Feed	Catalyst	T	P	Contact		X	Carbon selectivity													Ref
				WHSV	τ															
		°C	Atm	h^{-1}	g-min/ml	%	O4	O6	O8	O12	O16	DO8	DO16	A8	A12	A16	Al4	Al6	Al8	Al12	
Butanol	**HAP**	**375**	**1**	**0.72**	**-**	**74.2**	**5.7**	**0**	**10.0**	**0**	**0**	**8.0**	**0**	**47.3**	**0**	**0**	**4.8**	**0**	**10.3**	**0**	15
Butanol	Sr-HAP	400	1	0.80	-	31.9	15.2	0	0	0	0	0	0	39.9	0	0	12.7	0	7.7	0	63
Hexanol	**HAP**	**375**	**1**	**-**	**2100**	**74.2**	**0**	**5.7**	**0**	**18.0**	**0**	**0**	**0**	**0**	**47.3**	**0**	**0**	**4.8**	**0**	**10.3**	15
Octanol	**HAP**	**375**	**1**	**-**	**2100**	**74.2**	**0**	**0**	**5.7**	**0**	**10.0**	**0**	**8.0**	**0**	**0**	**57.6**	**0**	**0**	**4.8**	**0**	15
	A4	**HAP**				**74.2**	**5.7**	**0**	**10.0**	**0**	**0**	**8.0**	**0**	**47.3**	**0**	**0**	**4.8**	**0**	**10.3**	**0**	
M	**A6**	**HAP**	**375**	**1**	**0.023**		**74.2**	**0**	**5.7**	**0**	**18.0**	**0**	**0**	**0**	**0**	**47.3**	**0**	**0**	**4.8**		**10.3**	-
	A8	**HAP**				**74.2**	**0**	**0**	**5.7**	**0**	**10.0**	**0**	**8.0**	**0**	**0**	**57.6**	**0**	**0**	**4.8**	**0**	

S5.5 Oligomerization

Light olefin oligomerization is a widely studied chemistry. This kind of process is relevant both for traditional refining industries, where it can be employed to upgrade low molecular weight olefins into heavier products, as well as in the sustainable fuel industry where it is a corner stone in the design of strategies for the production of advanced fuels[64,65]. The oligomerization of light olefins yields a product consisting of a mixture of heavier olefins. The carbon distribution observed in the final products is a function of the mechanism followed by the catalyst, the feed composition, and the catalyst itself. For example, Ziegler-Natta catalysts and Ni-based catalysts, whose chemistry is described in terms of a Cossee-Arlman mechanism yield a product that follows a Schultz-Flory distribution[23,66]. In contrast, metallocene catalysts are highly selective toward olefin dimers[67]. In this work we are concerned with the oligomerization of different light olefins: ethylene (Technology 5, part of Technology group 2), propene (Technology 6, part of Technology group 3), isobutene (Technology 7, part of Technology group 4), propene/isobutene mixtures (Technology 8, part of Technology group 5), butene (Technology 9, part of Technology group 6), hexene (Technology 10, part of Technology group 7), octene (Technology 11, part of Technology group 8), and mixtures of these species (Technology 12, part of Technology group 9). For each of these technologies, oligomerization catalysts have been reported. In tables S5.8-S5.15 we present a brief summary of the catalysts available to perform these chemistries, the catalyst clusters used in this work, and the selected catalyst for process synthesis. The different criteria used for the clustering process are detailed in table S5.16. Although we have emphasized the use of heterogeneous catalysts, in ethylene oligomerization there is data available detailing the use of homogeneous catalysts, thus for completeness we have included some homogeneous processes in Table S5.8. Finally, we highlight that the data presented in Table S5.15 for a mixed olefin stream are inferred based on results obtained with HZSM-5 with pure olefins, and constitute only an approximation to the more complex behavior of the system that would exist in a real production plant.

Table S5.8 Catalyst used for ethylene oligomerization

	T	P	Contact		X	Carbon Selectivity															Ref.
			WHSV	GHSV		P1	P3	O2	O4	O6	DO4	DO6	DO8	Al4	A4	A5	A6	A7	A8	E4	COx	
	°C	Atm	h^{-1}	h^{-1}	%																
Ni-LASA	300	15	6	-	53.7	0.0	0.0	0.6	73.5	1.3	14.3	6.6	0.3	3.5	0.0	0.0	0.0	0.0	0.0	0.0	0.0	68
H-ZSM-5	450	1	14.2	-	58	0.0	13.6	42.0	20.7	11.8	0.0	0.0	0.0	0.0	0.0	0.0	0.0	0.0	0.0	0.0	0.0	69
SAPO-34	450	1	17.3	-	54.4	15.4	3.3	43.3	24.6	11.3	0.0	0.0	0.0	0.0	0.0	0.0	0.0	0.0	0.0	0.0	0.0	70
SAPO-34	450	1	4.6	-	77.9	28.5	4.6	35.1	16.6	9.9	0.0	0.0	0.0	0.0	0.0	0.0	0.0	0.0	0.0	0.0	0.0	70
Ni-MCM-41	400	1	1.03	-	42.5	0.0	0.0	46.6	39.6	0.0	3.0	0.0	0.0	0.0	0.0	0.0	0.0	0.0	0.0	0.0	0.0	48
D-IWI	350	1	0.027	-	40.0	0.0	0.0	52.7	29.0	5.4	2.0	0.0	0.0	0.0	0.0	0.0	0.0	0.0	0.0	0.0	0.0	71
Alphabutol	50	30	-	4	80	0.0	0.0	0.0	93.0	0.0	7.0	0.0	0.0	0.0	0.0	0.0	0	0	0	0	0	72
Chevron	180	230	-	0.25	90	0	0	0	14	0	13	15	0	12.5	10	0	8	6.5	5.5	15.5	0	73
Alphaselect	130	70	-	-	-	0.0	0.0	0.0	35.0	0.0	30.0	21.0	0.0	14.0	0.0	0.0	0	0	0	0	0	72
Ni-AlSBA-15	150	30	10	-	91	0.0	0.0	0.0	45.0	0.0	31.0	19.0	0.0	5.0	0.0	0.0	0.0	0.0	0.0	0.0	0.0	74
Ni(2.7)-B-im	120	35	2.1	-	65.7	0.0	0.0	0.2	47.3	0.3	11.5	10.7	1.4	11.5	8.2	8.2	0.0	0.0	0.0	0.0	0.0	75
Ni(5.0)-B-im	120	35	2.1	-	87.2	0.0	0.0	0.1	34.5	0.3	8.9	13.3	1.4	16.1	11.8	12.8	0	0	0	0	0	75
NiSAIA	120	35	2	-	95.2	0.0	0.0	0.0	35.9	0.0	24.7	16.4	0.0	10.2	4.6	0.0	3.1	2.3	1.5	0.8	0.4	76
NiSAIB	120	35	2	-	98.5	0.0	0.0	0.0	19.6	0.0	14.8	23.3	0.0	19.2	11.0	0.0	5.5	3.1	1.7	1.4	0.4	76
NiSAII	120	35	2	-	98.9	0.0	0.0	0.0	26.6	0.0	17.0	25.9	0.0	14.1	8.1	0.0	3.9	2.2	1.2	1.0	0.0	76
5Ni/NB	120	35	2	-	80	0.0	0.0	0.0	32.7	0.0	54.2	0.0	0.0	0.0	0.0	13.1	0.0	0	0	0	0	77
40NiNaY	115	35	2	-	96.4	0.0	0.0	0.0	38.2	0.0	19.7	15.1	0.0	13.1	7.0	0.0	4.0	1.9	1.0	0	0	76
Ni-AlSBA-15	150	10	10	-	60	0.0	0.0	0.0	77.0	0.0	17.0	4.0	0.0	2.0	0.0	0.0	0.0	0.0	0.0	0.0	0.0	74
Ni(2.0)-B-ex	120	35	2.1	-	39.4	0.0	0.0	0.1	67.4	0.3	10.1	6.0	1.0	5.1	4.2	5.8	0.0	0.0	0.0	0.0	0.0	75
Ni-AlKIT-6	60	30	7.5	-	47.0	0.0	0.0	0.0	80.0	0.0	19.0	1.0	0.0	0.0	0.0	0.0	0.0	0.0	0.0	0.0	0.0	78

Table S5.9 Catalysts used for propene oligomerization

	T	P	Contact		X	Carbon selectivity														Ref.
			WHSV	LHSV		C5	C6	C7	C8	C9	C10	C11	C12	C13	C14	C15	C16	C18	C21	
	°C	Atm	h^{-1}	h^{-1}	%															
HZSM-5	284	24	0.7	-	90	0.9	4.5	5.8	7.8	18.5	9.7	11.2	17.4	6.9	5.2	6.0	6.1	0.0	0.0	79
HZSM-5	270	34	4.03	-	77.7	0.0	10.7	0.0	0.0	36.5	0.0	0.0	37.4	0.0	0.0	11.9	0.0	3.5	0.0	80
2.21Ni/HZSM-5	270	34	4.03	-	75.4	0.0	5.2	0.0	0.0	30.9	0.0	0.0	36.8	0.0	0.0	20.8	0.0	6.3	0.0	80
pell-SAPO-11	220	50	12	-	95	0.0	65.0	0.0	0.0	27.0	0.0	0.0	8.0	0.0	0.0	0.0	0.0	0.0	0.0	81
23%P-Kieselguhr	215	72	0.8	-	93.6	0.0	50.2	0.0	0.0	29.1	0.0	0.0	13.7	0.0	0.0	7.0	0.0	0.0	0.0	82
H-ZSM-23	185	35	0.24	-	91.1	0.0	58.7	0.0	0.0	20.1	0.0	0.0	11.0	0.0	0.0	6.4	0.0	2.4	1.4	83
ZSM-22	180	68	4.4	-	100	18.0	40.0	0.0	0.0	30.0	0.0	0.0	12.0	0.0	0.0	0.0	0.0	0.0	0.0	84
H-ZSM-23	240	35	0.31	-	100	0.0	16.2	0.0	0.0	20.9	0.0	0.0	23.9	0.0	0.0	19.5	0.0	13.4	6.1	83
3.5%P- 55/45 Si/Al2O2	215	72	0.8	-	85	0.0	30.9	0.0	0.0	17.8	0.0	0.0	22.2	0.0	0.0	29.1	0.0	0.0	0.0	82
HZSM-5	189	24	0.7	-	90	0.2	2.7	1.9	3.4	34.2	4.2	5.1	31.0	2.2	4.2	9.1	1.8	0.0	0.0	79
Montmorillonite	171	61	1.6	-	85	0.0	10.0	0.0	0.0	34.0	0.0	0.0	25.0	0.0	0.0	18.0	0.0	11.0	2.0	85
H-ZSM-57	150	70	2.13	-	95.14	0.1	1.9	1.6	2.5	65.3	1.9	0.0	17.3	9.2	0.0	0.0	0.0	0.0	0.0	86
6.9%-SO3-10NiO-Al2O2	50	60	-	1	83	0.0	76.0	0.0	0.0	17.0	0.0	0.0	7.0	0.0	0.0	0.0	0.0	0.0	0.0	87

Table S5.10 Catalysts for the oligomerization of Propene/Isobutene blends

	T	P	Contact WHSV	X	Carbon Selectivities										Ref
					C5	C6	C7	C8	C9	C10	C11	C12	C13	C15	
	°C	Atm	h^{-1}	%											
SPA	**160**	**35**	**1.5**	**65**	**1.3**	**7.9**	**33.0**	**23.4**	**23.9**	**0.0**	**0.0**	**7.5**	**0.0**	**3.0**	[88]
H-ZSM-57	150	60	2.9	C3:86, C4:83	0.0	1.0	4.0	24.0	23.0	29.0	8.0	7.0	4.0	0.0	[89]
CT275	**120**	**14**	**1.1**	**100**	**1.6**	**3.3**	**7.5**	**41.2**	**0.0**	**6.9**	**1.3**	**38.2**	**0.0**	**0.0**	[52]
Amberlyst 36	140	14	1.1	C4 99, C3 89	1.5	3.3	7.5	41.2	0.0	6.9	1.3	38.2	0.0	0.0	[52]
MTW/AL2O3	120	34	2.7	50.3	0.3	1.8	33.5	25.4	0.0	11.2	0.0	14.7	0.0	13.1	[88]
MTW-10%P H3PO4	**120**	**34**	**1.6**	**53.5**	**0.1**	**0.6**	**18.4**	**33.7**	**0.0**	**3.1**	**0.0**	**43.0**	**0.0**	**1.1**	[88]

Table S5.11 Catalysts for isobutene oligomerization

	T	P	Contact WHSV	X	Carbon Selectivities							Ref.
					C6	C8	C10	C12	C14	C16	C20	
	°C	Atm	h^{-1}	%								
Sulfated titanium	**140**	**40**	**2.5**	**100**	**0.0**	**38.0**	**0.0**	**60.0**	**0.0**	**2.0**	**0.0**	[90]
H-ZSM-Y-P	**100**	**1**	**176.3**	**93**	**0.0**	**13.0**	**0.0**	**75.0**	**0.0**	**12.0**	**0.0**	[91]
Amberlyst 15	100	1	2.5	98	0.0	8.0	0.0	82.0	0.0	10.0	0.0	[92]
H-ZSM-Y-P	50	1	176.3	99.5	0.0	48.0	0.0	44.0	0.0	8.0	0.0	[91]

Table S5.12 Catalysts for butene oligomerization

	T	P	Contact WHSV	X	Carbon selectivity														Ref.
					PC6	PC8	PC10	C5	C6	C7	C8	C9	C10	C12	C14	C16	C18	C20	C24	
	°C	Atm	h^{-1}	%																
ATHZ5-Cs	**300**	**15**	**6**	**100**	**0.0**	**0.0**	**0.0**	**0.0**	**15.0**	**0.0**	**85.0**	**0.0**	**0.0**	**0.0**	**0.0**	**0.0**	**0.0**	**0.0**	**0.0**	[93]
H-ZSM-57	**200**	**70**	**2.13**	**81.71**	**0.0**	**0.0**	**0.0**	**0.2**	**0.3**	**1.0**	**80.1**	**1.7**	**1.3**	**11.3**	**0.5**	**3.6**	**0.0**	**0.0**	**0.0**	[86]
H-ZSM-57	165	70	2.13	94.6	0.0	0.0	0.0	0.1	0.3	0.8	61.3	1.9	3.1	19.0	1.7	12.0	0.0	0.0	0.0	[86]
H-Ferrierite	150	63	3.17	48.5	0.2	3.1	0.7	0.0	1.8	0.0	63.9	0.0	4.5	16.4	0.9	3.5	0.6	0.7	0.0	[94]
2A-Co/C-230	**80**	**31**	**0.25**	**29**	**0.0**	**0.0**	**0.0**	**0.0**	**0.0**	**0.0**	**94.4**	**0.0**	**0.0**	**5.6**	**0.0**	**0.0**	**0.0**	**0.0**	**0.0**	[95]
ASA13	**120**	**35**	**8**	**76**	**0.0**	**0.0**	**0.0**	**0.0**	**0.0**	**0.0**	**58.8**	**0.0**	**0.0**	**28.2**	**0.0**	**9.4**	**0.0**	**3.6**	**0.0**	[96]
Nafion	120	35	8	87	0.0	0.0	0.0	0.0	0.0	0.0	53.3	0.0	0.0	26.6	0.0	14.7	0.0	5.4	0.0	[96]
ASA	120	35	7	87.6	0.0	0.0	0.0	0.0	0.0	0.0	58.2	0.0	0.0	21.6	0.0	7.8	0.0	0.0	0.0	[96]
ZSM-5-50	**230**	**40**	**2**	**100**	**0.0**	**0.0**	**0.0**	**0.0**	**7.0**	**0.0**	**18.0**	**0.0**	**0.0**	**35.0**	**0.0**	**25.0**	**0.0**	**0.0**	**5.0**	[97]
HZSM-5	225	36	0.11	95	0.0	0.0	0.0	0.0	7.0	0.0	23.0	0.0	0.0	22.0	0.0	20.0	0.0	13.0	15.0	[98]
H-ZSM-23	205	36	0.21	95.4	0.0	0.0	0.0	0.0	0.0	0.0	26.2	0.0	0.0	43.0	0.0	21.9	0.0	7.0	2.2	[83]
Amberlyst-70	170	17	0.63	99	0.0	0.0	0.0	0.0	7.0	0.0	20.0	0.0	0.0	22.0	0.0	26.0	0.0	17.0	8.0	[98]
H-Ferrierite	150	63	0.18	98.9	0.8	6.8	3.9	0.0	0.8	0.0	11.6	0.0	5.5	16.7	7.1	16.0	6.0	13.1	0.0	[94]

Table S5.13 Catalysts for hexene oligomerization

Catalyst	T	P	Contact WHSV	Contact LHSV	X	Carbon selectivity			Ref.
	°C	Atm	h-1	h-1	%	PC9	C12	C18	
Al-MTS	200	50	0.4		80	0.00	48.00	34.00	[99]
SO4/ZrO2	**100**	**8**	**-**	**1.2**	**85**	**0.00**	**78.00**	**22.00**	[100]
HZSM-5	170	40	0.15	-	85	17.50	73.00	9.50	[101]
ASA	170	40	0.15	-	88	11.50	61.50	27.50	[101]

Table S5.14 Catalysts for octene oligomerization

Catalyst	Temperature	Pressure	Contact		Carbon selectivity			Ref.
			WHSV	X	C12	C16	C18	
	°C	Atm	h^{-1}	%				
ASA	**150**	**40**	**0.5**	**70**	**10.00**	**90.00**	**0.00**	101
6.9%-SO3-Al2O2	100	70	2	70	63.00	27.00	10.00	87
HZSM-5	**170**	**40**	**0.25**	**50**	**20.00**	**80.00**	**0.00**	101

Table S5.15 Oligomerization of a mixed olefin blend

		T	P	WHSV	X	Carbon selectivity														Ref.
						C5	C6	C7	C8	C9	C10	C11	C12	C13	C14	C15	C16	C18	C20	C24	
		°C	atm	h^{-1}	%																
HZSM5	**C3**	**200**	**40**	**0.2**	**90**	**0.2**	**2.7**	**1.9**	**3.4**	**34.2**	**4.2**	**5.1**	**31.0**	**2.2**	**4.2**	**9.1**	**1.8**	**0.0**	**0.0**	**0.0**	15
	C4				**95**	**0.0**	**7.0**	**0.0**	**23.0**	**0.0**	**0.0**	**0.0**	**22.0**	**0.0**	**0.0**	**0.0**	**20.0**	**0.0**	**13.0**	**15.0**	
	C5					**0.0**	**0.0**	**0.0**	**0.0**	**0.0**	**30.0**	**0.0**	**22.0**	**0.0**	**0.0**	**48**	**0.0**	**0.0**	**0.0**	**0.0**	
	C6				**85**	**0.0**	**0.0**	**0.0**	**0.0**	**17.5**	**0.0**	**0.0**	**73.0**	**0.0**	**0.0**	**0.0**	**0.0**	**9.5**	**0.0**	**0.0**	
	C7					**0.0**	**0.0**	**0.0**	**0.0**	**0.0**	**0.0**	**0.0**	**0.0**	**0.0**	**100**	**0.0**	**0.0**	**0.0**	**0.0**	**0.0**	
	C8				**50**	**0.0**	**0.0**	**0.0**	**0.0**	**0.0**	**0.0**	**0.0**	**20.0**	**0.0**	**0.0**	**0.0**	**80.0**	**0.0**	**0.0**	**0.0**	

Table S5.16 Table S5.6. Criteria applied for the clustering of catalyst used for the oligomerization reaction of light olefins

Olefin	Cluster	Temperature	Pressure	Conversion	Catalysis phase	Selectivity
Ethylene	Cluster 1	$T > 280°C$	$P > 1atm$	$35 < x < 75$	Heterogeneous	$O4 > 65$
	Cluster 2	$T > 280°C$	$P = 1atm$	$35 < x < 75$	Heterogeneous	$O3 + O4 > 65$
	Cluster 3	$T \leq 280°C$	$P > 1atm$	$x \geq 75$	Homogeneous	$O4 > 65$
	Cluster 4	$T \leq 280°C$	$P > 1atm$	$x \geq 75$	Homogeneous	$O4+> 65$
	Cluster 5	$T \leq 280°C$	$P > 1atm$	$x \geq 75$	Homogeneous	$O4+> 65$
	Cluster 6	$T \leq 280°C$	$P > 1atm$	$x \geq 75$	Heterogeneous	$O4+> 65$
	Cluster 7	$T \leq 280°C$	$P > 1atm$	$35 < x < 75$	Heterogeneous	$O4 > 65$
Propene	Cluster 1	$T > 280°C$	$P > 1atm$	$x \geq 75$	Heterogeneous	$O9+> 75$
	Cluster 2	$T \leq 280°C$	$P > 1atm$	$x \geq 75$	Heterogeneous	$O9+> 75$
	Cluster 3	$T \leq 280°C$	$P > 1atm$	$x \geq 75$	Heterogeneous	$O9+> 75$
	Cluster 4	$T \leq 280°C$	$P > 1atm$	$x \geq 75$	Heterogeneous	$O9+> 75$
Propene/Isobutene	Cluster 1	$T \leq 280°C$	$P > 1atm$	$35 < x < 75$	Heterogeneous	$O9+\leq 35$
	Cluster 2	$T \leq 280°C$	$P > 1atm$	$x \geq 75$	Heterogeneous	$O9+> 35$
	Cluster 3	$T \leq 280°C$	$P > 1atm$	$35 < x < 75$	Heterogeneous	$O9+> 35$
Isobutene	Cluster 1	$T \leq 280°C$	$P > 1atm$	$x \geq 75$	Heterogeneous	$O12+\leq 35$
	Cluster 2	$T \leq 280°C$	$P = 1atm$	$x \geq 75$	Heterogeneous	$O12+> 70$
Butene	Cluster 1	$T > 280°C$	$P > 1atm$	$x \geq 75$	Heterogeneous	$O10+\leq 30$
	Cluster 2	$T \leq 280°C$	$P > 1atm$	$x \geq 75$	Heterogeneous	$O10+\leq 30$
	Cluster 3	$T \leq 280°C$	$P > 1atm$	$35 < x < 75$	Heterogeneous	$O10+\leq 30$
	Cluster 4	$T \leq 280°C$	$P > 1atm$	$x \geq 75$	Heterogeneous	$30 \leq O10+\leq 50$
	Cluster 5	$T \leq 280°C$	$P > 1atm$	$x \geq 75$	Heterogeneous	$O10+\geq 35$
Hexene	Cluster 1	$T \leq 280°C$	$P > 1atm$	$x \geq 75$	Heterogeneous	$O9+\geq 90$
Octene	Cluster 1	$T \leq 280°C$	$P > 1atm$	$x \geq 70$	Heterogeneous	$O9+\geq 90$
	Cluster 2	$T \leq 280°C$	$P > 1atm$	$35 < x < 75$	Heterogeneous	$O9+\geq 90$
Mixed olefins	Cluster 1	$T \leq 280°C$	$P > 1atm$	Function of olefin	Heterogeneous	$O9+\geq 90$

S5.12 Higher alcohol etherification

The etherification of higher alcohols is a chemistry that has received recent attention due to the suitability of ethers of higher alcohols as diesel replacement or even as a diesel additive. This chemistry yields as a main product an ether mixture, the by-products are essentially constituted by olefins, additionally a stochiometric amount of waste water is produced. The etherification reaction can proceed with pure alcohol streams as feed, or with blends of different alcohols. In feeds consisting of alcohol blends it is known that a high fraction of linear vs branched alcohols favors selectivity toward ethers, when this fraction gets reduced selectivity toward olefins increases. In this work we are interested in the etherification of pure streams of butanol, hexanol, and octanol, as well as in the etherification of mixed alcohol streams. As in other chemistries etherification of the pure streams has been designed considering the experimental results obtained with the given feedstock. The etherification of mixed streams, on the other hand is complex, we have assumed in this case the existence of a catalyst that yields a product stream consisting only of ethers in which each alcohol reacts with itself. To account for the effect of linearity of the alcohols on the product distribution we have modified the selectivity toward ether and olefin depending on the degree of branching. In Table S5.17 we present the catalysts available for this process for each of the substrates of interest.

Table S5.17 Catalysts for the etherification of higher alcohols

Feed	Catalyst	T	P	Contact WHSV	X	Carbon selectivity							Ref.
		°C	Atm	h^{-1}	%	E8	E12	E16	O4	O6	O8	Ar	
Butanol	**Amberlyst 70**	**150**	**20**	**0.83**	**58.1**	**97**	**0**	**0**	**3**	**0**	**0**	**0**	15
Butanol	g-Al2O3	250	1	0.9	59	86	0	0	14	0	0	0	102
Butanol	USY	170	1	0.3	63	98	0	0	2	0	0	0	102
Butanol	BEA	170	1	0.3	68	94	0	0	6	0	0	0	102
Butanol	Amberlyst36	130	1	0.3	79	82	0	0	18	0	0	0	102
Butanol	Amberlyst70	135	1	0.6	63	86	0	0	14	0	0	0	102
Hexanol	**Amberlyst 70**	**150**	**20**	**0.83**	**77.7**	**0**	**96.7**	**0**	**100**	**3.3**	**0**	**0**	15
Hexanol	Amberlyst 70	190	21	9.8	70.9	0	86.9	0	0	13.1	0	0	103
Hexanol	Nafion NR50	190	21	9.8	66.1	0	93.4	0	0	6.6	0	0	103
Hexanol	BEA25 zeolite	190	21	9.8	53.8	0	88.8	0	0	11.2	0	0	103
Octanol	Amberlyst 39	150	20	9.68	29.5	0	0	95	0	0	5	0	104
Octanol	**Amberlyst 70**	**250**	**20**	**0.83**	**65**	**0**	**0**	**87.4**	**0**	**0**	**1.7**	**10.9**	15
Mixed alcohols	**A2**	**Amberlyst 70**	**250**	**20**	**0.83**	**65**	**87.4**	**0**	**0**	**1.7**	**0**	**0**	**10.9**	-
	A6					**65**	**0**	**87.4**	**0**	**0**	**1.7**	**0**	**10.9**	
	A6_2					**65**	**0**	**40.7**	**0**	**0**	**51.4**	**0**	**7.9**	
	A8					**65**	**0**	**0**	**87.4**	**0**	**0**	**1.7**	**10.9**	
	A8_2					**65**	**0**	**0**	**40.7**	**0**	**0**	**51.4**	**7.9**	

S5.14 Hydrogenation reactions

Olefins are more reactive than paraffins and in fuel products they tend to form gums[6]. As a consequence, the amount of olefins in a final fuel products is typically constrained (less than 18% in gasoline, 2% in jet fuel, and 20% in diesel). Since many of the chemistries studied (dehydration, and oligomerization) produce olefins instead of paraffins, it is important to have a technology for the hydrogenation of paraffins. This option is added to give the superstructure more flexibility. This technology is mature; thus, we are not interested in exploring catalytic options and we have added only one module designed using a Coper molybdenum catalyst[59,105] operated at 350°C, 36 atm, with a WHSV of $3h^{-1}$. This process proceeds with full conversion and 100% selectivity of olefins to paraffins.

S6. Flowsheets associated with the modules employed in the superstructure

In this section we present a brief description of the different modules used for the realization of each technology. These modules were designed and simulated using the software ASPEN plus® V10. In a few instances, which are indicated, the designs and data were obtained from the literature. Heat integration was pursued in each case using Aspen Energy Analyzer®. For heat integration a target-based approach was first implemented, and then a Heat Exchanger Network (HEN) with performance close to the target was designed. The ΔT_{min} used to design the HEN was determined in each case by inspecting a plot of total annualized cost of the HEN versus ΔT_{min}. For consistency we assume that all streams entering and leaving the module are at 35°C and 1 ATM, this assumption may be relaxed in a further design stage.

S6.1 Ethanol dehydration

Ethanol dehydration using Syndol® catalyst (M1)

Processes based on Syndol® catalyst for the dehydration of ethanol are well established, in this work we have used the data and design reported by Mohsenzadeh and coworkers, details about the process can be consulted in the original publication[20].

Ethanol dehydration using MCM-41 catalyst (M2-M4)

The dehydration process using MCM-41 as catalyst is very simple provided that the single pass conversion is 100% and the reported carbon selectivity to ethylene is equal to 1. The process layout (Figure S6.1) consists of a reactor operated at 350°C which is designed as a furnace, followed by a flash tank (operated at 1°C, right above freezing temperature) designed to condense most of the water on the stream leaving the reactor. The gas stream leaving the flash tank is fed to a molecular sieving unit responsible for removing the remaining water on that stream, such that almost pure ethylene is obtained as the main product, and a stream consisting mainly of water is obtained as a waste product. Although the whole process operates at atmospheric pressure we ha added a pump to account for pressure losses through the different units. In terms of layout, modules M2-M4 are identical. The difference between these modules stems from the fact that M2 is designed considering that the feedstock is ethanol 50%, M3 ethanol 83%, and M4 ethanol 100%. In practice the difference between feedstocks implies that the size of the units in modules M2-M4 is different. Furthermore, the heat exchanger network required in each case is also different provided that the heat load is different in each case.

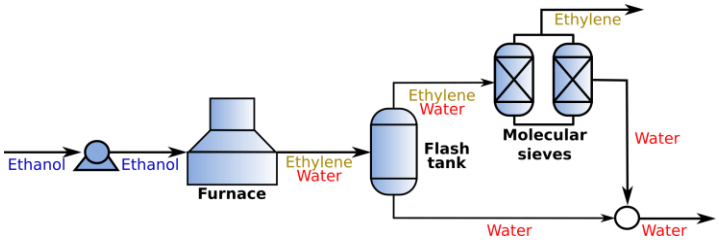

Figure S6.1 Layout of the processes used to dehydrate ethanol using MCM-41 as catalyst.

Ethanol dehydration using La-PHZSM (M5-M7)

The layout of modules designed for the dehydration of ethanol using La-PHZSM (Figure S6.2) is very similar to the layout of modules designed based on MCM-41. La-PHZSM display full conversion of ethanol and it is very selective toward ethylene, with only a small amount of hydrocarbons ($\sim 0.1\%$) been obtained as co-product. The process is designed to operate at atmospheric pressure, and uses a separation strategy based on the condensation of water and hydrocarbon byproducts in a flash tank followed by molecular sieving of the humid ethylene gas stream. The main difference observed for La-PHZSM modules is the reactor design. In this case a lower temperature is required (240°C), thus instead of using a furnace we have employed a series of adiabatic modules with inter-stage heating. As in the

previous case the three modules associated with this design (M5-M7) differ from each other in the substrate they are designed to process: M5 is designed for ethanol 50%, M6 for ethanol 83%, and M7 for ethanol 100%.

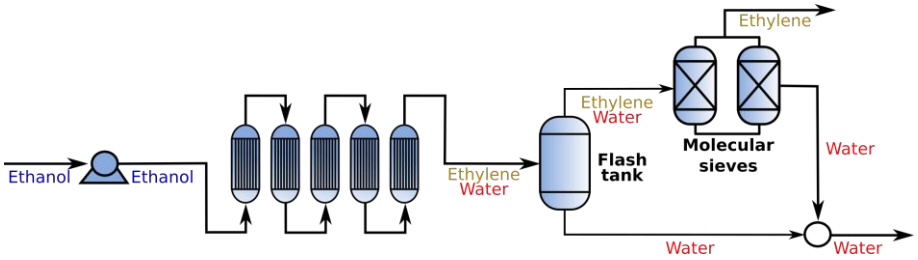

Figure S6.2. Processes for the dehydration of ethanol using La-PHZSM.

S6.2 Simultaneous dehydration and oligomerization of ethanol

Vertimas™ process (M8)

The Vertimas™ process and catalyst have been developed and continuously improved by Hannon and coworkers[41]. The process design and economics used in this work are based on recently reported results that can be consulted in the reference publication[41].

Simultaneous dehydration and oligomerization of ethanol using P-HZSM (M9-M10)

There are two modules designed using P-HZSM as catalyst (M9-M10). These modules have the same layout (Figure 6.3) except for the presence of a recycle stream in module M10 (indicated as a red dashed arrow). Both modules make use of a furnace reactor operated at 550°C and 2 Atm. The output stream from the reactor contains four kinds of products: olefins of interest (ethylene, propene, and isobutene), water, light products, and heavy products (modelled through this work as naphthalene). To properly define the recycle stream in M10 we assume a two-step reaction. In the first step ethanol is dehydrated to ethylene. In the second step the ethylene produced is oligomerized to other products. The first step occurs at 100% single pass conversion, while the second step occurs at 72.8% conversion. Following the reactor there is a flash tank operated at 2 atm and 55°C. This flash tank splits the reactor output into two products: a gas stream, containing a large fraction of the olefin products of interest (ethylene, propene, and isobutene) and a small amount of water; and a liquid stream, containing a fraction of the olefins of interest, most of the water produced during the dehydration step, and the heavy products of ethylene oligomerization. The gas stream is fully dehydrated in a molecular sieving unit, and further compressed to 6 Atm, before been sent to a cryogenic distillation train. This distillation train consist of two columns (Column 3 and Column 4) and yields three products: an ethylene rich stream, a stream consisting of a propene/isobutene blend, and a stream containing minor light by-products that is used to produce electricity. In M9 the ethylene stream leaves the system as a product. In contrast in M10 this stream is recycled back to the reactor. The liquid stream leaving the flash tank is feed to a sequence of two distillation columns (Column 1 and Column 2). The first of these columns recovers as a distillate product the fraction of olefins of interest dissolved in the liquid stream leaving the flash tank. The distillate product of Column 1 is blended with the dehydrated gas stream leaving the molecular sieving unit. On the other hand, the bottoms of Column 1 contain only water and heavy products resulting from oligomerization. This bottom stream is sent to Column 2 that produces waste water as distillate and a stream rich in heavy products in the bottom. In this work we have assumed that these heavy products are burned to produce electricity.

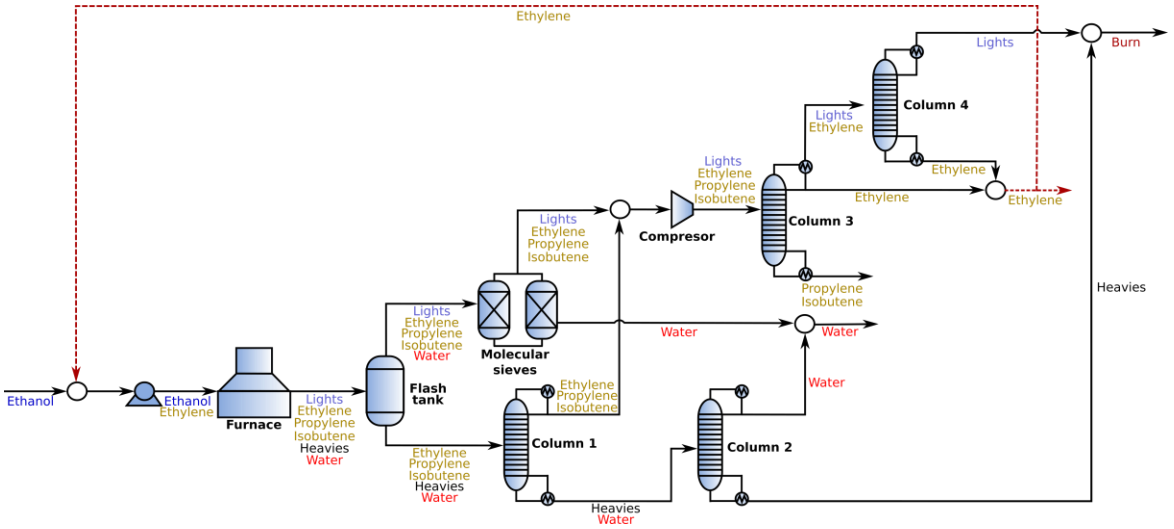

Figure S6.3 Modules used for simultaneous dehydration and oligomerization of ethanol using P-HZSM (M9-M10). In M10 the recycle stream indicated as a red dashed arrow exists; conversely, in M9 this stream leaves the module as a product.

S6.3 Ethanol condensation

Ethanol condensation using $ZnZrO_2$ (M11)

The condensation of ethanol using $ZnZrO_2$ proceeds in a furnace reactor operated at 450°C and 14 atm (Figure S6.4). Conversion under these conditions reaches 100%, therefore no recycle streams are needed. The product of the reactor consists of olefins (isobutene, ethylene and propene), some light ends (methane, and hydrogen), and waste products (CO_2 and water). The stream leaving the reactor enters a flash tank operated at 14atm and 54°C, this flash tank condenses most of the water resulting from the reaction. The gas stream leaving the flash tank is compressed to 35 atm and dehydrated in a molecular sieving unit. The dehydrated product enters a cryogenic distillation column, this column yields a distillate consisting of a blend of ethylene, the light end products and CO_2; this stream is used for electricity generation. The bottoms of the column constitute the product of interest and consists of a blend of propene and isobutene, as well as some other minor byproducts obtained in the reaction.

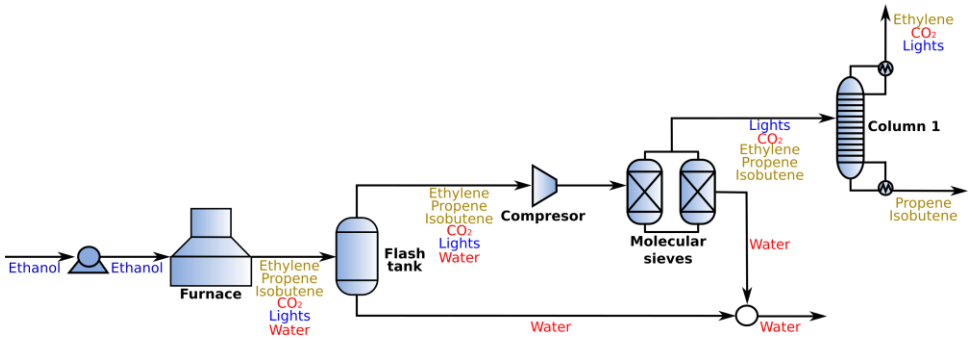

Figure S6.4 Process flowsheet for ethanol condensation using $ZnZrO_2$.

Ethanol condensation using In_2O_2-Zeoliteβ (M12)

This process is characterized by using a furnace reactor operated at 460°C and atmospheric pressure. The reactor product contains propene and isobutene as olefins of interest, as well as minor amounts of ethylene, butane and ethane. Other minor products include aromatics and acetone; additionally, the reaction generates hydrogen as byproduct. Finally, water and CO_2 are obtained as waste

products. The stream leaving the reactor is dehydrated by means of a flash tank operated at 25°C and 1 atm, and a molecular sieving unit that removes the water remnants not condensed in the flash tank. The gas stream leaving the molecular sieving unit is compressed in a multistage system to 20 atm. This compressed stream enters a cryogenic section consisting of a flash drum and a distillation column. The flash drum is designed to remove the non-condensable hydrogen, which is used for electricity generation. The condensed stream leaving the second flash tank is feed to a cryogenic distillation column, whose top product contains the light ends of the reactor product (methane, traces of H_2, CO_2, and ethylene), this stream is also used for electricity generation. The bottom stream on the other hand is the product of interest and it consists mainly of propene and isobutene, but it also contains other products obtained in the condensation reaction (*e.g.* aromatics, acetone, and butane).

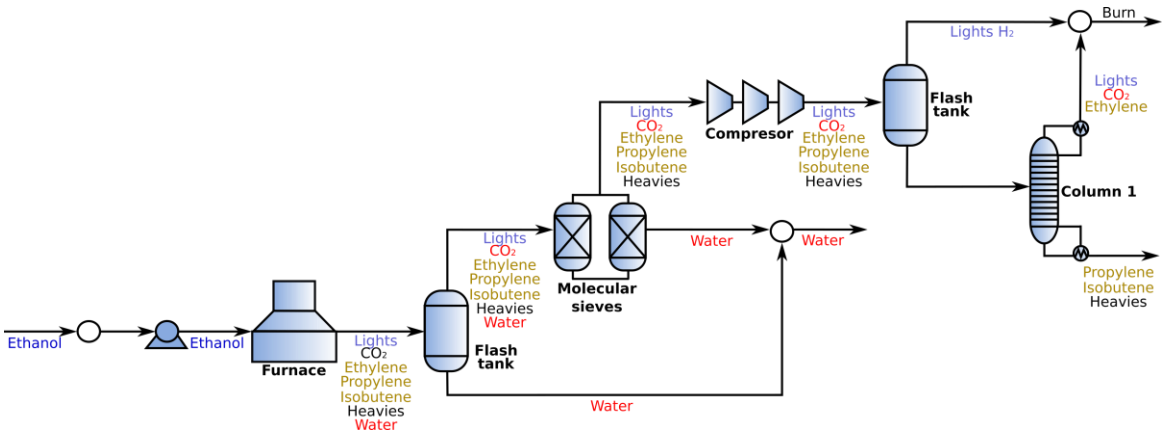

Figure S6.5 Process flowsheet for ethanol condensation using In_2O_2-Zeoliteβ.

Ethanol condensation using $LaZrO_2$ (M13)

The condensation process using $LaZrO_2$ (Figure S6.6) proceeds in a furnace reactor operated at 460°C and 30 atm; under these conditions ethanol single pass conversion reaches a value of 93.6%. The stream leaving the reactor contains unconverted ethanol, the main products propylene and ethylene, light ends hydrogen and methane, and waste products carbon dioxide and water. The stream laving the reactor is fed to flash drum operated at 30 atm and 35°C. The flash tank splits the product into two fractions, a gas stream containing the products of interest and the light ends; and a liquid stream, containing mainly water and unconverted ethanol. The gas stream leaving the flash drum is dehydrated in a molecular sieving unit before entering a cryogenic distillation train consisting of two columns (Column 1 and Column2). This distillation train is responsible for splitting the product into three streams: a propylene rich stream, an ethylene rich stream, and a waste stream mainly containing CO_2. The liquid stream leaving the flash drum is distillated (Column 3) such that a top product with a composition close to the water-ethanol azeotrope is obtained. The top product is recycled back to the reactor. While the bottom product consisting almost exclusively of water is disposed as waste. Note that all distillation columns have been designed using a partial condenser, the gas stream leaving the partial condensers are mixed and used for electricity generation. These streams contain mainly Hydrogen, methane, and ethylene that could not be recovered due to vapor-liquid equilibrium restrictions.

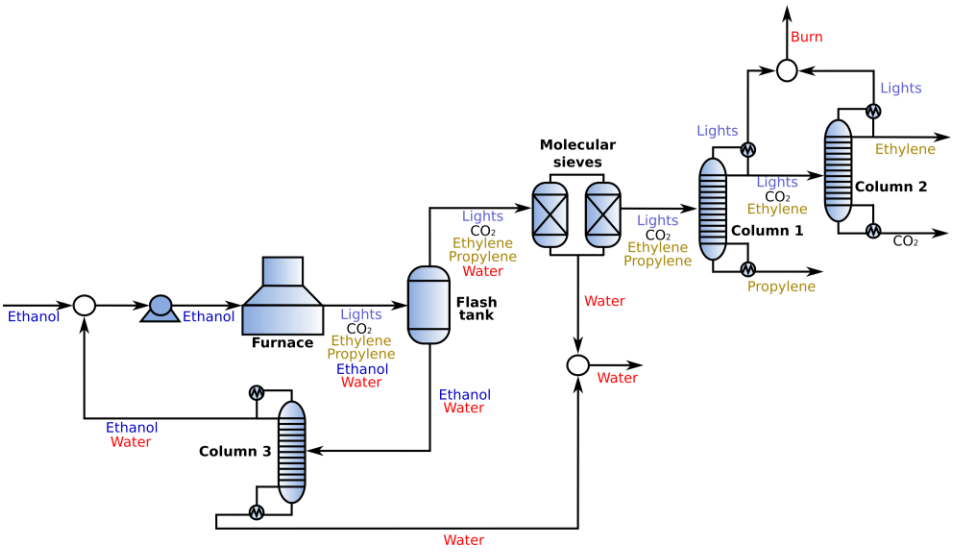

Figure S6.6 Process flowsheet for ethanol condensation using $LaZrO_2$

S6.4 Guerbet coupling of ethanol

Guerbet coupling of ethanol using Ni-La_2O_3-γ-Al_2O_3 (M14-M15)

For the design of modules M14 and M15 we have relied on the results reported by Nezam and coworkers[55] (Figure S6.7). These authors report the use of a reactor designed as a heat exchanger that operates at 230°C and 100 atm, under these conditions conversion reaches a value of 35%. Interestingly, the authors demonstrate that this low conversion value has a positive effect on the economics of their process by enabling the simplification of the separation train. The outlet stream from the reactor contains: unconverted ethanol, higher alcohols, light ends, and waste water. The separation train used consists of three distillation columns: in the first one, higher alcohols are obtained as a bottom product while water and the rest of species leaving the reactor are distilled at the top. The distillate of the first column is fed to a second distillation column whose top product consist mainly of light ends, this stream is used for electricity generation. The bottom product of the Column 2 is fed to Column 3, that yields an azeotropic ethanol-water blend as a top product, and waste water at the bottom. The difference between modules M14 and M15 is given by the absence/presence of a forth column (highlighted in Figure S6.7 by means of a dashed square) used to separate butanol from the other higher alcohols.

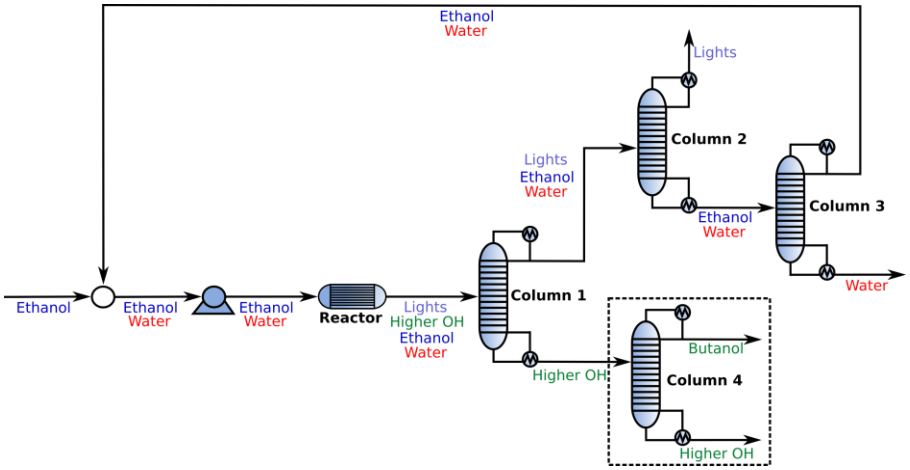

Figure S6.7 Processes for Guerbet coupling of ethanol condensation using Ni-La_2O_3-γ-Al_2O_3. Column 4 is highlighted using a dashed square to indicate that it is present in M14 but not in M15.

Guerbet coupling of ethanol using Ni(8%)-γ-Al_2O_3 (M16-M17)

Modules M16 and M17 are designed based on the use of Ni(8%)-γ-Al_2O_3 as catalyst. The process consists of an adiabatic reactor whose entrance temperature is 250°C operated at 176 atm. Conversion reported under these conditions is 35%. The products of the reactor are first split in a flash drum operated at 40°C and 5 atm. This drum separates the non-condensable fraction, mainly hydrogen, from the condensable products, mainly higher alcohols, waste water, and unconverted ethanol. The non-condensable portion is used for electricity generation. The liquid fraction is sent to a distillation column whose bottom product consist of higher alcohols (C4+), and whose top product is a nearly azeotropic mixture of water and ethanol. This azeotropic mixture is subsequently dehydrated in a molecular sieving unit and then used as a recycle stream. A second flash drum is used to remove a small fraction of byproducts present in the recycle stream thus preventing the build up of minor species. Modules M16 and M17 differ from each other in the presence/absence of a second distillation column (dashed square in Figure S6.7). The function of this second column is to separate butanol from other higher alcohols.

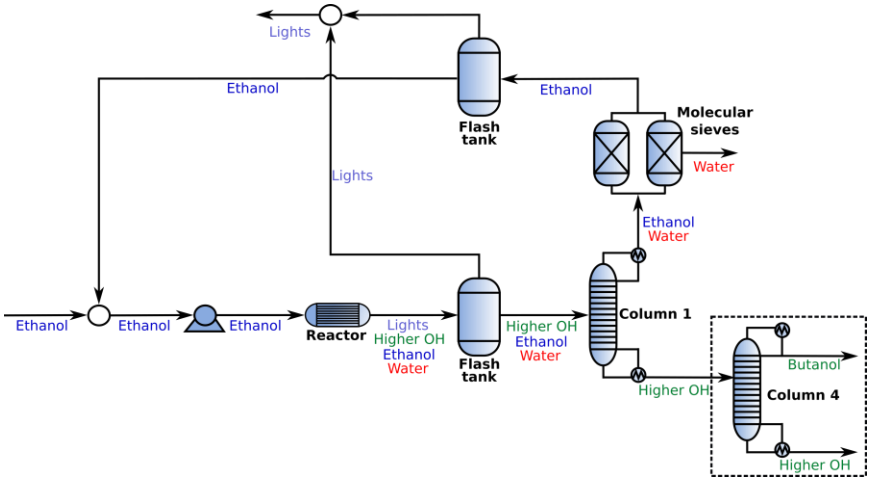

Figure S6.8 Processes for Guerbet coupling of ethanol condensation using *Ni(8%)-γ-Al_2O_3*. Column 2 is highlighted using a dashed square to indicate that it is present in M16 but not in M17.

Guerbet coupling of ethanol using Ca-HAP (M18-M20, M25-M27, and M28-M29)

Ca-HAP is a common catalyst used for the Guerbet coupling of ethanol. It is known that depending on the conversion the product profile changes, thus we have synthesized modules for three different single pass conversions: 25% (*M25-M27*) (Figure S6.9), 50% (*M18-M20*) (Figure S6.10), and 75% (*M28-M29*) (Figure S6.11). As an initial approximation we have not considered the use of carrier gases, this simplification reflects the future state of the art rather than current results more focused in characterizing the catalyst. Processes operated at medium and high conversions (50% and 75%) are significantly similar; in contrast, processes operated at low conversion present a completely different layout. This kind of difference has also been reported by Nezam and coworkers[55]. The conversion processes at the three conversion levels can be described in terms of three processing sections: a core section where the reactor is located (light-blue shaded region in Figures S6.9-S6.11), and two satellite sections designed to accomplish the required separations (light-green and light-yellow regions in Figures S6.9-S6.11). The core section consists in all cases of an adiabatic reactor with an inlet temperature of 350°C operated at 1 atm, followed by a flash tank, and a distillation train. The flash tank is operated at atmospheric pressure and a temperature close to 50°C. The flashing operation splits the condensable and non-condensable fractions. We have found that the non-condensable fraction contains a significant amount of unconverted ethanol. Therefore, this fraction is sent to a distillation column that recovers ethanol as a bottom product and obtains light products (hydrogen and ethylene) at the top, ethanol is recycled to the process while the

light products can used for electricity generation or oligomerized to heavier olefins if economically advantageous. This column requires refrigeration but it is not cryogenic. The condensable fraction leaving the flash tank is feed to a distillation train consisting of a single column in the low conversion process, and of two columns in the medium and high conversion processes. In all cases the bottom product of the first column contains higher alcohols and heavy products, and it is essentially water free. The top product on the other hand contains water, ethanol, and in the medium and high conversion processes a portion of the butanol produced in the reaction (approximately 30% of the butanol produced in the 50% conversion design, and close to 100% in the 75% conversion design). In the low conversion process the top product is recycled once fully dehydrated in a molecular sieving unit. In contrast, in the medium and high conversion processes the presence of butanol in the top product makes necessary the use of a second distillation column, that recovers an azeotropic blend of ethanol and water at the top, and an azeotropic blend of butanol and water at the bottom. The top product is dehydrated in a molecular sieving unit and recycled back to the reactor, while the bottom product is sent to the first satellite separation section (light yellow region) where distillation operations and phase separations are used to break the azeotrope, such that pure butanol can be recovered. This satellite section is only required in the medium and high conversion processes (Figures S6.10-S6.11). In all cases there is a second separation satellite section (light green area) consisting of a train of distillation columns. These columns are responsible of fractionating the produced higher alcohols. The number of columns in this section is the fundamental difference among modules designed to operate with the same reactor conversion (*e.g. M25-M27*).

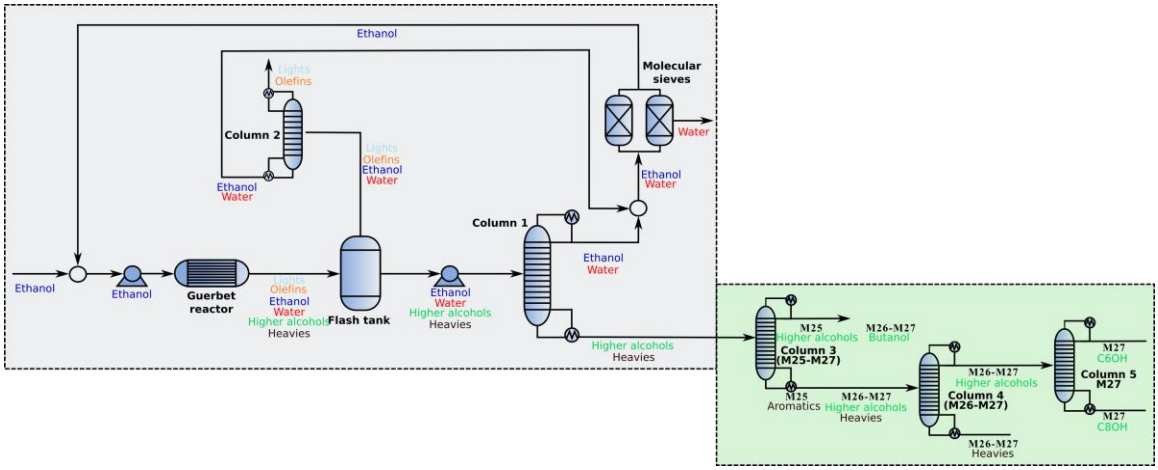

Figure S6.9 Processes for Guerbet coupling of ethanol using Ca-HAP with 25% conversion (M25-M27). Optional columns used in modules M25-M27 are indicated in the green area.

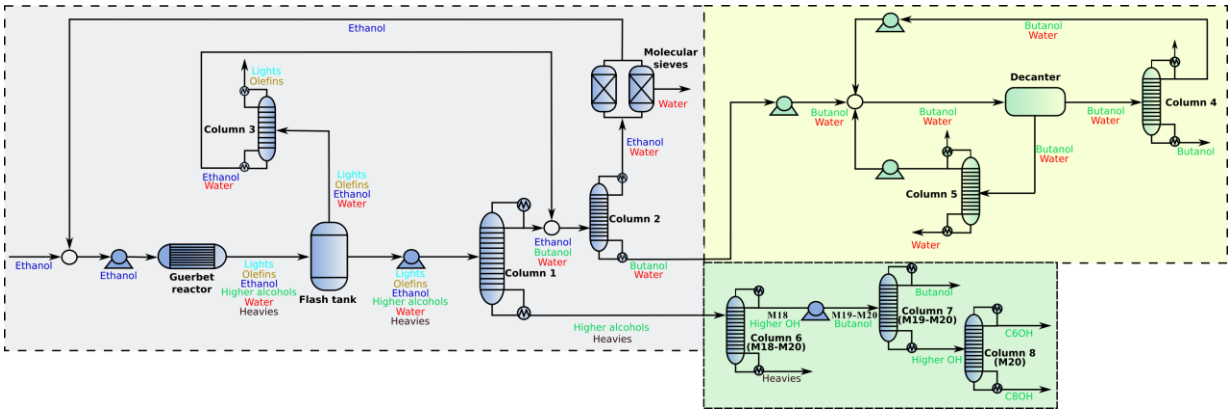

Figure S6.10 Processes for Guerbet coupling of ethanol using Ca-HAP with 50% conversion (*M18-M20*)). Optional columns used in modules M25-M27 are indicated in the green area.

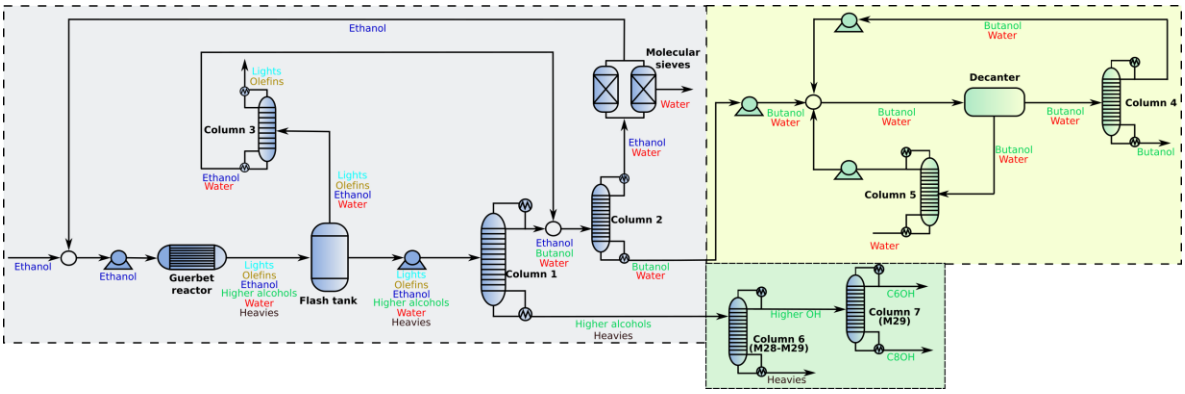

Figure S6.11 Processes for Guerbet coupling of ethanol using Ca-HAP with 75% conversion (M28-M29). Optional columns used in modules M28-M29 are indicated in the green area.

Guerbet coupling of ethanol using Pa-Hydrotalcite (M21-M22)

In terms of layout the processes designed using Pa-Hydrotalcite (Figure S6.12) as catalyst are similar to those described for Ca-Hap with 50% or 75% conversion. There are however some slight differences: First, the ethanol recoverty column used to split the gas stream leaving the flash tank is not used in this case. Second, the fraction of butanol that is send to the butanol recovery section (light yellow area) changes, and in this case is 72%. Third, the catalyst conversion achived is 63%. Finally, the alcohol fractionation section is also differenet such that only one column is required. This column is preent in Module 22, and absent in module 21.

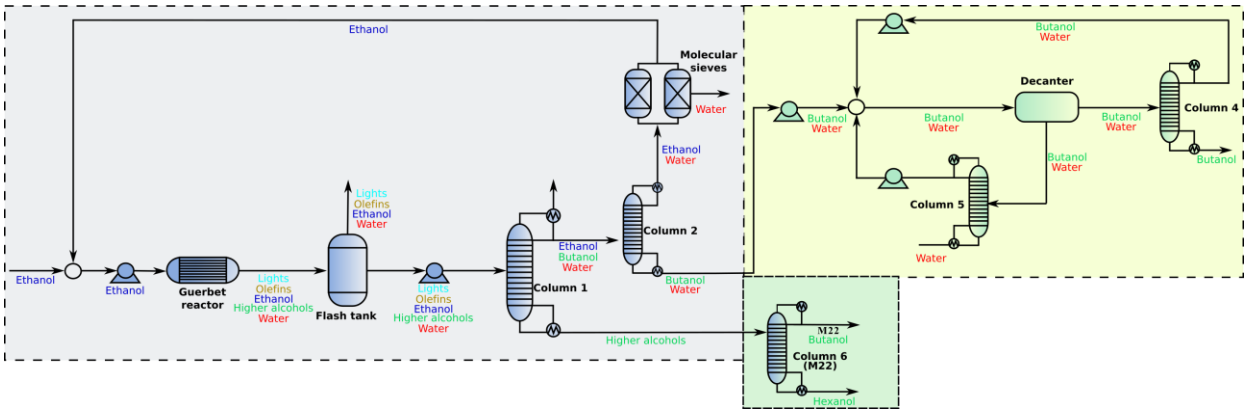

Figure S6.12 Processes for Guerbet coupling of ethanol using *Pa-Hydrotalcite* (M21-M22). Optional columns used in modules M21-M22 are indicated in the green area.

Guerbet coupling of ethanol using Pd-MgO (M23-M24)

The process used for the Guerbet coupling of ethanol using Pd-MgO is presented in Figure S6.14. The layout is similar to the one previously described (see Pd-Hydrotalcite catalyst and CA-HAP). However, the operating conditions of the different unit operations are different. Specifically, the adiabatic reactor used requires an entrance temperature of 250°C, and operates at 34 atm. Furthermore, in this case we have considered the use of nitrogen as a carrier gas. This implies the use of a multistage compressor to feed make-up nitrogen to the system, as well as the installation a carrier gas recycle loop. Recovery of most of the nitrogen and its recycling is enabled by the high-pressure operation (34 atm) of the flash drum. An additional advantage of operating this drum at high pressure is the increased efficiency in condensing unconverted ethanol and products of the condensation reaction. As in previous cases we show in Figure S6.13 optional distillation columns in a green square area. In this case we have one column which is absent in M23, and present in M24.

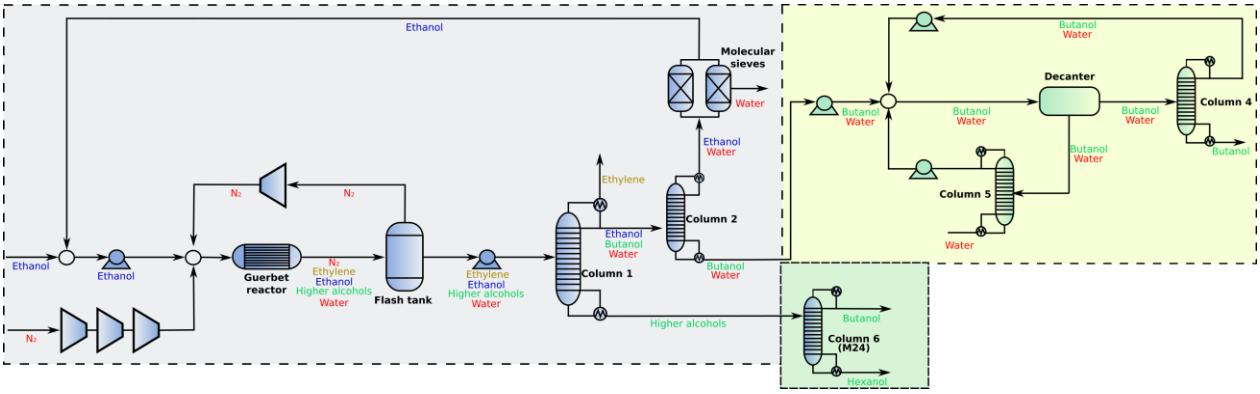

Figure S6.13 Processes for Guerbet coupling of ethanol using Pd-MgO (M23-M24). Optional columns used in modules M23-M24 are indicated in the green area.

S6.5 Ethylene oligomerization

Processes for ethylene oligomerization using Ni-LASA as catalyst (M30-M32)

The oligomerization of ethylene using Ni-LASA catalyst (Figure S6.14) proceeds in a furnace reactor operated at 300°C and 15 atm, conversion under these conditions is close to 50%. The separation system consists of a flash drum operated at -5°C and the reactor pressure. This flash drum produces a gas stream containing mainly ethylene that is recycled back to the reactor and a liquid stream that is send to a cryogenic distillation column (Column 1). The top product of this column is ethylene which is recycled. The bottom product contains the products of the oligomerization reaction (O4+ olefins), and it is fed to a sequence of distillation columns (number of columns varies between M30-M32). These columns are responsible for fractionating the oligomerization products into different olefins as indicated in the figure. In addition to the elements described the system requires the installation of a multistage compressor used to increase the pressure of the ethylene feed.

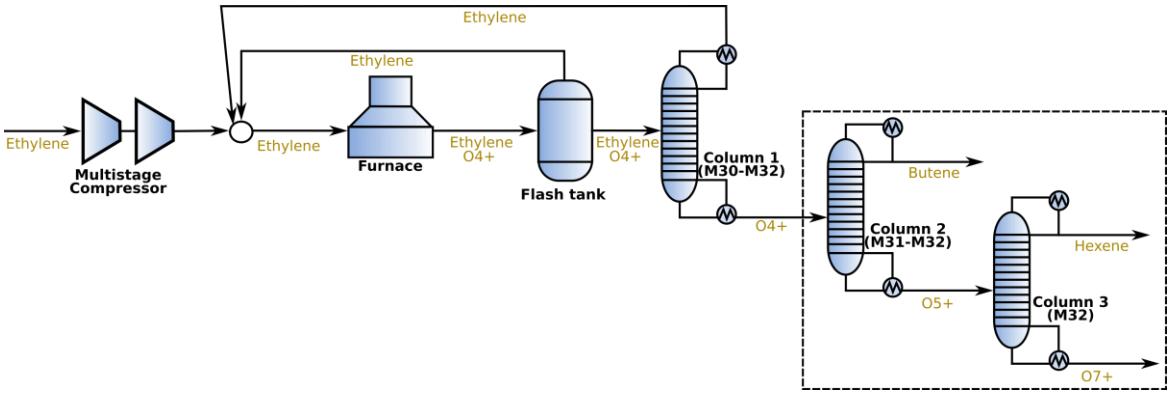

Figure S6.14 Processes for ethylene oligomerization using Ni-LASA as catalyst (M30-M32). Optional columns used in modules M30-M32 are indicated by a dashed square.

Processes for ethylene oligomerization using HZSM-5 as catalyst (M33-M35)

Processes for the oligomerization of ethylene using HZSM-5 (Figure S6.15) occur in a furnace reactor operated at 450°C, at atmospheric pressure, conversion under these conditions reaches 58%, making necessary a design with recycle streams. The product of the reactor is pressurized to 9 atm by means of a multistage compressor equipped with and intermediate condensation drum. The compressed product is fed to a distillation column that produces as a top product a blend of ethylene and methane, and as a bottom product a blend of O3+ olefins. The top product of is further pressurized to 40 atm using a pump and sent to a second distillation column where methane and ethylene are fractionated. Methane

is used for electricity generation while ethylene is recycled to the reactor. On the other hand, the bottom product of the first column is sent in M34 and M35 to a distillation train characteristic of each module. Products of this distillation train are olefin streams of different composition.

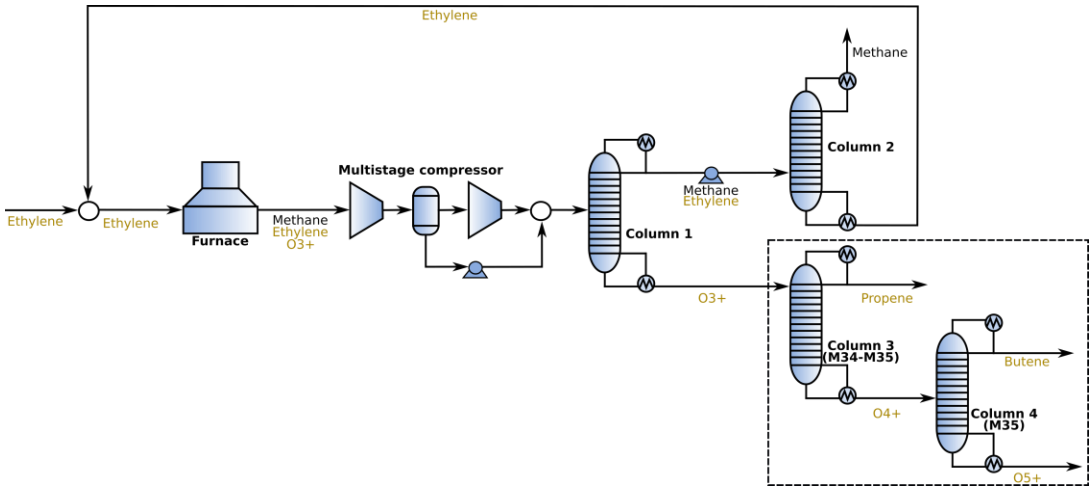

Figure S6.15 Processes for ethylene oligomerization using HZSM-5 as catalyst (M33-M35). Optional columns used in modules M33-M35 are indicated by a dashed square.

Alphabutol™ (M36) and Alphaselect™ (M37) processes

The Alphabutol™ and Alphaselect™ processes are based on the use of a homogenous catalysts. These processes are commercial and can be licensed by companies if required. Economic and process data are available in the work of Forestiere and coworkers[72].

Processes for ethylene oligomerization using NiSAIB as catalyst (M38-M40)

The oligomerization of ethylene in the nickel-based catalyst NiSAIB proceeds at 120°C and 35 atm, reaching 100% conversion (Figure S6.16). Since the temperature is lower the reactor is designed as a heat exchanger. The output of the reactor consists of a blend of O4+ olefins, that is fed in modules M39-M40 to a train of distillation columns that split the product into different fractions of interest. The use of a multistage compressor is required to pressurize the incoming ethylene fed.

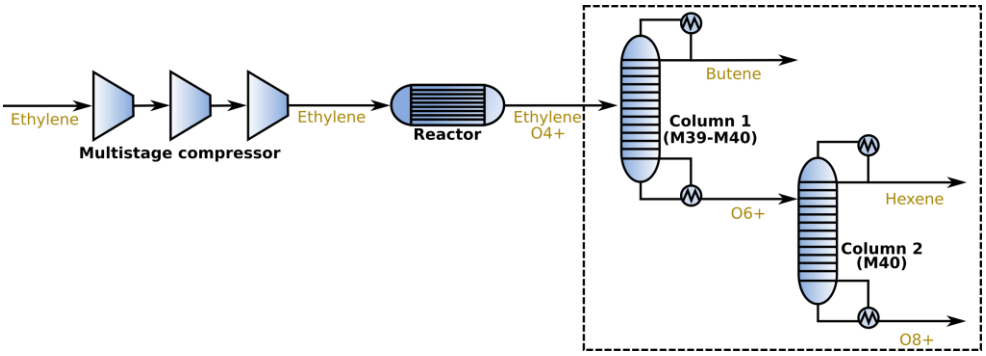

Figure S6.16 Processes for ethylene oligomerization using NiSAIB as catalyst (M38-M40). Optional columns used in modules M38-M40 are indicated by a dashed square.

Processes for ethylene oligomerization using NiAISBA as catalyst (M41-M43)

The layout of processes for the oligomerization of ethanol using NiAISBA as catalyst is shown in Figure S6.17. The process, which is very similar to the one used with Ni-LASA (Figure S6.14), consists of a reactor operated at 10 atm and 150°C. The reactor reaches a single pass conversion of 60%, and

considering the operating temperature is designed as a heat exchanger. Products from the reactor are fed to a flash tank that recovers unconverted ethylene. The liquid fraction from the flash drum is fed to a distillation column (Column 1). This column recovers the remaining ethylene still present, and produces a bottom stream containing the oligomerization products. Finally, the oligomerization products are fed to a distillation train for further fractionation.

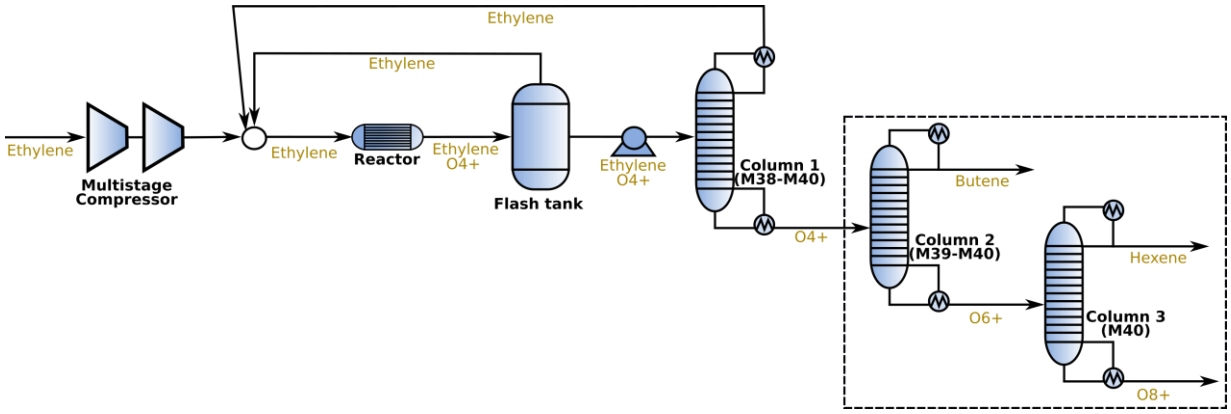

Figure S6.17 Processes for ethylene oligomerization using NiSAIB as catalyst (M38-M40). Optional columns used in modules M38-M40 are indicated by a dashed square.

Chevron-Philips™ processes for ethylene oligomerization (M44-M46)

The Chevron-Phillips process for the oligomerization of ethylene is well known, in this work we have followed, with some modifications, the layout presented by Lapin and coworkers[73] (Figure S6.18). Briefly, the process consists of a homogeneous reactor that operates at high temperature (180°C) and pressure (230 atm). The reactor reaches a single pass conversion close to 90% and it is followed by flash tank (operated at 29 atm and 60°C) whose gas product is recycled and consists mainly of ethylene. The liquid product of the flash tank contains the reactor products as well as the catalyts, this product is fed to a quenching tower where the catalyst reacts with sodium hydroxide. This quenching tower has been modelled in this work by means of a stochiometric reactor. The product of the quenching tower is fed to a decanter such that an aqueous phase containing catalyst is produced and a product phase containing mainly hydrocarbons is obtained. The product phase is dehydrated in a molecular sieve unit, and then fed to a cryogenic distillation column that recovers the remaining ethylene as a top product, and produces a blend of olefins at the bottom. This olefin blend is finally fed to a distillation train for further fractionation.

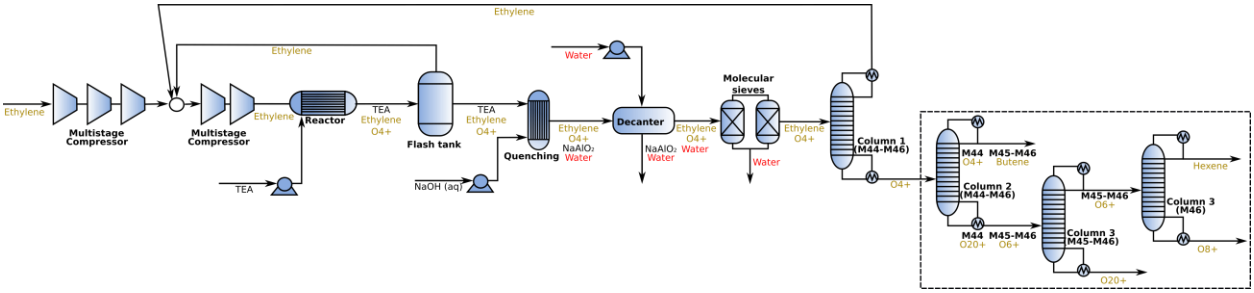

Figure S6.18 Chevron-Phillips process for the oligomerization of ethylene (M44-M46).

S6.6 Propene oligomerization

Processes for propene oligomerization using Ni-HZSM-5 as catalyst (M47-48)

Oligomerization of propene in a Ni-HZSM-5 catalyst proceeds in reactor designed as a heat exchanger operated at 270°C and 34 atm. Single pass conversion achieved is close to 75%. Since the

reactor operates at high pressure the process requires the installation of a compression system comprised of a multistep compressor and a pump. The separation process associated consists first of a distillation column that recovers unreacted propene as a top product. This column produced in its bottoms a blend of oligomerization products. This stream constitutes the final product (M47) or can be sent to further fractionation in a second distillation column (M48).

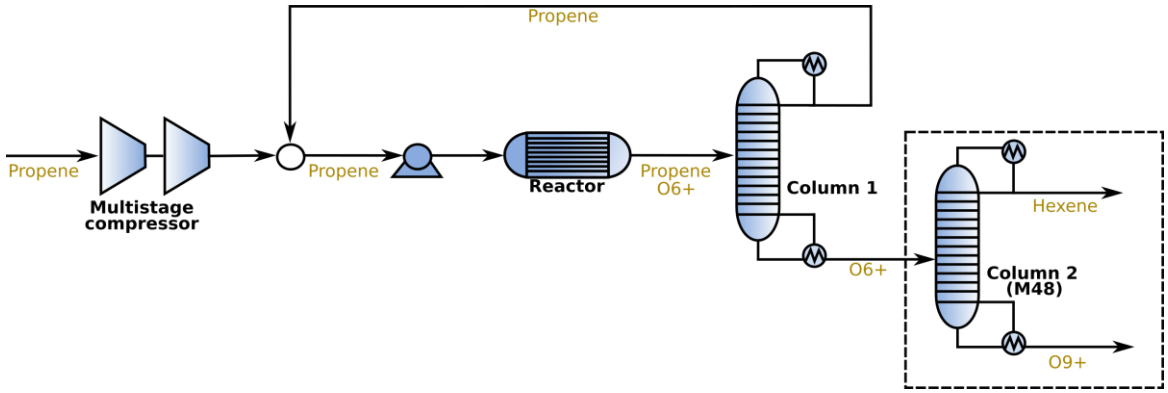

Figure S6.19 Processes for the oligomerization of propene Ni-HZSM-5 as catalyst (M47-48). Optional columns are shown surrounded by a dashed square.

Processes for propene oligomerization using Pell-SAPO-11 (M49-M50) or HZSM-23 (M51-M52) as catalysts

Processes flowsheets for the oligomerization of propene in Pell-SAPO-11 or HZSM-23 catalysts are identical and very simple (Figure S6.20). They differ from each other in the operating conditions: in the case of Pell-SAPO-11 the reactor operates at 50 atm and 220°C; in contrast, for HZSM-23 the reaction proceeds at 35 atm and 250 °C. In both cases 100% conversion is attained. The process flowsheet required consists of an initial compression system , followed by a reactor and an optional distillation column (used in M50 and M52). The compression system contains a multistage compressor followed by a pump, and the reactor is designed as a heat exchanger.

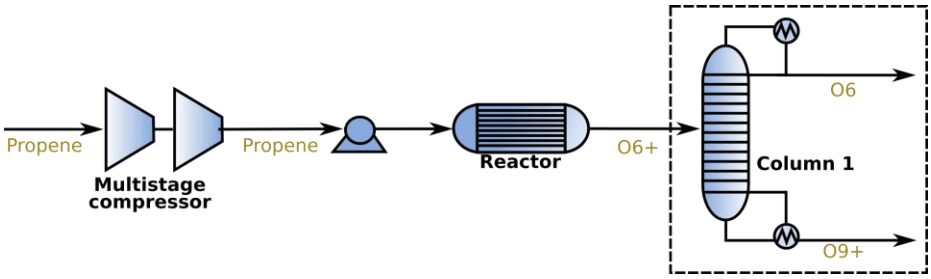

Figure S6.20 Processes for the oligomerization of propene using Pell-SAPO-11 (M49-M50) or HZSM-23 (M51-M52) as catalyst. Optional columns are shown surrounded by a dashed square.

Processes for propene oligomerization using SO_3-10%-NiO-γ-Al_2O_2 (M53-M54)

The oligomerization process of propene in SO_3-10%-NiO-γ-Al_2O_2 (Figure S6.21) proceeds at 50°C and 35 atm, reaching a single pass conversion close to 85%. The reactor is designed as a heat exchanger, and operates using propane as a carrier. The ratio of propene/propane at the reactor entrance is adjusted to be 0.25. The products of the reactor are fed to a distillation column that separates the carrier and the unreacted propene and recycle them back to the reactor. The bottom product of this column constitutes the final product in M53, or it is fed to a second column for further fractionation in M54. Since the reaction proceeds at high pressure we use a multistage compressor and a pump to raise the pressure of the fed streams to the reaction conditions.

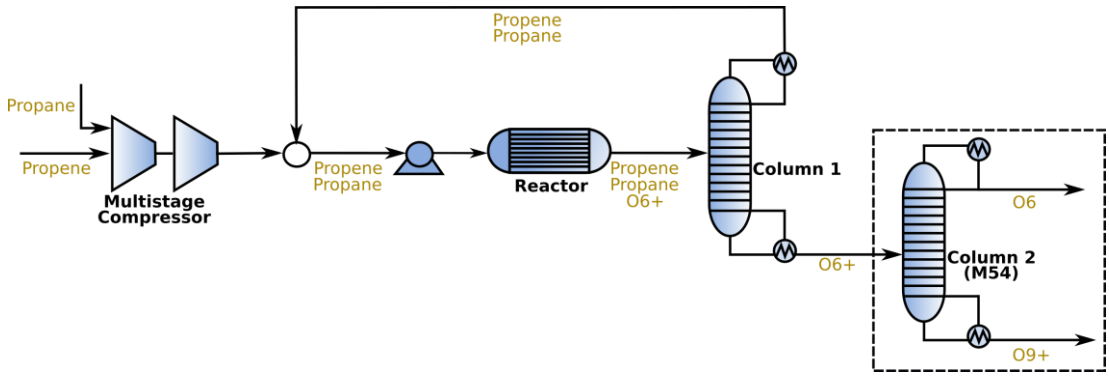

Figure S6.21 Processes for the oligomerization of propene using SO_3-10%-NiO-γ-Al_2O_2 as catalyst (M53-M54). Optional columns are shown surrounded by a dashed square.

S6.7 Oligomerization of isobutene blends

Process for isobutene oligomerization using H-Zeolite-Y-P (M55)

Isobutene oligomerization using HY zeolite can be performed at 100°C and atmospheric pressure. Conversion under these conditions reaches 93% such that only a small recycle stream is needed. The process occurs in a reactor designed as a heat exchanger (Figure S6.22). The separation train consist of a single distillation column responsible for recovering the unreacted isobutene and yielding O8+ olefins as a bottom product.

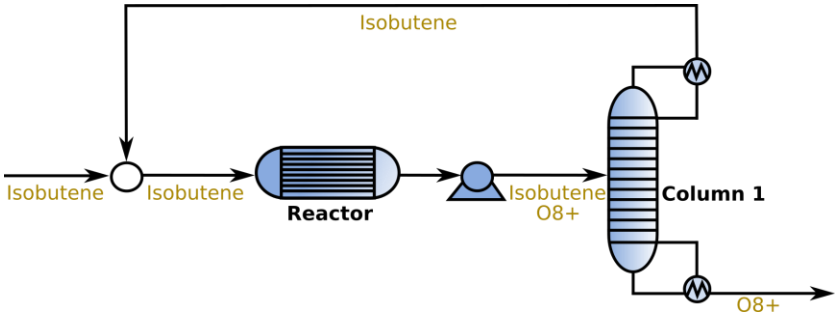

Figure S6.22 Process for the oligomerization of isobutene using H-Zeolite-Y-P as catalyst (M55).

Process for isobutene oligomerization using Sulfated titania (M56)

Isobutene oligomerization using sulfated titania as catalyst (Figure S6.23) occurs in a reactor designed as a heat exchanger that operates at 140°C and 40 atm. The reactor reaches 100% single pass conversion, thus no recycle streams are needed. The product obtained does not require separation operations and consists of a O8+ blend of olefins. Pressurization to the reactor conditions is achieved in a two-stage compressor followed by a pump.

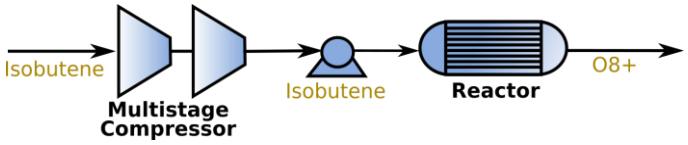

Figure S6.23 Processes for the oligomerization of isobutene using Sulfated titania as catalyst (M56).

S6.8 Oligomerization of propene/isobutene blends

Oligomerization of propene/isobutene blends using SPA (M57-M58) or MTW-10%P-H_3PO_4 (M61-M62)

The oligomerization of propene/isobutene blends using solid phosphoric acid (SPA) or MTW-10%P-H_3PO_4 occurs in a heat exchanger reactor operated at 160°C and 35 atm in both cases (Figure S6.24). The single pass conversion for both propene and isobutene is 65% in SPA, and 50% in MTW-10%P-H_3PO_4. The products from the reactor are fed to a distillation column that recovers unreacted propene and isobutene as a distillate, and at the bottom produces O6+ olefins. This blend constitutes the final product in M57 and M61, or it is fed to a second column for further fractionation in M58 and M62.

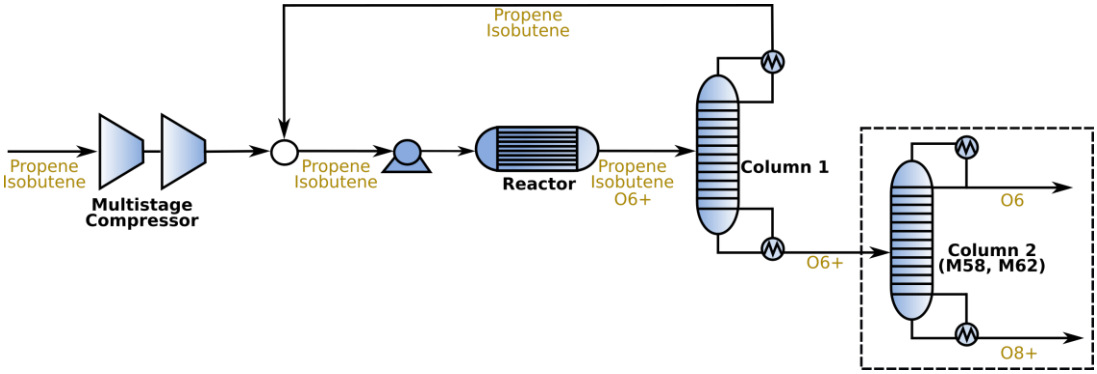

Figure S6.24 Processes for the oligomerization of propene/isobutene blends using SPA as catalyst (M57-M58). Optional columns are shown surrounded by a dashed square.

Process for the oligomerization of propene/isobutene blends using CT275 (M59-M60)

The process for the oligomerization of propene/isobutene blends using CT275 (Figure S6.25) consists of a reactor designed as a heat exchanger, a multistage compressor required to reach the operating conditions, and an optional distillation column that is used in M60 to split the product into a fraction rich in O6 olefins and another fraction rich in O8+ olefins. The reactor operates at 120°C and 14 atm and reaches a 100% conversion.

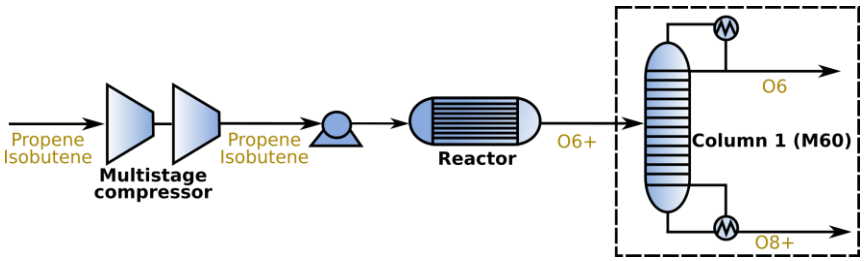

Figure S6.25 Processes for the oligomerization of propene/isobutene blends using CT275 as catalyst (M59-M60). Optional columns are shown surrounded by a dashed square.

S6.9 Butene oligomerization

Processes for the oligomerization of butene using ATHZ5-Cs (M63-M64)

Butene oligomerization using ATHZ5-CS, proceeds in a furnace reactor operated at 300°C and 15 atm (Figure S6.26). The reactor reaches a 100% single pass conversion. Compression of butene to the reacting pressure is achieved by using a compressor followed by a pump. A distillation column is used in M64 to fractionate the reactor products into an O6 rich olefin mixture (top product) and an O8+ olefin mixture (bottom product).

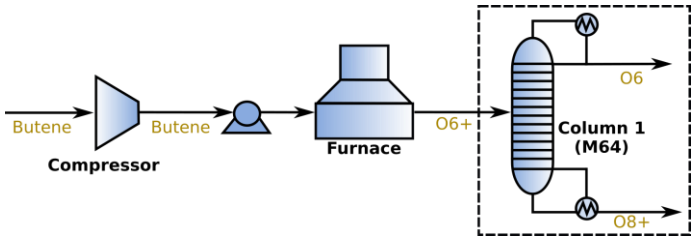

Figure S6.26 Processes for the oligomerization of butene using ATHZ5-Cs as catalyst (M63-M64). Optional columns are shown surrounded by a dashed square.

Processes for the oligomerization of butene using HZSM-57 (M65-M66)

Oligomerization of butene using HZSM-57 proceeds at 200°C and 70 atm in a reactor designed as a heat exchanger (Figure S6.27). The reaction takes place in the presence of propane as diluent such that the molar ratio of butene/propane at the entrance of the reactor is equal to one. Butene conversion under these conditions is close to 80%. The products of the reactor are fed to a distillation column (Column 1), the top product of this column contains the diluent and unreacted butene, this top product is recycled back to the reactor. The bottom product of the first distillation column consist of O6+ olefins and constitutes the final product in M65. On the other hand, in M66 this bottom product is fed to a second distillation column (Column 2) that separates the O6 fraction at the top and O8+ products at the bottom. Compression of the fed products to the reaction conditions is achieved by means of a multistage compressor followed by a pump.

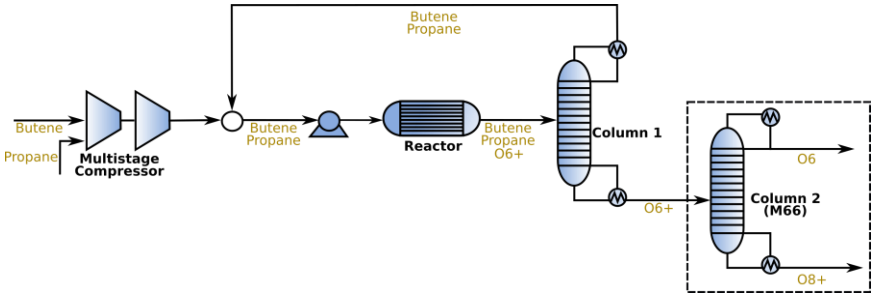

Figure S6.27 Processes for the oligomerization of butene using HZSM-57 as catalyst (M65-M66). Optional columns are shown surrounded by a dashed square.

Process for the oligomerization of butene using 2A-Co-C-230 (M67) or ASA-13 (M68)

Oligomerization of butene using 2A-Co-C-230 or ASA-13 (M68) occurs in a heat exchanger reactor, operated at 80°C and 31 atm in the first case, or 120°C and 35 atm in the second one (Figure S6.28). Single pass conversion in the reactor is 30% (2A-Co-C-230) or 76% (ASA-13). The products of the reactor are feed to a distillation column, such that the distillate (constituted mainly of unreacted butene) is recycled back to the reactor; the bottom product consist of C8+ olefins and constitutes the final product. Pressurization of the fed is achieved using a single stage compressor connected in series with two pumps.

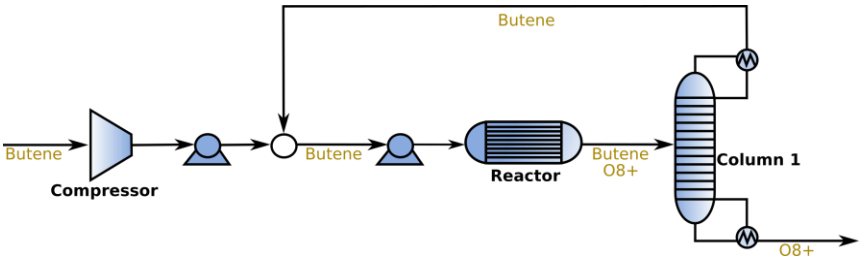

Figure S6.28 Processes for the oligomerization of butene using 2A-Co-C-230 (M67) or ASA-13 (M68) as catalysts.

Process for the oligomerization of butene using HZSM5 (M69)

The process for the oligomerization of butene using HZSM5 zeolite is very simple (Figure S6.29), it consists of a heat exchanger reactor operated at 230°C and 40 atm that achieves 100% conversion. The fed to the module is pressurized using a single stage compressor followed by a pump. There is no need for separation operations in this case.

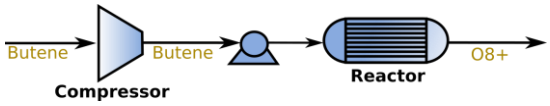

Figure S6.29 Processes for the oligomerization of butene using HZSM5 (M69).

S6.10 Hexene oligomerization

Process for the oligomerization of hexene using SO_4/ZrO_2 (M70)

Oligomerization of hexene in SO_4/ZrO_2 is performed in a heat exchanger reactor operated at 100°C and 8 atm (Figure S6.30). The reactor reaches a single pass conversion of 85%. The reactor products are fed to a distillation column producing unreacted hexene at the top and O12+ olefins at the bottom. Since the reactant is liquid pressurization to the reactor conditions only requires a pump.

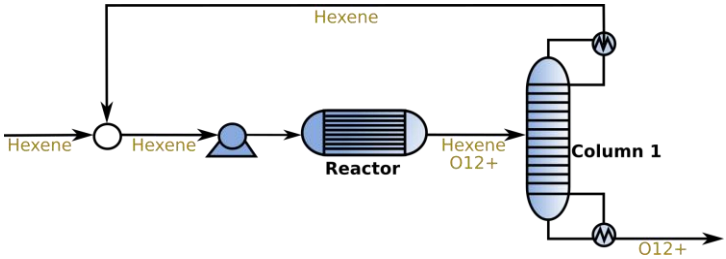

Figure S6.30 Processes for the oligomerization of hexene using SO_4/ZrO_2 (M70).

S6.11 Octene oligomerization

Processes for the oligomerization of octene using ASA (M71) or HZSM-5 (M72)

Process flowsheets for the oligomerization of octene using ASA or HZSM-5 are identical (Figure S6.31), and consist of a reactor operated at 150°C and 40 atm in the first case, or at 170°C and 40 atm in the second one. Conversion reaches a value of 70% for ASA and 50% for HZSM-5. The products of the reactor are split in a distillation column that produces a recycle stream rich in octene, and a product stream containing O12+ olefins.

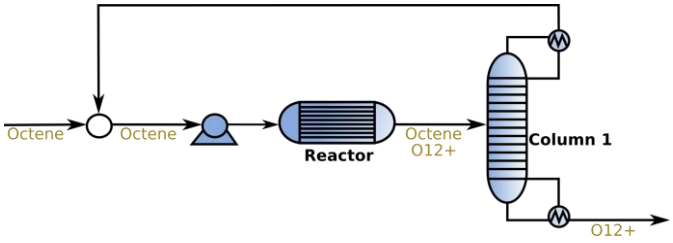

Figure S6.31 Processes for the oligomerization of octene ASA (M71) or HZSM-5 (M72)

S6.12 Oligomerization of olefin blends O3-O8

Process for the oligomerization of octene using ATHZ5-Cs (M73)

The product composition obtained after the oligomerization of a blend of olefins is a function of the fed composition. In this work we have synthesized a process (Figure S6.32) making some simplifying

assumptions: first, we have assumed that the conversion of individual species is not a function of the fed composition; and second, we have assumed that the product distribution obtained is the result of the self-oligomerization of the species present in the fed. Although these are strong assumptions they allow to have a first approximation to the problem without the need of implementing more complex kinetic models. The process designed is based on the use of ATHZ5-Cs, a catalyst effective in the oligomerization of individual olefins in the range O3-O8. We have assumed that an oligomerization temperature of 200°C at 40 atm is sufficient to achieve conversions of 90% for O4-O5, 85% for O6-O7, and 50% for O8, these values are consistent with experimental values observed for the pure species under similar conditions[15]. Importantly, nor ethylene neither olefins with more than eight carbons are oligomerized to any extent. The process proceeds in a heat exchanger reactor. Products of the reactor are fed to a distillation column such that the top product contains olefins in the range O3-O8 that are recycled, while the bottom product contains O9+ olefins that constitute the final module product. Pressurization of the feed is done by means of a single stage compressor and a pump.

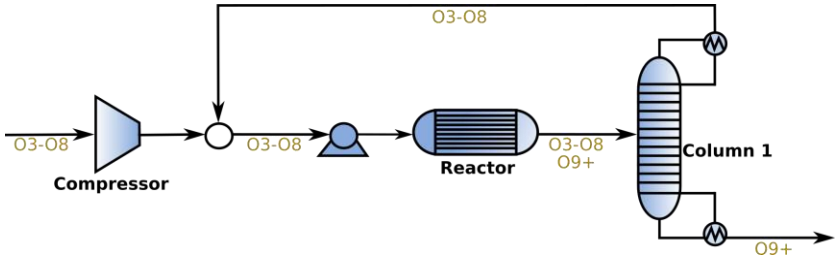

Figure S6.32 Processes for the oligomerization of olefin blends (O3-O8) using ATHZ5-Cs as catalyst (M73)

S6.13 Butanol dehydration

Process for the butanol dehydration using AM-11 (M74)

Butanol dehydration proceeds in a heat exchanger reactor operated at 250°C and atmospheric pressure (Figure S6.33). Conversion under these conditions is 100%. The product of the reactor consists of water and butene. These products are separated first using a flash tank refrigerated to 15°C and operated at 1 atm, followed by a distillation column whose top product is butene and whose bottom product is waste water.

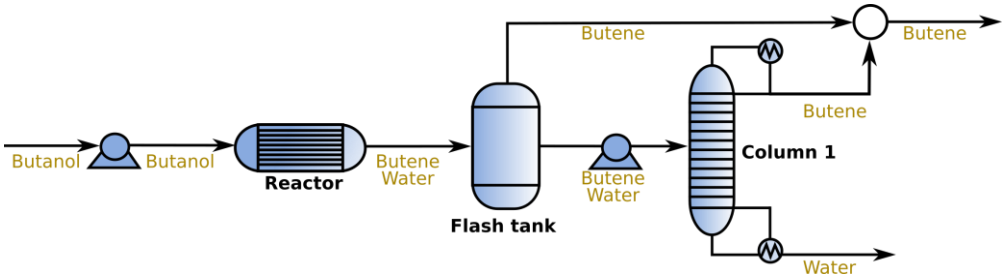

Figure S6.33 Process for butanol dehydration using AM-11 as catalyst (M74).

S6.14 Butanol etherification

Process for butanol dehydration using Amberlyst-70 (M75)

Etherification of butanol proceeds at 250°C and 20 atm in an isothermal reactor that reaches a 65% single pass conversion. Products of the reaction include ethers of eight carbons, water resulting from the partial dehydration and a small amount of butene, resulting from a side reaction (Figure S6.34). The separation process makes use first of a decanter. This decanter produces a waste water stream, and an organic stream that is fed to a distillation train consisting of two columns. The first of these columns yields ethers as a bottom product and a mixture of olefins, unreacted butanol and water at the top. The top

products is further separated in a second column that produces an azeotropic blend of butanol and water at the top, and pure butanol at the bottom. The azeotropic blend is recycled to the decanter, while the butanol stream is recycled to the reactor. This second column is designed using a partial condenser. The gas stream leaving the partial condenser contains a blend of butene, water and butanol and it is used for electricity generation.

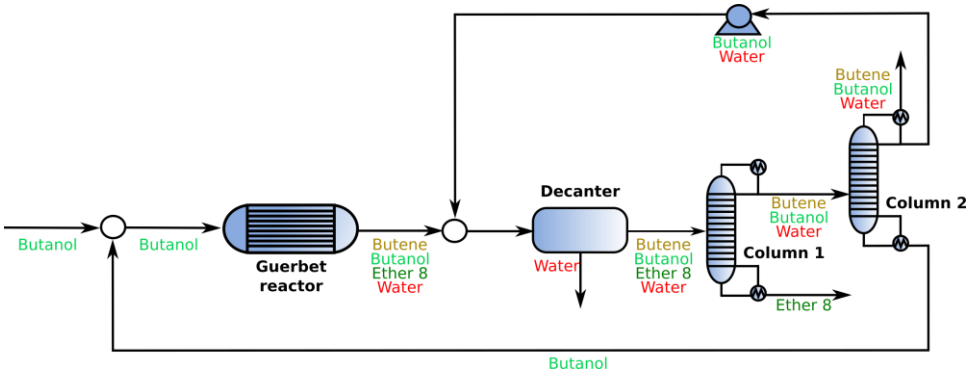

Figure S6.34 Process for butanol etherification using Amberlyst 70 as catalyst (M75).

S6.15 Guerbet coupling of butanol

Process for Guerbet coupling of butanol using Ca-HAP (M76)

Guerbet coupling of butanol proceeds in an adiabatic reactor operated at atmospheric pressure with an entrance temperature of 375°C (Figure S6.35). Under these conditions butanol conversion reaches 65%. The main product of the condensation reaction is 2-ethyl-hexanol; other co-products and by-products include olefins (O4 and O8), aldehydes (Al4 and Al8), heavy species, and hydrogen. Additionally, waste water is formed during the reaction. The reactor products are fed to a flash drum. The gas stream leaving this drum consists mainly of hydrogen and is used for electricity generation. On the other hand, the liquid stream contains the condensable species, this stream is fed to a distillation column (Column 1) that splits the products such that at the bottom of the column 2-ethyl-hexanol and heavy products are obtained; while all other species are sent to the top. The bottom product is fractionated in Column 3, obtaining 2-ethyl-hexanol as a top product and heavy products at the bottom. The distillate stream is the main product of the module, while the bottom stream is used for electricity generation. The top product of the first column is sent to Column 2, this column produces a blend of O8 olefins and butanol as a bottom product, and a blend of butanol, butanal, and water at the top. The bottom product is split in Column 6 producing butanol that recycled to the reactor, and O8 olefins that are products. The top product, on the other hand, is send to a separation sub-system consisting of a decanter, and Columns 3 and 4, this systems enabes the recovery of the remaining butanol and butanal (top product of Column 4), which are recycled to the reactor. The subsystem also produce waste water as a product (decanter).

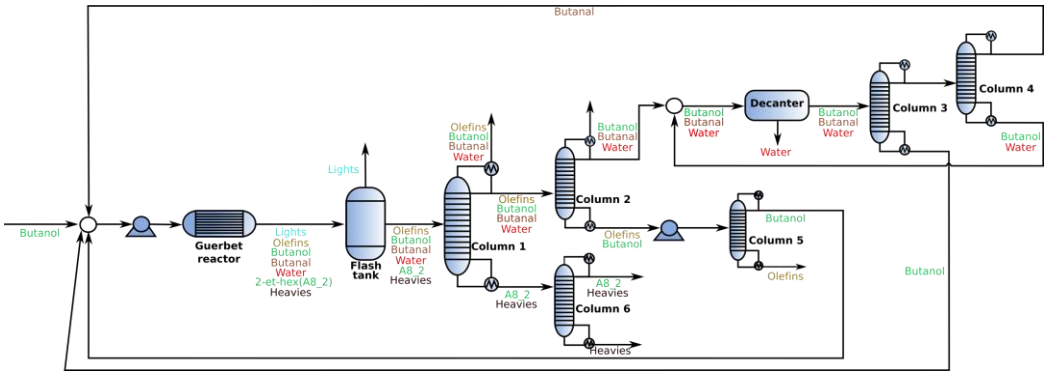

Figure S6.35 Process for Guerbet coupling of butanol Ca-HAP as catalyst (M76).

S6.16 Hexanol dehydration

Process for Hexanol dehydration using Syndol® catalyst (M77)

The dehydration of hexanol using Syndol® catalyst proceeds in an isothermal reactor designed as a furnace (Figure S6.36). The reactor is operated at 350°C and atmospheric pressure. Conversion reaches 94%. The products of the reactor are separated by means of a simple separation train consisting of a three-phase decanter and a distillation column. The decanter, operated at 35°C and 1 atm, produces a gas stream consisting of light species (mainly hydrogen), additionally two liquid streams are obtained, one organic containing unconverted hexanol and hexene, and one containing mostly water that is sent for waste treatment. The liquid organic phase leaving the flash drum is separated in the distillation column, such that pure hexene is obtained as a top product, and unreacted hexanol at the bottom, this bottom product is recycled back to the reactor.

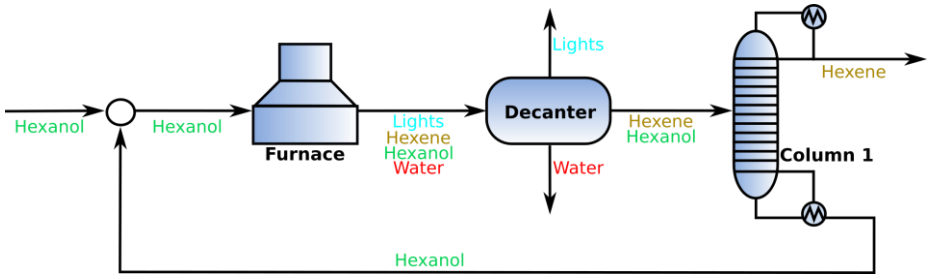

Figure S6.36 Process for hexanol dehydration using Syndol® catalyst (M77).

S6.17 Hexanol etherification

Process for Hexanol etherification using Amberlyst 70 catalyst (M78)

The etherification of hexanol using Amberlyst 70 is performed in an isothermal reactor operated at 150°C and 20 atm, single pass conversion in this system is 77%. Products from the reactor include ethers of 12 carbons (E12), a minor amount of hexene (O6), and water. These products are fed to a distillation column that recovers the ether fraction as a bottom product; and the olefins, water and unreacted alcohol at the top. The water-hexanol mixture obtained at the top of Column 1 presents an azeotrope, which is broken by using a phase splitting unit, followed by a distillation column (Column 2). This distillation column produces almost pure hexanol at the bottom, which is recycled to the reactor; and the azeotropic blend of water and hexanol at the top which is recycled to the decanter for phase splitting.

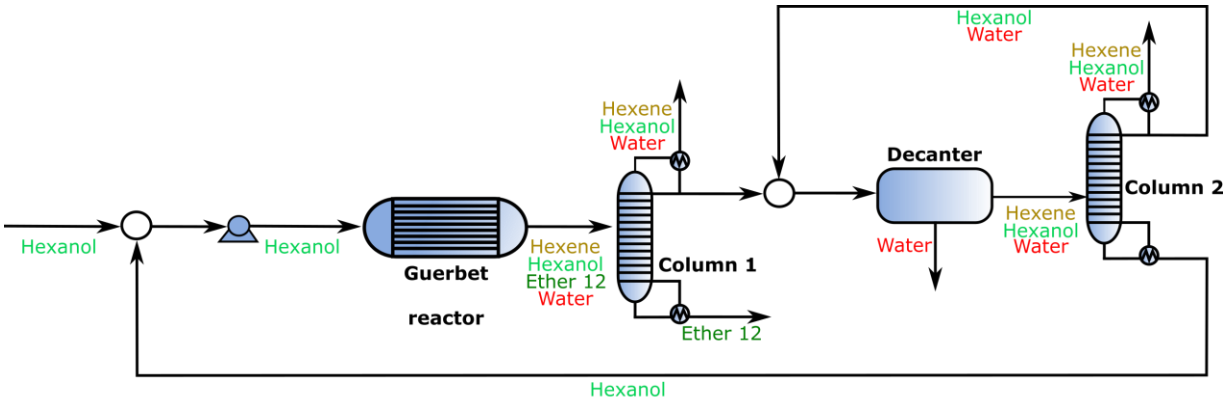

Figure S6.37 Process for hexanol etherification using Amberlyst 70 as catalyst (M78).

S6.18 Guerbet coupling of hexanol

Process for Guerbet coupling of hexanol using Ca-HAP (M79)

The process designed for the Guerbet Coupling of hexanol consists of an adiabatic reactor with an entrance temperature of 375°C and operated at atmospheric pressure, followed by a separation train (Figure S6.38). In the reactor hexanol reaches 75% single pass conversion. The product consists of a blend of higher alcohols (A12), olefins (O6 and O12), aldehydes (Al6 and Al12), light products (mainly H_2), heavy products, and waste water. Products of the reactor are first fed to a flash drum operated at 35°C and atmospheric pressure. The gas stream leaving this drum contains most of the hydrogen, while the liquid stream contains all other condensable species. This liquid stream is fed to a distillation column that split the product in two fractions: the bottom product containing the species with 12 carbon atoms or more (*i.e.* A12, O12, Al12, and heavy products), and the distillate containing other products (A6, O6, Al6, and water). The bottom product of the first column is further separated in a second column (column 3) yielding an olefin rich stream as top product and A12 alcohols at the bottom. On the other hand, the top product of Column 1 is fed to a sub-system consisting of a decanter and a distillation column, this subsystem is designed to break the azeotrope existing between hexanol and water allowing to separate the unreacted hexanol from the waste water.

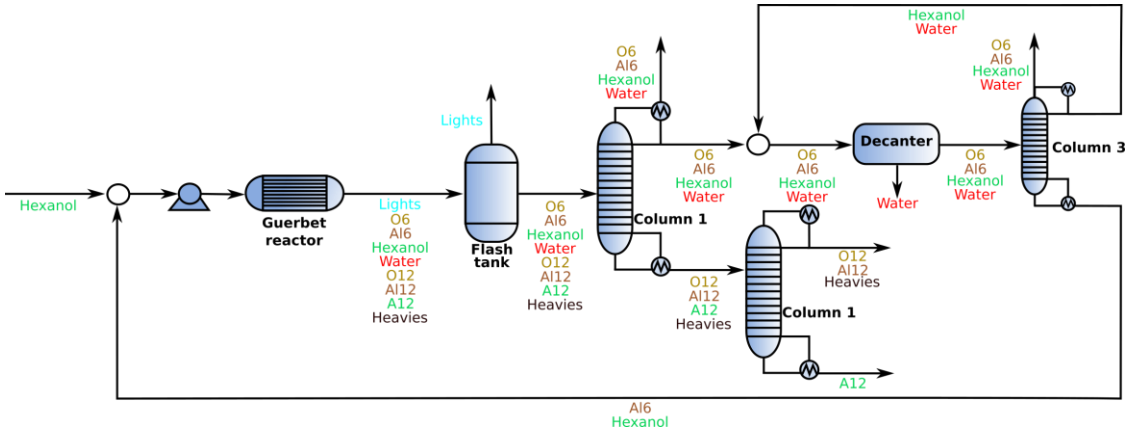

Figure S6.38 Process for Guerbet coupling of hexanol using Ca-HAP as catalyst (M79).

S6.19 Octanol dehydration

Process for Octanol dehydration using Syndol® catalyst (M80)

Dehydration of octanol takes place in a process consisting of a furnace reactor operated at 350°C and atmospheric pressure, followed by a distillation column (Figure S6.39). Conversion in the reactor is close to 100%. The main products of the reactor are octene and water, with minor amounts of hydrogen, aldehydes and ethers resulting from side reactions. The products of the reactor are separated in a distillation column such that waste water is obtained as a distillate, while octene and oxygenated molecules are obtained as the main product at the bottom of the column.

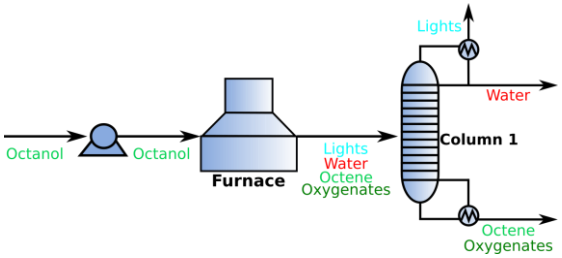

Figure S6.39 Process for dehydration of octanol using Syndol® catalyst (M80).

S6.20 Octanol etherification

Process for Octanol etherification using Amberlyst catalyst (M81)

Octanol etherification occurs in an isothermal reactor designed as a heat exchanger, operated at 250°C and 20 atm (Figure S6.40). Conversion under these conditions is 65%. The main products of the reaction are ethers with eight carbons (E8); other by-products include olefins (O8), heavy products, hydrogen, and waste water. The separation system consists of a distillation column that splits the reactor output into an ether rich stream (bottoms), and a top product containing unconverted octanol, water, olefins, and light product. The light products are separated using a partial condenser in the first column. The rest of the distillate is fed to a decanter that produces a water rich phase that is send for waste treatment, and an organic phase, that is fed to a second distillation column. The bottom product of this second column contains essentially pure octanol and it is recycled to the reactor, while the top product is an azeotropic blend of octanol and water that is sent back to the decanter.

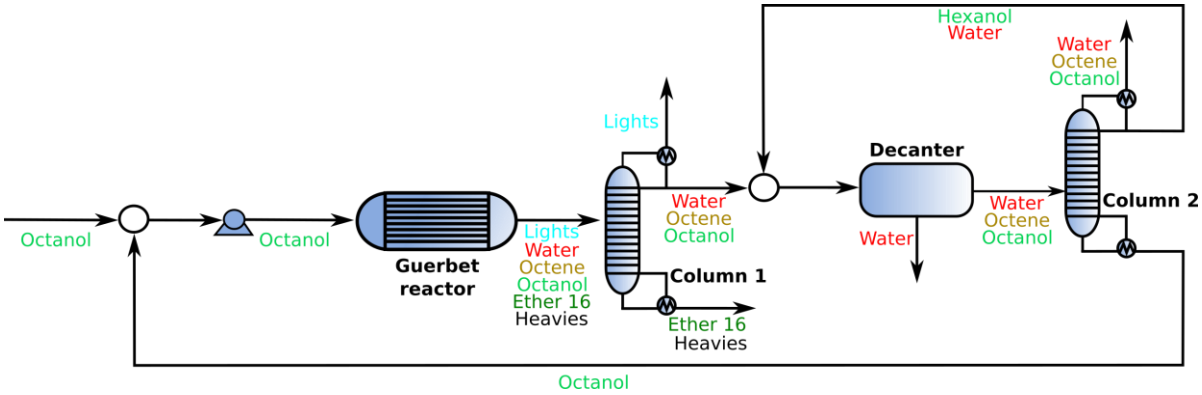

Figure S6.40 Process for octanol Etherification using Amberlyst® as catalyst (M81).

S6.21 Guerbet coupling of octanol

Process for Guerbet coupling of octanol using Ca-HAP (M80)

Guerbet coupling of octanol occurs in an adiabatic reactor with entrance temperature equal to 375°C, operated at atmospheric pressure, single pass conversion under these conditions is 75%. Reactor products include alcohols of 16 carbons, olefins (O8, O16), hydrogen, and waste water. The separation train starts with a flash tank (35°C and 1 atm) that yields a gas stream containing light products, used for electricity generation, and a liquid stream with all condensable species. The liquid stream is fed to a distillation column that produces a distillate containing species with less than 8 carbons and water; and a bottom product containing species with more than 16 carbons. The bottom product is further separated using two distillation columns (Columns 2 and 3) that yield as final products an alcohol (A16) rich stream, a stream that is used for electricity generation, and an olefin (O16) rich stream. The top product of the first column contains the unreacted octanol, olefins with eight carbons, and the water. This mixture forms an azeotrope that is broken using of a phase separation operation (decanter) that produces two liquid streams, one enriched in water, that is sent for waste treatment; and another phase still containing some water but enriched in octanol and O8 olefins. This phase is split using distillation Columns 4 and 5. These columns produce three streams of interest: one with the remaining waste water, one enriched in O8 olefins, and one with unreacted octanol that is recycled to the reactor.

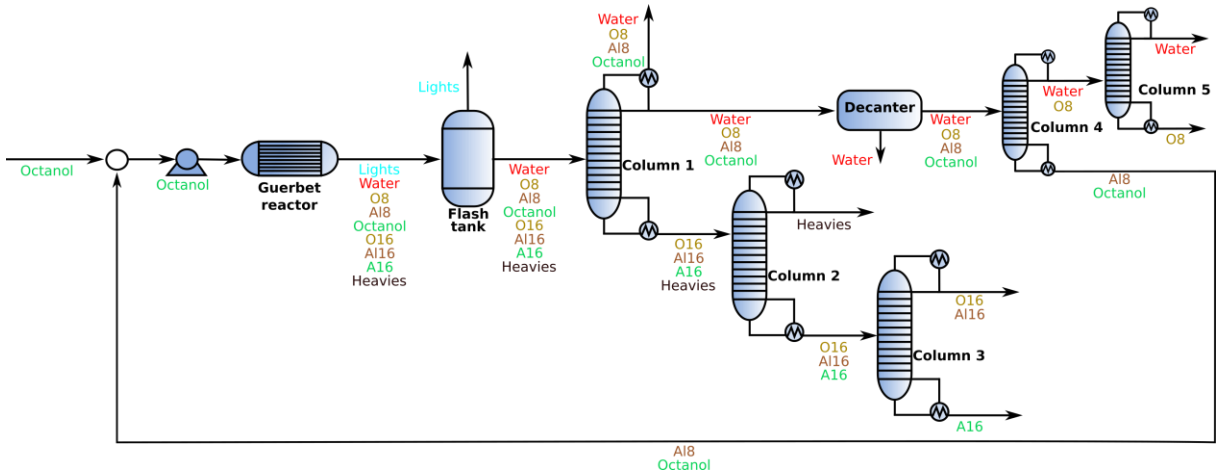

Figure S6.41 Process for Guerbet coupling of octanol using Ca-HAP as catalyst (M82).

S6.22 Mixed alcohol dehydration

Process for mixed alcohol dehydration using Syndol® catalyst (M83-M84)

The dehydration of mixed alcohols takes place in a furnace reactor operated at 350°C and atmospheric pressure (Figure S6.42). Conversion reached for all alcohols in the fed is assumed to be 100%. Products from the reactor include olefins in the same carbon range as the fed alcohols (*i.e.* O4+) and water. These products are fed to a distillation column (Column 1), whose top product contains O4-O7 olefins, and whose bottom product contains water and O8+ olefins. The bottom product is further separated in a second column (Column 2) that yields waste water as a top product and O8+ olefins at the bottom. On the other hand, the top product of column 1 constitute in itself a final product in M83, or it is split into O4 olefins and O6 olefins in distillation Column 3 in M84.

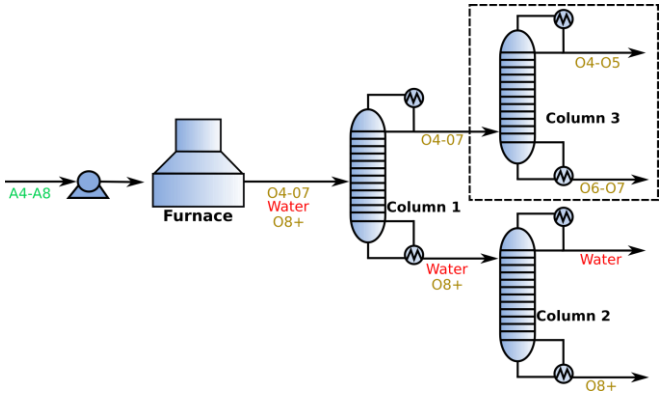

Figure S6.42 Processes for mixed alcohol dehydration using Syndol® catalyst (M83-M84). Optional columns are shown surrounded by a dashed square.

S6.23 Mixed alcohols etherification

Process for mixed alcohols etherification using Amberlyst catalyst (M85)

In this work we consider the etherification of mixtures of alcohols in the carbon range A4-A8. In order to have a first approximation to the process we have made two simplifying assumptions: first, that the conversion of each alcohol is not a function of the composition; and second that the ether distribution is the result of self-condensation reactions. In a more detailed study these assumptions may be relaxed, here we rely on them to gain some insight into the process without requiring detailed models of the reaction kinetics. The process consists of a reactor designed as a heat exchanger operated at 250°C and

20 atm followed by a separation train (Figure S6.43). We have assumed that conversion of every alcohol is identical and equal to 65%. The products obtained from the reactor include olefins (O4-O8) ethers (E8-E16), heavy species, water, and hydrogen. The separation train includes a flash drum, six distillation columns, and two decanters. Products of the reactor are first fed to a flash drum (35°C and 20 atm) that produces a gas phase containing most of the hydrogen, which is used for electricity generation, and a liquid phase with the condensable species. The liquid phase is fed to Column 1, that yields a bottom product rich in alcohols with eight carbons, heavy ethers (E12 and E16), and heavy species; and a top product containing the remaining compounds. The bottom product is separated in Column 2, such that the unconverted alcohols (top product) are recycled back to the reactor, while the bottom product consisting essentially of heavy species and ethers is one of the products of the module. The top product of the first column contains a mixture of water, alcohols, olefins and ethers, this top product is complex and present different azeotropes. To separate this mixture, we make use first of a decanter, that produces two streams: one lean in water (directed to Column 3), and one rich in water (directed to Column 5). The stream lean in water, also containing O6 olefins and alcohols, is further separated using Columns 3 and 4, such that a product rich in O6 olefins is obtained (top of Column 4), and a stream containing A4-A6 alcohols is recycled to the reactor (bottom of Column 4). The water rich stream, that also contains E8 ethers, unconverted A6 alcohols, and olefins (O8), is separated using two distillation columns (Columns 5 and 6) and a decanter; these unit operations allow obtaining individual streams rich in E8 ether (output from decanter 2), O8 olefin (top product of Column 6), waste water (output from decanter 2), and unconverted A6 alcohol (bottom product Column 6), this last stream is recycled back to the reactor.

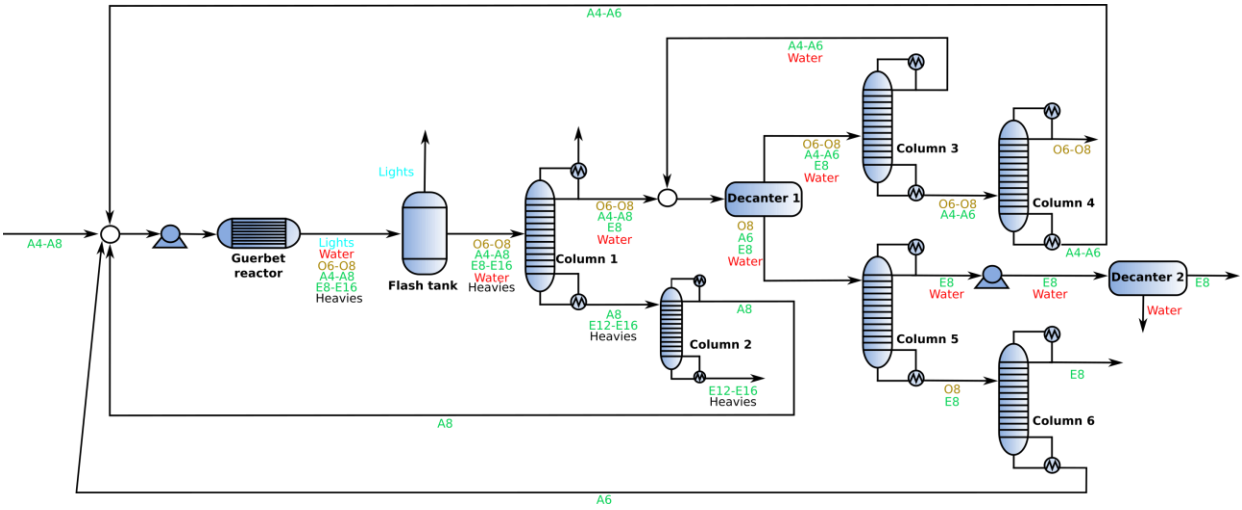

Figure S6.43 Processes for mixed alcohol etherification using Amberlyst 70 as catalyst (M85).

S6.24 Guerbet coupling of mixed alcohols

Process for Guerbet coupling of mixed alcohols using Ca-HAP (M86)

As in the previous case we consider Guerbet coupling of alcohols with four to eight carbons. The assumptions made regarding the independence of conversion from fed composition and the consideration of only self-coupling reactions holds valid for this module. The process designed consists of an adiabatic reactor with entrance temperature of 375°C operated at 1 atm, followed by a separation train containing a flash tank, three distillation columns and a decanter. Conversion of all alcohols is assumed constant and equal to 65%. The product from the reaction include alcohols resulting from the self-condensation reaction (A8, A12, and A16), olefins (O4, O6, O8, O12, and O16), aldehydes (Al4, Al6, Al8, Al12, Al16), waste water, and hydrogen. The product from the reactor is fed to a flash tank (35°C and 1 atm) that yields a gas stream containing hydrogen, and a liquid stream with all condensable species. This

liquid stream is fed to a distillation column whose bottom product is a blend of the chemical species with more than eight carbons. This stream is the final product of the module. On the other hand, the top stream of the column contains alcohols and aldehydes with less than eight carbons, and minor amounts of olefins (O4-O8). This top stream is fed to a subsystem containing two distillation columns and a decanter. This subsystem produces a waste water stream (bottom of Column 3), and a stream containing A4 and A6 unconverted alcohols that is recycled to the reactor. Note that unconverted octanol is not recycled to the reactor leaving the system as part of the bottom product of Column 1.

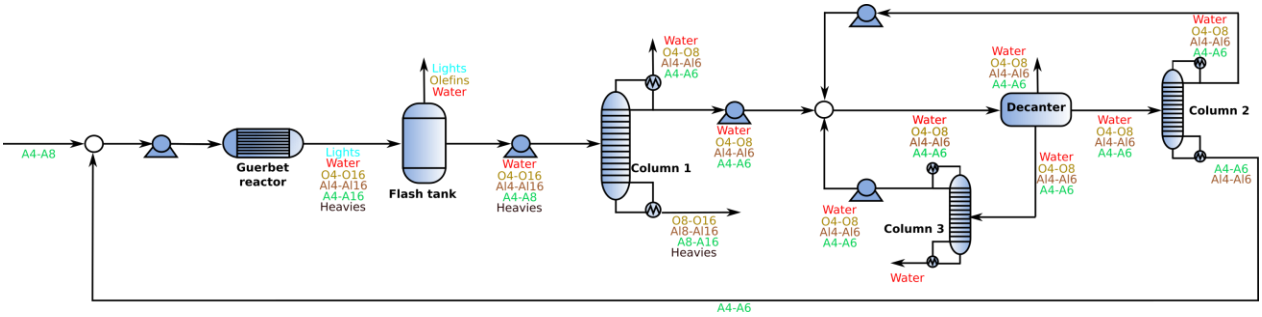

Figure S6.44 Process Guerbet coupling of mixed alcohols using Ca-HAP as catalyst (M86).

S6.25 Olefin hydrogenation

The hydrogenation of olefins takes place in an isothermal reactor designed as a furnace operated at 350°C and 36 atm (Figure S6.45). The ratio of hydrogen/olefins is adjusted to be equal to two. This reaction is well known and very efficient, and we can safely assume that 100% conversion is achieved. The output stream from the reactor includes paraffins and the excess of hydrogen. This output stream is fed to a flash drum, that allows to recover hydrogen, and yields a condensed phase containing the paraffins. The recovered hydrogen is recompressed and recycled to the reactor. The condensed phase is fed to a fractionation system, this system splits the paraffins into seven fractions according to their molecular weight: P1-P3 (electricity), P4-P8 (gasoline or electricity), P9-P10 (gasoline, jet fuel or electricity), P11-P12 (gasoline, jet fuel, diesel or electricity), P13-P16 (jet fuel, diesel or electricity), P16-P20 (diesel or electricity), P20+ (electricity). The design of this separation system is a function of the paraffin composition, such that the number of distillation columns and their operating conditions change with the product composition. Instead of designing a large number of modules each suitable to separate a different blend of paraffins, which could be unpractical, we have decided to assume that the separation of these fractions is possible and that the cost of achieving these separations is not dominant in the biorefinery as a whole. This assumption is justified for an initial process screening based on the results that we have obtained in which capital and operating cost are not dominant factors.

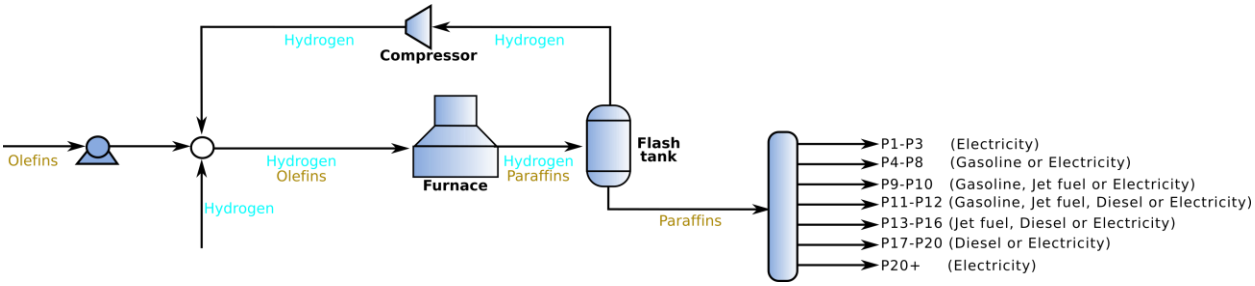

Figure S6.45 Process for olefin hydrogenation using CoMo (M87).

S7. Financial and cost assumptions

All financial and cost assumptions in this work are presented in Table S7-1. Parameters used for financial evaluation as well as installation factors have been obtained from the NREL reports and we have

kept them constant to facilitate comparisons[3]. The costs of ethanol feedstocks have been calculated as follows: For ethanol 100% we have used results from NREL report on lignocellulosic ethanol production plant[3]. For ethanol 83% and 50% we have adjusted the capital and operating costs of the equipment required (molecular sieves and rectification column) to purify ethanol streams leaving the beer column[41]. Based on the updated costs we have recalculated the minimum selling price and we have used this value as input. The cost of other chemicals has been obtained when possible from commercial vendors. In the case of catalyst however, there are many cases in which a commercial quote is not available, in these cases we have used the recently developed tool CatCost[TM](106). In a few instances estimation of the catalyst price using cat-cost was not possible due to lack of information on the catalyst preparation processes, in these cases we have estimated the cost using a related catalyst.

Table S7-1. Financial and cost assumptions used in this study.

		Source
General parameters		
Scaling exponent for capital cost equation (α)	0.72	[107]
Reference capacity of the NREL ethanol conversion plant (β^{NREL})	126.8 mol/s	3
Conversion efficiency from heat to electricity (δ)	0.4	Assumed
Financial variables		
Equity	40%	
Loan interest	8%	
Loan term (years)	10	
Operation period (years)	30	
Annualization factor (θ^{af})	0.1165	
Depreciation period (years)	7	
Construction period (years)	3	
% year -2	8%	
% year -1	60%	3
% year 0	32%	
Startup time (years)	0.25	
Feedstock use (% of Normal)	50%	
Variable cost (% of Normal)	75%	
Fixed cost (% of Normal)	100%	
Discount rate	10%	
Income tax	21%	
Working capital (% of FCI)	5%	
Base year for analysis	2007	
Direct costs		
OSBL (% of ISBL)	40%	3
Warehouse (% of ISBL)	4%	
Site (% of ISBL)	9%	
Additional piping (% of ISBL)	4.5%	
Indirect costs		
Proratable expenses (% TDC)	10%	
Field development (% TDC)	10%	3
Home Office & construction fee (% TDC)	20%	
Contingency (% TDC)	40%	
Other cost (Start-Up, permits, etc.)	10%	
Materials		
Lignocellulosic ethanol price 100% ($/kg)	0.7232	3
Lignocellulosic ethanol price 87% ($/kg)	0.6591	Calculated
Lignocellulosic ethanol price 50% ($/kg)	0.5076	Calculated
Gasoline ($/kg)	2	Assumed
Diesel ($/kg)	2	Assumed
Jet Fuel ($/kg)	2	Assumed
Electricity sale price θ_j^E ($/J)	1.5×10^{-8}	[108]
N2 ($/kg)	0.1345	[109]
H2 ($/kg)	1.07	[105]
NaOH ($/kg)	0.086	[110]
Propane ($/kg)	1.37	[111]
Syndol ($/kg)	20.48	[20]
MCM-41 ($/kg)	103.5	[105]
HZSM5 ($/kg)	8.60	[113]
Vertimas ($/kg)	25.81	[41]
P-HZSM ($/kg)	8.60	[112]
$ZnZrO_2$ ($/kg)	59.28	Catcost
In_2O_3-Zβ ($/kg)	101.62	Catcost
$LaZrO_2$ ($/kg)	215.81	Catcost
Ni-La_2O_3-γ-Al_2O_3 ($/kg)	105.34	[55]

Ni(8%)-γ-Al_2O_3 ($/kg)	109.63	Catcost
Ca-HAP ($/kg)	8	Catcost
Pd-Hydrotalcite ($/kg)	100.99	Catcost
Pd-MgO ($/kg)	702.00	Catcost
Ni-LASA ($/kg)	134.56	Assumed
NiSAIB ($/kg)	90.33	Catcost
Ni-AlSBA ($/kg)	48.44	Catcost
TEA ($/kg)	2.58	[113]
2.21%Ni-HZSM-5 ($/kg)	148.00	Catcost
Pell-SAPO ($/kg)	15.00	Catcost
HZSM-23 ($/kg)	7.00	Catcost
SO_3-10%-NiO-γ-Al_2O_2 ($/kg)	7.25	Catcost
H-Zeolite-Y-P ($/kg)	81.18	[114]
Sulfated Titania ($/kg)	25.36	Catcost
Solid Phosphoric Acid (SPA) ($/kg)	0.69	[115]
CT275 ($/kg)	1.30	[116]
MTW-10%P-H_3PO_4 ($/kg)	15.76	Catcost
ATHZ5-CS ($/kg)	17.70	Catcost
HZSM-57 ($/kg)	10.55	Assumed
2A-Co-C-230 ($/kg)	40.59	Catcost
ASA ($/kg)	0.69	[117]
SO_4-ZrO_2 ($/kg)	16.24	[118]
AM11 ($/kg)	34.91	Catcost
Amberlyst 70® ($/kg)	120.64	[119]
CoMo ($/kg)	0.71	[105]
Utilities		
Refrigerant 4th generation ($/J)	7.85×10^{-6}	
Refrigerant 3rd generation ($/J)	5.46×10^{-6}	
Refrigerant 2nd generation ($/J)	3.09×10^{-6}	
Refrigerant 1st generation ($/J)	2.52×10^{-6}	
Water ($/J)	1.97×10^{-7}	
Low pressure steam ($/J)	1.76×10^{-6}	[3,108]
Medium pressure steam ($/J)	2.04×10^{-6}	
High pressure steam ($/J)	2.32×10^{-6}	
Hot Oil ($/J)	3.25×10^{-6}	
Fired Heat ($/J)	3.95×10^{-6}	
Electricity ($/J)	1.48×10^{-8}	
Waste management		
Waste treatment ($/Kg)	5.9×10^{-4}	[59]

S8. Capital and operating costs associated with each module

Table S8-1. Capital cost (θ_i^{CC}), operating cost (θ_i^{OC}), and reference incoming mass flow rate (θ_i^{F}) for the modules used in the superstructure. Additionally, we present the consumption rate for each module associated with the different sources used in this work.

	Cost associated parameters			**Source consumption rate ϕ_j^{SRC}**			
	θ_i^{F}	θ_i^{CC}	θ_i^{OC}	H2	N2	H2O	Propylene
	[Kg/s]	[MM$]	[MM$/year]	[mol/mol]	[mol/mol]	[mol/mol]	[mol/mol]
M1	11.7200	67.5143	11.3448	-	-	-	-
M2	8.1259	23.2543	5.2469	-	-	-	-
M3	6.3200	17.7540	4.5803	-	-	-	-
M4	5.8400	15.6182	4.6038	-	-	-	-
M5	6.5687	27.6007	2.3652	-	-	-	-
M6	6.3200	20.5594	2.8139	-	-	-	-
M7	5.8400	19.5104	2.0307	-	-	-	-
M8	6.6400	37.1550	3.7514	-	-	-	-
M9	5.8400	34.4799	3.1361	-	-	-	-
M10	5.8400	38.1363	3.3997	-	-	-	-
M11	8.1259	42.4432	5.9634	-	-	-	-
M12	8.1259	60.9343	14.1602	-	-	-	-
M13	8.1259	29.6878	4.5249	-	-	-	-
M14	5.8400	71.9693	9.1009	-	-	-	-
M15	5.8400	75.0653	9.2771	-	-	-	-
M16	5.8400	69.0357	6.0393	-	-	-	-
M17	5.8400	74.1157	6.3861	-	-	-	-
M18	5.8400	60.6095	6.2655	-	-	-	-
M19	5.8400	68.2789	6.4266	-	-	-	-
M20	5.8400	73.3088	6.5348	-	-	-	-
M21	5.8400	55.6695	3.0971	-	-	-	-
M22	5.8400	51.3197	3.1620	-	-	-	-
M23	5.8400	91.8654	7.7415	-	0.13	-	-

M24	5.8400	101.2107	7.4173	-	0.13	-	-
M25	5.8400	115.8451	7.3628	-	-	-	-
M26	5.8400	126.6243	7.3309	-	-	-	-
M27	5.8400	109.9918	7.6939	-	-	-	-
M28	5.8400	91.9283	10.1025	-	-	-	-
M29	5.8400	93.8322	10.1458	-	-	-	-
M30	3.5600	22.5364	1.6429	-	-	-	-
M31	3.5600	21.9040	1.7653	-	-	-	-
M32	3.5600	23.2332	1.2050	-	-	-	-
M33	3.5600	27.8263	2.7839	-	-	-	-
M34	3.5600	28.6679	2.6981	-	-	-	-
M35	3.5600	28.8114	2.7617	-	-	-	-
M36	1.0400	44.3963	3.0950	-	-	-	-
M37	3.8600	251.7766	24.4300	-	-	-	-
M38	3.5600	17.0344	2.4684	-	-	-	-
M39	3.5600	18.6349	2.6079	-	-	-	-
M40	3.5600	18.7459	2.6602	-	-	-	-
M41	3.5600	17.6883	1.6068	-	-	-	-
M42	3.5600	20.2133	1.7897	-	-	-	-
M43	3.5600	22.6796	1.8525	-	-	-	-
M44	3.5600	56.7558	4.3441	-	-	230.522	-
M45	3.5600	57.4074	4.7869	-	-	230.522	-
M46	3.5600	56.9467	4.4153	-	-	230.522	-
M47	1.6000	14.1679	1.3756	-	-	-	-
M48	1.6000	17.0998	1.4754	-	-	-	-
M49	1.6000	10.9631	0.9590	-	-	-	-
M50	1.6000	12.3536	2.2947	-	-	-	-
M51	1.6000	11.0540	1.1363	-	-	-	-
M52	1.6000	11.2641	1.1672	-	-	-	-
M53	1.6000	11.0541	1.9160	-	-	-	0.000044
M54	1.6000	12.4273	1.9922	-	-	-	0.000044
M55	1.9500	2.9981	0.8557	-	-	-	-
M56	1.9500	9.3010	0.9702	-	-	-	-
M57	1.6600	10.9599	1.0298	-	-	-	-
M58	1.6600	13.3257	1.1724	-	-	-	-
M59	1.6600	9.4306	1.0918	-	-	-	-
M60	1.6600	10.5957	1.1309	-	-	-	-
M61	1.6600	11.7334	1.3242	-	-	-	-
M62	1.6600	16.7119	1.4054	-	-	-	-
M63	1.9500	6.4163	0.8951	-	-	-	-
M64	1.9500	7.4613	0.8757	-	-	-	-
M65	1.9500	15.5277	1.2065	-	-	-	0.000124
M66	1.9500	17.2684	1.3399	-	-	-	0.000124
M67	1.9500	10.2647	5.7666	-	-	-	-
M68	1.9500	12.7611	1.1509	-	-	-	-
M69	1.9500	5.9621	0.8075	-	-	-	-
M70	2.9200	3.2819	2.6182	-	-	-	-
M71	3.9000	5.3750	1.2500	-	-	-	-
M72	3.9000	6.3461	2.3094	-	-	-	-
M73	2.0500	12.3582	1.6341	-	-	-	-
M74	3.5000	7.2191	1.6628	-	-	-	-
M75	2.0600	15.3206	3.3880	-	-	-	-
M76	2.0600	37.2263	6.0222	-	-	-	-
M77	4.8300	12.8471	2.3881	-	-	-	-
M78	2.8400	19.7283	3.9508	-	-	-	-
M79	2.8400	17.1414	7.0855	-	-	-	-
M80	6.1500	26.1506	2.8073	-	-	-	-
M81	3.6200	19.4324	5.4136	-	-	-	-
M82	3.6100	31.6932	9.2858	-	-	-	-
M83	4.4900	18.7353	2.6842	-	-	-	-
M84	4.4900	22.3192	2.8720	-	-	-	-
M85	2.9900	31.3188	5.6806	-	-	-	-
M86	2.6400	28.0074	7.3453	-	-	-	-
M87	2.2800	7.2100	0.6850	0.02147	-	-	-

S9. Processes for ethanol upgrading to diesel as a function of cetane number

In figure S10.1 we show a Sankey diagram for the optimal solutions obtained for a diesel biorefineries when different constraints on the cetane number are imposed.

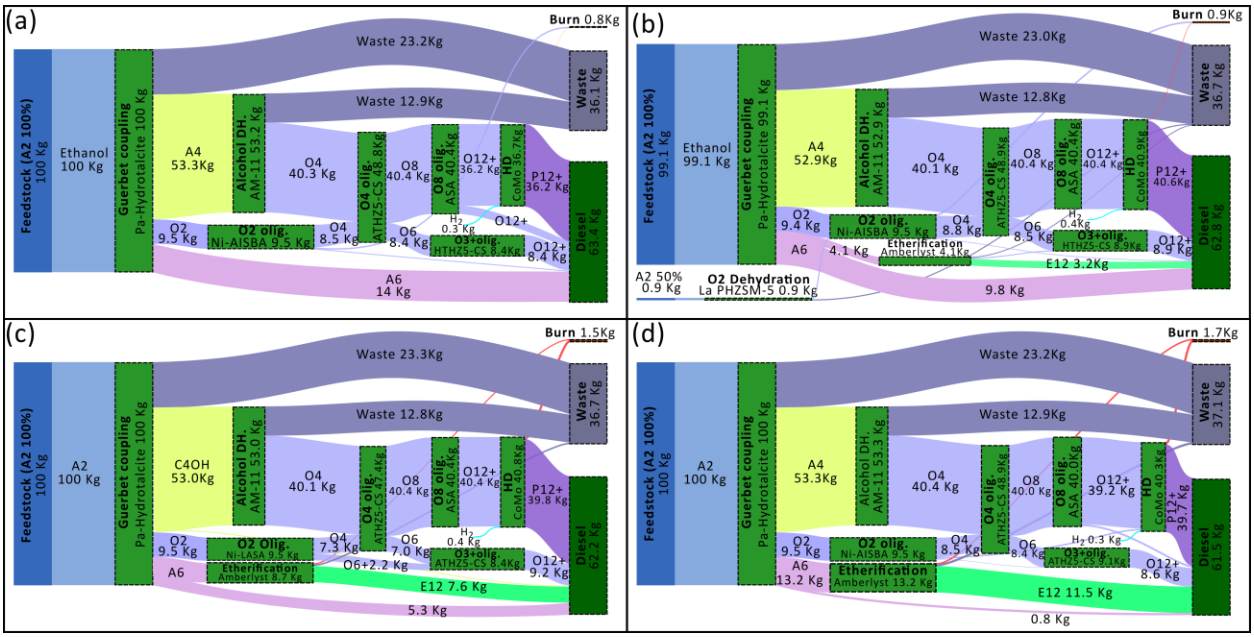

Figure S9.1 Sankey diagrams of optimal biorefineries as a function of cetane number (a) $40 \leq CN \leq 61.4$ (b)$CN = 70$ (c) $CN = 80$ (d) $CN = 90$

S10. Strategies to dealing with price uncertainty

Once an optimal design has been found it is possible to reduce the effect of fuel price variability by redirecting process flows within the biorefinery in such a way that production of final products is adjusted based on the market conditions. In order to be able to gain this kind of flexibility the process units within the biorefinery need to be overdesigned such that they can handle flows larger than usual. The optimal redistribution of flows within the biorefinery is obtained by formulating an optimization problem to maximize profit, while fixing the process units and their capacities. In this case the process units correspond to the solution of the initial optimization problem, and the capacities are calculated using the selected overdesign factor. We note that adding flexibility comes at the expense of increasing the capital cost of the biorefineries.

REFERENCES

(1) Kong, L.; Sen, S. M.; Henao, C. A.; Dumesic, J. A.; Maravelias, C. T. A Superstructure-Based Framework for Simultaneous Process Synthesis, Heat Integration, and Utility Plant Design. *Comput. Chem. Eng.* **2016**, *91*, 68–84. https://doi.org/10.1016/j.compchemeng.2016.02.013.

(2) Kim, J.; Sen, S. M.; Maravelias, C. T. An Optimization-Based Assessment Framework for Biomass-to-Fuel Conversion Strategiest. *Energy Environ. Sci.* **2013**, *6*, 1093–1104. https://doi.org/10.1039/c3ee24243a.

(3) Humbird, D.; Davis, R.; Tao, L.; Kinchin, C.; Hsu, D.; Aden, A.; Schoen, P.; Lukas, J.; Olthof, B.; Worley, M.; et al. *Process Design and Economics for Biochemical Conversion of Lignocellulosic Biomass to Ethanol: Dilute-Acid Pretreatment and Enzymatic Hydrolysis of Corn Stover*; Golden, Colorado, 2011. https://doi.org/10.2172/1013269.

(4) Dahmen, M.; Marquardt, W. Model-Based Design of Tailor-Made Biofuels. *Energy and Fuels* **2016**, *30* (2), 1109–1134. https://doi.org/10.1021/acs.energyfuels.5b02674.

(5) ASTM D4814−14b. *Standard Specification for Automotive Spark-Ignition Engine Fuel*; 2014.

https://doi.org/10.1520/D4814-11B.1.6.

(6) ASTM D1655-19a. *Standard Specification for Aviation Turbine Fuels*; 2010. https://doi.org/10.1520/D1655-10.2.

(7) Bacha, J.; Freel, J.; Gibbs, A.; Gibbs, L.; Hemighaus, G.; Hoekman, K.; Horn, J.; Ingham, M.; Jossens, L.; Kohler, D.; et al. Diesel Fuels Technical Review. *Chevron Glob. Mark.* **2007**, 1–116. https://doi.org/10.1063/1.3575169.

(8) Dahmen, M.; Marquardt, W. Model-Based Formulation of Biofuel Blends by Simultaneous Product and Pathway Design. *Energy and Fuels* **2017**, *31* (4), 4096–4121. https://doi.org/10.1021/acs.energyfuels.7b00118.

(9) Ng, L. Y.; Andiappan, V.; Chemmangattuvalappil, N. G.; Ng, D. K. S. A Systematic Methodology for Optimal Mixture Design in an Integrated Biorefinery. *Comput. Chem. Eng.* **2015**, *81*, 288–309. https://doi.org/10.1016/j.compchemeng.2015.04.032.

(10) Hashim, H.; Narayanasamy, M.; Yunus, N. A.; Shiun, L. J.; Muis, Z. A.; Ho, W. S. A Cleaner and Greener Fuel: Biofuel Blend Formulation and Emission Assessment. *J. Clean. Prod.* **2017**, *146*, 208–217. https://doi.org/10.1016/j.jclepro.2016.06.021.

(11) König, A.; Neidhardt, L.; Viell, J.; Mitsos, A.; Dahmen, M. Integrated Design of Processes and Products: Optimal Renewable Fuels. *Comput. Chem. Eng.* **2020**, *134*. https://doi.org/10.1016/j.compchemeng.2019.106712.

(12) Yanowitz, J.; Ratcliff, M. A.; McCormick, R. L.; Taylor, J. D.; Murphy, M. J. Compendium of Experimental Cetane Numbers Compendium of Experimental Cetane Numbers. **2017**, No. February.

(13) Kubic, W. L. *A Group Contribution Method for Estimating Cetane and Octane Numbers*; 2016.

(14) McCormick, R. L.; Fioroni, G.; Fouts, L.; Christensen, E.; Yanowitz, J.; Polikarpov, E.; Albrecht, K.; Gaspar, D. J.; Gladden, J.; George, A. Selection Criteria and Screening of Potential Biomass-Derived Streams as Fuel Blendstocks for Advanced Spark-Ignition Engines. *SAE Int. J. Fuels Lubr.* **2017**, *10* (2), 442–460. https://doi.org/10.4271/2017-01-0868.

(15) Eagan, N. M.; Moore, B. J.; McClelland, D. J.; Wittrig, A. M.; Canales, E.; Lanci, M. P.; Huber, G. W. Catalytic Synthesis of Distillate-Range Ethers and Olefins from Ethanol through Guerbet Coupling and Etherification. *Green Chem.* **2019**. https://doi.org/10.1039/c9gc01290g.

(16) Wallner, T.; Ickes, A.; Lawyer, K. Analytical Assessment of C2-C8 Alcohols as Spark-Ignition Engine Fuels. *Lect. Notes Electr. Eng.* **2013**, *191 LNEE* (VOL. 3), 15–26. https://doi.org/10.1007/978-3-642-33777-2_2.

(17) Çakmak, A.; Kapusuz, M.; Özcan, H. Experimental Research on Ethyl Acetate as Novel Oxygenated Fuel in the Spark-Ignition (SI) Engine. *Energy Sources, Part A Recover. Util. Environ. Eff.* **2020**, *00* (00), 1–16. https://doi.org/10.1080/15567036.2020.1736216.

(18) Saldana, D. A.; Starck, L.; Mougin, P.; Rousseau, B.; Pidol, L.; Jeuland, N.; Creton, B. Flash Point and Cetane Number Predictions for Fuel Compounds Using Quantitative Structure Property Relationship (QSPR) Methods. *Energy and Fuels* **2011**, *25* (9), 3900–3908. https://doi.org/10.1021/ef200795j.

(19) Anastas, P. T.; Zimmerman, J. B. Design through the 12 Principles of Green Engineering. *Environ. Sci. Technol.* **2003**, *35*, 94–1001. https://doi.org/10.1039/b411954c.

(20) Mohsenzadeh, A.; Zamani, A.; Taherzadeh, M. J. Bioethylene Production from Ethanol: A Review and Techno-Economical Evaluation. *ChemBioEng Rev.* **2017**, *4* (2), 75–91. https://doi.org/10.1002/cben.201600025.

(21) Fan, D.; Dai, D. J.; Wu, H. S. Ethylene Formation by Catalytic Dehydration of Ethanol with Industrial Considerations. *Materials (Basel).* **2013**, *6* (1), 101–115. https://doi.org/10.3390/ma6010101.

(22) Zhang, M.; Yu, Y. Dehydration of Ethanol to Ethylene. *Ind. Eng. Chem. Res.* **2013**, *52* (28), 9505–9514. https://doi.org/10.1021/ie401157c.

(23) Eagan, N. M.; Kumbhalkar, M. D.; Buchanan, J. S.; Dumesic, J. A.; Huber, G. W. Chemistries and Processes for the Conversion of Ethanol into Middle-Distillate Fuels. *Nat. Rev. Chem.* **2019**, *3* (4), 223–249. https://doi.org/10.1038/s41570-019-0084-4.

(24) Arvidsson, M. and Lundin, B. Process Integration Study of a Biorefinery Producing Ethylene from Lignocellulosic Feedstock for a Chemical Cluster, Chalmers University of Technology, 2011.

(25) Haishi, T.; Kasai, K.; Iwamoto, M. Fast and Quantitative Dehydration of Lower Alcohols to Corresponding Olefins on Mesoporous Silica Catalyst. *Chem. Lett.* **2011**, *40* (6), 614–616. https://doi.org/10.1246/cl.2011.614.

(26) Zhan, N.; Hu, Y.; Li, H.; Yu, D.; Han, Y.; Huang, H. Lanthanum-Phosphorous Modified HZSM-5 Catalysts in Dehydration of Ethanol to Ethylene: A Comparative Analysis. *Catal. Commun.* **2010**, *11* (7), 633–637. https://doi.org/10.1016/j.catcom.2010.01.011.

(27) Duan, C.; Zhang, X.; Zhou, R.; Hua, Y.; Zhang, L.; Chen, J. Comparative Studies of Ethanol to Propylene over HZSM-5/SAPO-34 Catalysts Prepared by Hydrothermal Synthesis and Physical Mixture. *Fuel Process. Technol.* **2013**, *108*, 31–40. https://doi.org/10.1016/j.fuproc.2012.03.015.

(28) Zhang, X.; Wang, R.; Yang, X.; Zhang, F. Comparison of Four Catalysts in the Catalytic Dehydration of Ethanol to Ethylene. *Microporous Mesoporous Mater.* **2008**, *116* (1–3), 210–215. https://doi.org/10.1016/j.micromeso.2008.04.004.

(29) Ramesh, K.; Jie, C.; Han, Y. F.; Borgna, A. Synthesis, Characterization, and Catalytic Activity of Phosphorus Modified H-ZSM-5 Catalysts in Selective Ethanol Dehydration. *Ind. Eng. Chem. Res.* **2010**, *49* (9), 4080–4090. https://doi.org/10.1021/ie901666f.

(30) Le Van Mao, R.; Nguyen, T. M.; McLaughlin, G. P. The Bioethanol-to-Ethylene (B.E.T.E.) Process. *Appl. Catal.* **1989**, *48* (2), 265–277. https://doi.org/10.1016/S0166-9834(00)82798-0.

(31) Nguyen, T. T. N.; Ruaux, V.; Massin, L.; Lorentz, C.; Afanasiev, P.; Maugé, F.; Bellière-Baca, V.; Rey, P.; Millet, J. M. M. Synthesis, Characterization and Study of Lanthanum Phosphates as Light Alcohols Dehydration Catalysts. *Appl. Catal. B Environ.* **2015**, *166–167*, 432–444. https://doi.org/10.1016/j.apcatb.2014.12.004.

(32) Nguyen, T. M.; Le Van Mao, R. Conversion of Ethanol in Aqueous Solution over ZSM-5 Zeolites. *Appl. Catal.* **1990**, *58* (1), 119–129. https://doi.org/10.1016/s0166-9834(00)82282-4.

(33) Becerra, J.; Quiroga, E.; Tello, E.; Figueredo, M.; Cobo, M. Kinetic Modeling of Polymer-Grade Ethylene Production by Diluted Ethanol Dehydration over H-ZSM-5 for Industrial Design. *J. Environ. Chem. Eng.* **2018**, *6* (5), 6165–6174. https://doi.org/10.1016/j.jece.2018.09.035.

(34) Ciftci, A.; Varisli, D.; Cem Tokay, K.; Asli Sezgi, N.; Dogu, T. Dimethyl Ether, Diethyl Ether & Ethylene from Alcohols over Tungstophosphoric Acid Based Mesoporous Catalysts. *Chem. Eng. J.* **2012**, *207–208*, 85–93. https://doi.org/10.1016/j.cej.2012.04.016.

(35) Varisli, D.; Dogu, T.; Dogu, G. Silicotungstic Acid Impregnated MCM-41-like Mesoporous Solid Acid Catalysts for Dehydration of Ethanol. *Ind. Eng. Chem. Res.* **2008**, *47* (12), 4071–4076. https://doi.org/10.1021/ie800192t.

(36) Brandão, P.; Philippou, A.; Rocha, J.; Anderson, M. W. Dehydration of Alcohols by Microporous Niobium Silicate AM-11. *Catal. Letters* **2002**, *80* (3–4), 99–102. https://doi.org/10.1023/A:1015444005961.

(37) Hsu, Y. S.; Wang, Y. L.; Ko, A. N. Effect of Sulfation of Zirconia on Catalytic Performance in the Dehydration of Aliphatic Alcohols. *J. Chinese Chem. Soc.* **2009**, *56* (2), 314–322. https://doi.org/10.1002/jccs.200900046.

(38) Makgoba, N. P.; Sakuneka, T. M.; Koortzen, J. G.; Van Schalkwyk, C.; Botha, J. M.; Nicolaides, C. P. Silication of γ-Alumina Catalyst during the Dehydration of Linear Primary Alcohols. *Appl. Catal. A Gen.* **2006**, *297* (2), 145–150. https://doi.org/10.1016/j.apcata.2005.09.003.

(39) Nel, R. J. J.; De Klerk, A. Dehydration of C5-C12 Linear 1-Alcohols over η-Alumina to Fuel Ethers. *Ind. Eng. Chem. Res.* **2009**, *48* (11), 5230–5238. https://doi.org/10.1021/ie801930r.

(40) Wright, M. E. Process for the Dehydration of Aqueous Bio-Derived Terminal Alcohols to Terminal Alkenes. US20120238788A1, 2012.

(41) Hannon, J. R.; Lynd, L. R.; Andrade, O.; Benavides, P. T.; Beckham, G. T.; Biddy, M. J.; Brown, N.; Chagas, M. F.; Davison, B. H.; Foust, T.; et al. Technoeconomic and Life-Cycle Analysis of Single-Step Catalytic Conversion of Wet Ethanol into Fungible Fuel Blendstocks. *Proc. Natl. Acad. Sci.* **2019**, 201821684. https://doi.org/10.1073/pnas.1821684116.

(42) Song, Z.; Takahashi, A.; Nakamura, I.; Fujitani, T. Phosphorus-Modified ZSM-5 for Conversion of Ethanol to Propylene. *Appl. Catal. A Gen.* **2010**, *384* (1–2), 201–205. https://doi.org/10.1016/j.apcata.2010.06.035.

(43) Xia, W.; Chen, K.; Takahashi, A.; Li, X.; Mu, X.; Han, C.; Liu, L.; Nakamura, I.; Fujitani, T. Effects of Particle Size on Catalytic Conversion of Ethanol to Propylene over H-ZSM-5 Catalysts - Smaller Is Better. *Catal. Commun.* **2016**, *73*, 27–33. https://doi.org/10.1016/j.catcom.2015.10.008.

(44) Furumoto, Y.; Harada, Y.; Tsunoji, N.; Takahashi, A.; Fujitani, T.; Ide, Y.; Sadakane, M.; Sano, T. Effect of Acidity of ZSM-5 Zeolite on Conversion of Ethanol to Propylene. *Appl. Catal. A Gen.* **2011**, *399* (1–2), 262–267. https://doi.org/10.1016/j.apcata.2011.04.009.

(45) Li, Y.; Liu, C.; Bai, Y.; Qiao, L.; Zhou, J. Ultrathin Hydrogen Diffusion Cloak. *Adv. Theory Simulations* **2017**, *1* (1), 1700004. https://doi.org/10.1002/adts.201700004.

(46) Xue, F.; Miao, C.; Yue, Y.; Hua, W.; Gao, Z. Sc2O3-Promoted Composite of In2O3 and Beta Zeolite for Direct Conversion of Bio-Ethanol to Propylene. *Fuel Process. Technol.* **2019**, *186* (November 2018), 110–115. https://doi.org/10.1016/j.fuproc.2018.12.024.

(47) Wang, F.; Xia, W.; Mu, X.; Chen, K.; Si, H.; Li, Z. A Combined Experimental and Theoretical Study on Ethanol Conversion to Propylene over Y/ZrO 2 Catalyst. *Appl. Surf. Sci.* **2018**, *439*, 405–412. https://doi.org/10.1016/j.apsusc.2017.12.253.

(48) Hayashi, F.; Iwamoto, M. Yttrium-Modified Ceria as a Highly Durable Catalyst for the Selective Conversion of Ethanol to Propene and Ethene. *ACS Catal.* **2013**, *3* (1), 14–17. https://doi.org/10.1021/cs3006956.

(49) Xia, W.; Wang, F.; Wang, L.; Wang, J.; Chen, K. Highly Selective Lanthanum-Modified Zirconia Catalyst for the Conversion of Ethanol to Propylene: A Combined Experimental and Simulation

Study. *Catal. Letters* **2019**, No. 0123456789. https://doi.org/10.1007/s10562-019-02916-2.

(50) Xia, W.; Mu, X.; Wang, F.; Chen, K.; Si, H.; Li, Z. Ethylene and Propylene Production from Ethanol over Sr or Bi Modified ZrO2 Catalysts. *React. Kinet. Mech. Catal.* **2017**, *122* (1), 473–484. https://doi.org/10.1007/s11144-017-1236-5.

(51) Iwamoto, M. Selective Catalytic Conversion of Bio-Ethanol to Propene: A Review of Catalysts and Reaction Pathways. *Catal. Today* **2015**, *242* (PB), 243–248. https://doi.org/10.1016/j.cattod.2014.06.031.

(52) Saavedra Lopez, J.; Dagle, R. A.; Dagle, V. L.; Smith, C.; Albrecht, K. O. Oligomerization of Ethanol-Derived Propene and Isobutene Mixtures to Transportation Fuels: Catalyst and Process Considerations. *Catal. Sci. Technol.* **2019**, *9* (5), 1117–1131. https://doi.org/10.1039/c8cy02297f.

(53) Liu, F.; Men, Y.; Wang, J.; Huang, X.; Wang, Y.; An, W. The Synergistic Effect to Promote the Direct Conversion of Bioethanol into Isobutene over Ternary Multifunctional CrxZnyZrzOn Catalysts. *ChemCatChem* **2017**, *9* (10), 1758–1764. https://doi.org/10.1002/cctc.201700154.

(54) Iwamoto, M.; Mizuno, S.; Tanaka, M. Direct and Selective Production of Propene from Bio-Ethanol on Sc-Loaded In2O3 Catalysts. *Chem. - A Eur. J.* **2013**, *19* (22), 7214–7220. https://doi.org/10.1002/chem.201203977.

(55) Nezam, I.; Peereboom, L.; Miller, D. J. Continuous Condensed-Phase Ethanol Conversion to Higher Alcohols: Experimental Results and Techno-Economic Analysis. *J. Clean. Prod.* **2019**, *209*, 1365–1375. https://doi.org/10.1016/j.jclepro.2018.10.276.

(56) Pang, J.; Zheng, M.; He, L.; Li, L.; Pan, X.; Wang, A.; Wang, X.; Zhang, T. Upgrading Ethanol to N-Butanol over Highly Dispersed Ni–MgAlO Catalysts. *J. Catal.* **2016**, *344*, 184–193. https://doi.org/10.1016/j.jcat.2016.08.024.

(57) Zhang, C.; Balliet, K.; Johnston, victor J. Catalyst and Processes for Producing Butanol US 8,962,897 B2. US 8,962,897 B2, 2012.

(58) Zhang, C.; Balliet, K.; Johnston, V. J. Catalyst and Processes for Producing Butanol US 9,024,090 B2. US 9,024,090 B2, 2012.

(59) Tan, E. C.; Snowden-Swan, L. J.; Abhijit-Dutta, M. T.; Jones, S.; Ramasamy, K. K.; Gray, M.; Dagle, R.; Padmaperuama, A.; Gerber, Ma.; Sahir, A. H.; et al. Comparative Techno-Economic Analysis and Process Design for Indirect Liquefaction Pathways to Distillate-Range Fuels via Biomass-Derived Oxygenated Intermediates Upgrading. *Biofuels, Bioprod. Biorefining* **2016**, *11*, 41–66. https://doi.org/doi.org/10.1002/bbb.1710.

(60) Zhang, C. Catalyst and Processes for Producing Butanol US 2014/0179958 A1. US 2014/0179958 A1, 2012.

(61) Zhang, C.; Borlik, M.; Weiner, H. Coated Hydrotalcite Catalyst and Processes for Producing Butanol. WO2014100131A1, 2014.

(62) Ghaziaskar, H. S.; Xu, C. C. One-Step Continuous Process for the Production of 1-Butanol and 1-Hexanol by Catalytic Conversion of Bio-Ethanol at Its Sub-/Supercritical State. *RSC Adv.* **2013**, *3* (13), 4271–4280. https://doi.org/10.1039/c3ra00134b.

(63) Ozer, R.; Fagan, P. J.; Calvarese, T. G. Conversion of Butanol to a Reaction Product Comprising 2-Ethylhexanol Using Hydroxyapatite Catalysts. US 8431753B2, 2013.

(64) Zacharopoulou, V.; Lemonidou, A. A. Olefins from Biomass Intermediates: A Review. *Catalysts*

2018, *8* (1). https://doi.org/10.3390/catal8010002.

(65) Lavrenov, A. V.; Karpova, T. R.; Buluchevskii, E. A.; Bogdanets, E. N. Heterogeneous Oligomerization of Light Alkenes: 80 Years in Oil Refining. *Catal. Ind.* **2016**, *8* (4), 316–327. https://doi.org/10.1134/S2070050416040061.

(66) Britovsek, G. J. P.; Malinowski, R.; McGuinness, D. S.; Nobbs, J. D.; Tomov, A. K.; Wadsley, A. W.; Young, C. T. Ethylene Oligomerization beyond Schulz-Flory Distributions. *ACS Catal.* **2015**, *5* (11), 6922–6925. https://doi.org/10.1021/acscatal.5b02203.

(67) Janiak, C.; Blank, F. Metallocene Catalysts for Olefin Oligomerization. *Macromol. Symp.* **2006**, *236*, 14–22. https://doi.org/10.1002/masy.200690047.

(68) Espinoza, R. L.; Nicolaides, C. P.; Korf, C. J.; Snel, R. Catalytic Oligomerization of Ethene over Nickel-Exchanged Amorphous Silica-Alumina; Effect of the Nickel Concentration. *Appl. Catal.* **1987**, *31* (2), 259–266. https://doi.org/10.1016/S0166-9834(00)80695-8.

(69) Lin, B.; Zhang, Q.; Wang, Y. Catalytic Conversion of Ethylene to Propylene and Butenes over H-ZSM-5. *Ind. Eng. Chem. Res.* **2009**, *48* (24), 10788–10795. https://doi.org/10.1021/ie901227p.

(70) Zhou, H.; Wang, Y.; Wei, F.; Wang, D.; Wang, Z. Kinetics of the Reactions of the Light Alkenes over SAPO-34. *Appl. Catal. A Gen.* **2008**, *348* (1), 135–141. https://doi.org/10.1016/j.apcata.2008.06.033.

(71) Frey, A. S.; Hinrichsen, O. Comparison of Differently Synthesized Ni(Al)MCM-48 Catalysts in the Ethene to Propene Reaction. *Microporous Mesoporous Mater.* **2012**, *164*, 164–171. https://doi.org/10.1016/j.micromeso.2012.07.015.

(72) Forestière, A.; Olivier-Bourbigou, H.; Saussine, L. Oligomerization of Monoolefins by Homogeneous Catalysts. *Oil Gas Sci. Technol.* **2009**, *64* (6), 649–667. https://doi.org/10.2516/ogst/2009027.

(73) Lappin, G. R.; Nemec, L. H.; Sauer, J. D.; Wagner, J. . Higher Olefins. In *Kirk-Othmer Encyclopedia of Chemical Technology*; Wiley & Sons, Inc.: New York, 2000; pp 709–728.

(74) Andrei, R. D.; Popa, M. I.; Fajula, F.; Hulea, V. Heterogeneous Oligomerization of Ethylene over Highly Active and Stable Ni-AlSBA-15 Mesoporous Catalysts. *J. Catal.* **2015**, *323*, 76–84. https://doi.org/10.1016/j.jcat.2014.12.027.

(75) Martínez, A.; Arribas, M. A.; Concepción, P.; Moussa, S. New Bifunctional Ni-H-Beta Catalysts for the Heterogeneous Oligomerization of Ethylene. *Appl. Catal. A Gen.* **2013**, *467*, 509–518. https://doi.org/10.1016/j.apcata.2013.08.021.

(76) Heveling, J.; Nicolaides, C. P.; Scurrell, M. S. Catalysts and Conditions for the Highly Efficient, Selective and Stable Heterogeneous Oligomerisation of Ethylene. *Appl. Catal. A Gen.* **1998**, *173* (1), 1–9. https://doi.org/10.1016/S0926-860X(98)00147-1.

(77) Moussa, S.; Arribas, M. A.; Concepción, P.; Martínez, A. Heterogeneous Oligomerization of Ethylene to Liquids on Bifunctional Ni-Based Catalysts: The Influence of Support Properties on Nickel Speciation and Catalytic Performance. *Catal. Today* **2016**, *277*, 78–88. https://doi.org/10.1016/j.cattod.2015.11.032.

(78) Beucher, R.; Andrei, R. D.; Cammarano, C.; Galarneau, A.; Fajula, F.; Hulea, V. Selective Production of Propylene and 1-Butene from Ethylene by Catalytic Cascade Reactions. *ACS Catal.* **2018**, *8* (4), 3636–3640. https://doi.org/10.1021/acscatal.8b00663.

(79) Wilshier, K. G. Propene Oligomerization over H-ZSM-5 Zeolite. *Stud. Surf. Sci. Catal.* **1988**, *36* (C), 621–625. https://doi.org/10.1016/S0167-2991(09)60559-0.

(80) Li, X.; Han, D.; Wang, H.; Liu, G.; Wang, B.; Li, Z.; Wu, J. Propene Oligomerization to High-Quality Liquid Fuels over Ni/HZSM-5. *Fuel* **2015**, *144*, 9–14. https://doi.org/10.1016/j.fuel.2014.12.005.

(81) Vaughan, J. S.; O'Connor, C. T.; Fletcher, J. C. Q. Propene Oligomerization and Xylene and Methyl-Pentene Isomerization over SAPO-11 and MeAPSO-11. *Stud. Surf. Sci. Catal.* **1994**, *84* (C), 1709–1716. https://doi.org/10.1016/S0167-2991(08)63723-4.

(82) Ward, J. W.; Delaney, D. D. Silica-Alumina Catalyst Containing Phosphorus. 5051386, 1991. https://doi.org/10.1016/0375-6505(85)90011-2.

(83) Blain, D. A.; Page, N. M.; Young, L. B. Olefin Oligomerization with Surface Modified Zeolite Catalyst. 5026933, 1991.

(84) Martens, J. A.; Verrelst, W. H.; Mathys, G. M.; Brown, S. H.; Jacobs, P. A. Tailored Catalytic Propene Trimerization over Acidic Zeolites with Tubular Pores. *Angew. Chemie - Int. Ed.* **2005**, *44* (35), 5687–5690. https://doi.org/10.1002/anie.200463045.

(85) Fetcher, J. C. .; Kojima, M.; O'Connor, C. T. Acidity and Catalytic Actiity of Synthetic Mica-Montmorillonite Part II: Propene Oligomerization. *Appl. Catal.* **1986**, *28*, 181–191.

(86) Mathys, G. M. K.; Dakka, J. M.; Marteens, M. M.; Martens, J. A.; Mishin, I. V.; Ravishankar, R.; Eijkhoudt, R. Alkene Oligomerization Process. 7112711B2, 2006.

(87) Fujie, H.; Imura, K.; Matsumoto, H.; Noh, T.; Nakanishi, K. Olefin Oligomerization Catalyst, Process for Preparing the Same, and Olefin Oligomerization Process Using the Same. 5883036, 1999.

(88) Nicholas, C. P. Applications of Light Olefin Oligomerization to the Production of Fuels and Chemicals. *Appl. Catal. A Gen.* **2017**, *543* (March), 82–97. https://doi.org/10.1016/j.apcata.2017.06.011.

(89) Martens, J. A.; Ravishankar, R.; Mishin, I. E.; Jacobs, P. A. Tailored Alkene Oligomerization with H-ZSM-57 Zeolite. *Angew. Chemie - Int. Ed.* **2000**, *39* (23), 4376–4379. https://doi.org/10.1002/1521-3773(20001201)39:23<4376::AID-ANIE4376>3.0.CO;2-2.

(90) Mantilla, A.; Tzompantzi, F.; Ferrat, G.; López-Ortega, A.; Alfaro, S.; Gómez, R.; Torres, M. Oligomerization of Isobutene on Sulfated Titania: Effect of Reaction Conditions on Selectivity. *Catal. Today* **2005**, *107–108*, 707–712. https://doi.org/10.1016/j.cattod.2005.07.153.

(91) Al-Kinany, M. C.; Al-Drees, S. A.; Al -Megren, H. A.; Alshihri, S. M.; Alghilan, E. A.; Al-Shehri, F. A.; Al-Hamdan, A. S.; Alghamdi, A. J.; Al-Dress, S. D. High-Quality Fuel Distillates Produced from Oligomerization of Light Olefin over Supported Phosphoric Acid on H-Zeolite-Y. *Appl. Petrochemical Res.* **2019**, *9* (1), 35–45. https://doi.org/10.1007/s13203-019-0225-1.

(92) Alcántara, R.; Alcántara, E.; Canoira, L.; Franco, M. J.; Herrera, M.; Navarro, A. Trimerization of Isobutene over Amberlyst-15 Catalyst. *React. Funct. Polym.* **2000**, *45* (1), 19–27. https://doi.org/10.1016/S1381-5148(00)00004-3.

(93) Zhang, L.; Ke, M.; Song, Z.; Liu, Y.; Shan, W.; Wang, Q.; Xia, C.; Li, C.; He, C. Improvement of the Catalytic Efficiency of Butene Oligomerization Using Alkali Metal Hydroxide-Modified Hierarchical Zsm-5 Catalysts. *Catalysts* **2018**, *8* (8). https://doi.org/10.3390/catal8080298.

(94) Kim, Y. T.; Chada, J. P.; Xu, Z.; Pagan-Torres, Y. J.; Rosenfeld, D. C.; Winniford, W. L.; Schmidt, E.; Huber, G. W. Low-Temperature Oligomerization of 1-Butene with H-Ferrierite. *J. Catal.* **2015**,

323, 33–44. https://doi.org/10.1016/j.jcat.2014.12.025.

(95) Xu, Z.; Chada, J. P.; Zhao, D.; Carrero, C. A.; Kim, Y. T.; Rosenfeld, D. C.; Rogers, J. L.; Rozeveld, S. J.; Hermans, I.; Huber, G. W. Production of Linear Octenes from Oligomerization of 1-Butene over Carbon-Supported Cobalt Catalysts. *ACS Catal.* **2016**, *6* (6), 3815–3825. https://doi.org/10.1021/acscatal.6b00655.

(96) Golombok, M.; De Bruijn, J. Dimerization of N-Butenes for High Octane Gasoline Components. *Ind. Eng. Chem. Res.* **2000**, *39* (2), 267–271. https://doi.org/10.1021/ie9906060.

(97) Flego, C.; Marchionna, M.; Perego, C. High Quality Diesel by Olefin Oligomerisation: New Tailored Catalysts. *Stud. Surf. Sci. Catal.* **2005**, *158 B* (ii), 1271–1278. https://doi.org/10.1016/s0167-2991(05)80474-4.

(98) Bond, J. Q.; Alonso, D. M.; Wang, D.; West, R. M.; Dumesic, J. A. Integrated Catalytic Concersion of Gamma-Valerolactone to Liquid Alkenes for Transportation Fuels. *Science (80-.).* **2010**, *327*, 1110–1114. https://doi.org/10.1126/science.1184362.

(99) Escola, J. M.; Van Grieken, R.; Moreno, J.; Rodriguez, R. Liquid-Phase Oligomerization of 1-Hexene Using Al-MTS Catalysts. *Ind. Eng. Chem. Res.* **2006**, *45* (22), 7409–7414. https://doi.org/10.1021/ie0603262.

(100) De Klerk, A. Oligomerization of 1-Hexene and 1-Octene over Solid Acid Catalysts, 2005, Vol. 44. https://doi.org/10.1021/ie0487843.

(101) Maseloane, M. A. Dimerization of Naphtha-Range Fischer-Tropsch Olefins into Diesel-Range Products over Zeolite H-ZSM-5 and Amorphous Silica-Alumina, University of Cape Town, 2011.

(102) Samoilov, V. O.; Ramazanov, D. N.; Nekhaev, A. I.; Egazar'Yants, S. V.; Maximov, A. L. Flow Reactor Synthesis of Cetane-Enhancing Fuel Additive from 1-Butanol. *Fuel Process. Technol.* **2015**, *140*, 312–323. https://doi.org/10.1016/j.fuproc.2015.08.021.

(103) Medina, E.; Bringué, R.; Tejero, J.; Iborra, M.; Fité, C. Conversion of 1-Hexanol to Di-n-Hexyl Ether on Acidic Catalysts. *Appl. Catal. A Gen.* **2010**, *374* (1–2), 41–47. https://doi.org/10.1016/j.apcata.2009.11.024.

(104) Casas, C.; Bringué, R.; Ramírez, E.; Iborra, M.; Tejero, J. Liquid-Phase Dehydration of 1-Octanol, 1-Hexanol and 1-Pentanol to Linear Symmetrical Ethers over Ion Exchange Resins. *Appl. Catal. A Gen.* **2011**, *396* (1–2), 129–139. https://doi.org/10.1016/j.apcata.2011.02.006.

(105) Tao, L.; Markham, J. N.; Haq, Z.; Biddy, M. J. Techno-Economic Analysis for Upgrading the Biomass-Derived Ethanol-to-Jet Blendstocks. *Green Chem.* **2017**, *19* (4), 1082–1101. https://doi.org/10.1039/c6gc02800d.

(106) Baddour, F. G.; Snowden-Swan, L.; Allsburg, K. M. Van; Super, J.; Tan, E.; Frye, J.; White, J.; Schaidle, J.; Talmadge, M.; Hensley, J.; et al. CatCost. 2018, pp 1–54.

(107) Lorenz Biegler; Grossmann;, I.; Westerberg, A. *Systematic Methods of Chemical Process Design*, First.; Prentice Hall: Upper Saddle River, 1999.

(108) Aspen Technology, I. Aspen Plus. 2017.

(109) N2 https://puritygas.ca/nitrogen-gas-costs/%0A.

(110) NaOH https://www.alibaba.com/product-detail/CAS-NO-1310-73-2-caustic_60763271661.html?spm=a2700.galleryofferlist.0.0.707c756cokN1ll.

(111) Propane https://www.nyserda.ny.gov/Researchers-and-Policymakers/Energy-Prices/Propane/Average-Propane-Prices%0A.

(112) HZSM5 https://www.alibaba.com/product-detail/Catalytic-cracking-catalyst-ZSM-5-for_1461857790.html?spm=a2700.details.deiletai6.2.6c591307ECoSFc&bypass=true.

(113) TEA https://www.alibaba.com/product-detail/Triethyl-Aluminium-TEAL- Used-As-Polyolefin_62295369824.html?spm=a2700.galleryofferlist.0.0.15a629d9 Db1LLv.

(114) ZEOLITE H-Y https://www.alibaba.com/product-detail/zeolite-H-Y-for-preparing-catalytic_60830743993.html?spm=a2700.galleryofferlist.0.0.61f942528esfGR&bypass=true.

(115) SPA https://www.alibaba.com/product-detail/Mytext-Solid-Phosphoric-Acid_60831957268.html?spm=a2700.galleryofferlist.0.0.147e7e1aRNk5FM&bypass=true.

(116) CT275 https://www.alibaba.com/product-detail/Factory-direct-Purolite-dowex-ion-exchange_60732119756.html?spm=a2700.galleryofferlist.0.0.565f3bbfC34UPp&s=p&bypass=true.

(117) Silica Alumina https://www.alibaba.com/product-detail/Customized-silica-alumina-catalyst-activated_60394176139.html?spm=a2700.7724857.normalList.42.4b3e425eHITT5P&bypass=true.

(118) ZrO2 https://www.alibaba.com/product-detail/Zirconium-dioxide-ZrO2-best-price-for_62425668138.html?spm=a2700.galleryofferlist.0.0.568b2d8akcmGXP&bypass=true.

(119) Bond, J. Q.; Upadhye, A. A.; Olcay, H.; Tompsett, G. A.; Jae, J.; Xing, R.; Alonso, D. M.; Wang, D.; Zhang, T.; Kumar, R.; et al. Production of Renewable Jet Fuel Range Alkanes and Commodity Chemicals from Integrated Catalytic Processing of Biomass. *Energy Environ. Sci.* **2014**, *7* (4), 1500–1523. https://doi.org/10.1039/c3ee43846e.